UNIVERSIDADE FEDERAL DE PERNAMBUCO

CENTRO DE TECNOLOGIA E GEOCIÊNCIAS

PROGRAMA DE PÓS-GRADUAÇÃO EM GEOCIÊNCIAS

GERMANO MARIO SILVA RAMOS

ANÁLISE DO POTENCIAL DE ARMAZENAMENTO DEFINITIVO DE CO_2 EM RESERVATÓRIOS COMPOSTOS POR ROCHAS VULCÂNICAS NA BACIA DE CAMPOS

Recife

2025

GERMANO MARIO SILVA RAMOS

ANÁLISE DO POTENCIAL DE ARMAZENAMENTO DEFINITIVO DE CO2 EM RESERVATÓRIOS COMPOSTOS POR ROCHAS VULCÂNICAS NA BACIA DE CAMPOS

Tese apresentada ao Programa de Pós-Graduação em Geociências da Universidade Federal de Pernambuco, como requisito parcial para obtenção do título de doutor em Geociências. Área de concentração: Geociências

Orientador: José Antonio Barbosa

Coorientador: Igor Fernandes Gomes

Recife

2025

.Catalogação de Publicação na Fonte. UFPE - Biblioteca Central

Ramos, Germano Mario Silva.
Análise do potencial de armazenamento definitivo de CO2 em reservatórios compostos por rochas vulcânicas na Bacia de Campos / Germano Mario Silva Ramos. - Recife, 2025.
114 f.: il.

Tese (Doutorado) - Universidade Federal de Pernambuco, Centro de Tecnologia e Geociências, Programa de Pós-Graduação em Geociências, 2025.
Orientação: José Antonio Barbosa.
Coorientação: Igor Fernandes Gomes.
Inclui referências.

1. Armazenamento geológico de CO2; 2. Mineralização de CO2; 3. Reservatórios vulcânicos; 4. Atributos sísmicos; 5. Modelagem geológica. I. Barbosa, José Antonio. II. Gomes, Igor Fernandes. III. Título.

UFPE-Biblioteca Central

GERMANO MARIO SILVA RAMOS

ANÁLISE DO POTENCIAL DE ARMAZENAMENTO DEFINITIVO DE CO_2 EM RESERVATÓRIOS COMPOSTOS POR ROCHAS VULCÂNICAS NA BACIA DE CAMPOS

Tese apresentada ao Programa de Pós-Graduação em Geociências da Universidade Federal de Pernambuco, como requisito parcial para obtenção do título de doutor em Geociências. Área de concentração: Geociências

BANCA EXAMINADORA

_____

Profa. Dra. Carla Joana Barreto
Universidade Federal de Pernambuco UFPE

_____

Prof. Dr. Francisco Hilário do Rego Bezerra (Examinador Externo)
Universidade Federal do Rio Grande do Norte UFRN

_____

Prof. Dr. Hélio Jorge Portugal Severiano Ribeiro (Examinador Externo)
Universidade Estadual do Norte Fluminense UENF

_____

Prof. Dr. Leonardo José do Nascimento Guimarães (Examinador Externo)
Universidade Federal de Pernambuco UFPE

_____

Prof. Dr. Tiago Siqueira de Miranda (Examinador Interno)
Universidade Federal de Pernambuco UFPE

AGRADECIMENTOS

Expressando minha profunda gratidão, gostaria de reconhecer aqueles que tornaram este trabalho possível e enriqueceram minha jornada acadêmica de forma indelével.

À minha família, alicerce incondicional e fonte inesgotável de amor e apoio, meu sincero agradecimento. Pai e mãe, Mavir e Gisa, sua presença constante, incentivo e respaldo foram essenciais para que eu pudesse me dedicar integralmente a este projeto, mesmo nos momentos mais desafiadores. Seu carinho, compreensão e sacrifícios tornaram esta conquista possível.

Ao Professor José Antonio Barbosa, meu orientador e amigo, minha eterna gratidão. Sua orientação valiosa, vasto conhecimento, experiência e paciência foram cruciais para o desenvolvimento deste estudo. Sua compreensão e apoio emocional me fortaleceram nos momentos em que as dificuldades pareciam intransponíveis. Obrigado por acreditar em mim, por me inspirar a buscar a excelência e por me guiar com sabedoria nesta jornada.

Ao Professor Virgínio Henrique, meu sincero agradecimento por sua amizade. Sua dedicação e compromisso com meu desenvolvimento acadêmico e pessoal foram verdadeiramente inspiradores.

À minha tia Marli, obrigado por suas orações incansáveis, palavras de encorajamento e apoio emocional inquebrantáveis, que me impulsionaram a superar os obstáculos e a não desistir diante dos desafios. Sua força e fé foram um bálsamo para minha alma nos momentos mais turbulentos.

Aos meus companheiros de curso e laboratório, Osvaldo, Roberta, Aline, Jefferson e Fernando, meu profundo agradecimento pela amizade verdadeira, pelo incentivo mútuo e por compartilharem comigo esta experiência inesquecível. Nossa jornada foi enriquecida pelos momentos de troca, apoio e crescimento compartilhados. Vocês tornaram esta caminhada mais leve e alegre. E a todos aqueles que cruzaram meu caminho e contribuíram, direta ou indiretamente, para a concretização desta conquista, minha sincera gratidão!

“A mente que se abre a uma nova ideia
jamais voltará ao seu tamanho original.”
Albert Einstein

RESUMO

As emissões de CO_2 de origem antropogênica se intensificaram nas últimas décadas e a concentração deste gás na atmosfera atingiu um novo pico de 425,38 ppm em 2024. Neste cenário, a produção de óleo e gás do intervalo pré-sal das bacias brasileiras de Santos e Campos apresenta um enorme desafio, devido às elevadas concentrações de CO2 existentes nos fluídos destes reservatórios. Desde o início da produção destas reservas a destinação encontrada tem sido a separação do CO2 e sua reinjeção nos reservatórios, para efeito de armazenamento e de auxílio na produção. O volume injetado alcança centenas de milhares de toneladas mensalmente. Esta pesquisa objetivou avaliar a possibilidade de uso da vasta quantidade de rochas basálticas da Formação Cabiúnas (*flooding basalts* - Neocomiano), posicionadas sobre o embasamento da região de plataforma da Bacia de Campos, para a realização de projetos de armazenamento geológico de CO2. A injeção em rochas basálticas apresenta a vantagem de prender de forma permanente o CO2 em estado sólido, o que representa uma alternativa mais segura e econômica de armazenamento geológico. Outras vantagens para esta proposta são: 1) as rochas estão na região de águas rasas, 2) não haveria limite de uso de água se a opção for injetar CO2 diluído, 3) as vasta quantidade de dados geofísicos e de poços que existem sobre a região por se tratar de área alvo de exploração da indústria petrolífera há décadas. A pesquisa utilizou um banco de dados com cerca de 180 poços, e um cubo de dados sísmicos 3D (PSTM/PSDM) que cobre a região dos campos de Badejo, Linguado e Pampo, que durante 30 anos produziram óleo em reservatórios basálticos nestas rochas. Na primeira parte da pesquisa os dados sísmicos e de poços foram utilizados para a modelagem de um reservatório hipotético nas rochas vulcânicas a partir do qual foram verificados o seu potencial em termos de parâmetros físicos para alcançar mineralização, e de volume de armazenamento. Uma segunda parte do projeto buscou demonstrar como os dados legados da indústria são úteis e valiosos para a realização de estudos preliminares para a determinação de locais mais favoráveis para a execução de projetos de injeção de CO2 em formações basálticas, tomando como exemplo os dados disponíveis sobre os reservatórios vulcânicos na unidade Cabiúnas. O estudo demonstrou o ótimo potencial em termos de parâmetros de reatividade e mineralização destas rochas, além da capacidade para receber vastos volumes de CO2, e que o uso de rotinas convencionais de interpretação e modelagem de dados legados permite avaliar características imprescindíveis na determinação das áreas mais favoráveis, como por exemplo a estimativa de porosidade que é controlada por processos diagenéticos e tectônicos, e pelos sistemas de falhas e fraturas.

Palavras-chave: Armazenamento Geológico de CO2; mineralização de CO_2; reservatórios vulcânicos; atributos sísmicos, modelagem geológica

ABSTRACT

The anthropogenic CO_2 emissions have intensified in recent decades, and the concentration of this gas in the atmosphere reached a new peak of 425.38 ppm in 2024. In this scenario, oil and gas production from the pre-salt interval of the Brazilian Santos and Campos basins presents a significant challenge due to the high concentrations of CO_2 present in the fluids of these reservoirs. Since the beginning of production from these reserves, the solution has been the separation of CO_2 and its reinjection into the reservoirs for storage and enhanced recovery purposes. The volume injected reaches hundreds of thousands of tons monthly. This research aimed to evaluate the possibility of using the vast basaltic deposits of the Cabiúnas Formation (flooding basalts - Neocomian), positioned over the basement in the Campos Basin platform region for CO_2 geological storage projects. Injecting CO2 into basaltic rocks has the advantage of permanently trapping the carbon in solid form through the mineralization mechanism, which represents a safer and more economical alternative for geological storage. Other advantages for this proposal include: 1) the rocks are located in shallow water regions, 2) there would be no water usage limit if the option is to inject diluted CO_2, and 3) the vast amount of geophysical and well data available on the region, as it has been explored for the petroleum industry for decades. The research utilized a database with about 180 wells and a 3D seismic data cube (PSTM/PSDM) covering the Badejo, Linguado, and Pampo fields, which have produced oil from basaltic reservoirs, which has produced oil for thirty years. In the first part of the research, seismic and well data were used to model a hypothetical reservoir in the volcanic rocks, aiming to analyze their potential in terms of physical parameters for achieving carbon mineralization and the storage capacity. The second part of the project aimed to demonstrate how legacy data from the industry are useful and valuable for preliminary studies to determine the most favorable sites for CO_2 storage projects in basaltic formations, using the example of the volcanic oil reservoirs from the Cabiúnas Formation. The study demonstrated the excellent potential in terms of reactivity and mineralization of these rocks, as well as the capacity to receive vast volumes of CO_2. Using conventional modeling and interpretation routines on the legacy data allows for evaluating essential characteristics, and determining the most favorable areas, such as porosity estimation, which is controlled by diagenetic and tectonic processes and fracture systems.

Keywords: CO_2 sequestration; CO_2 mineralization mechanism; CCS; Reservoir modeling; Basaltic rocks

SUMÁRIO

1 INTRODUÇÃO 10

1.1 ASPECTOS GERAIS 10

1.2 MOTIVAÇÃO E OBJETIVOS 15

1.3 ESTRUTURA DA TESE 19

2 METODOLOGIA 19

2.1 CONJUNTO DE DADOS E PRÉ-PROCESSAMENTO 19

2.2 ANÁLISE DE POÇOS E CARACTERÍSTICAS DO RESERVATÓRIO 21

2.3 QUANTIFICAÇÃO DA POROSIDADE 22

2.4 ESTIMATIVA DA CAPACIDADE DE ARMAZENAMENTO 23

2.5 CRIAÇÃO DE UM CUBO DE POROSIDADE COM O PLUGIN DE REDE NEURAL ARTIFICAL (RNA) 24

3 RESULTADOS OBTIDOS 25

4 ARTIGO 1 25

5 ARTIGO 2 45

6 CONCLUSÕES PRELIMINARES 97

7 REFERÊNCIAS 98

1 INTRODUÇÃO

1.1 ASPECTOS GERAIS

As emissões antropogênicas de dióxido de carbono (CO_2), que é um dos gases causadores do efeito estufa devido à absorção de radiação infravermelha térmica, representam uma ameaça à manutenção das atuais condições climáticas no planeta. As emissões poluentes se intensificaram de forma dramática durante as últimas décadas do século XX. O uso de combustíveis fósseis e a fabricação de cimento representam 75% do total de emissões de CO_2, enquanto os processos de mudança no uso do solo, especialmente desmatamentos e queimadas, são responsáveis por grande parte dos 25% restantes. Ao contrário das reduções demandadas para o cumprimento das metas climáticas globais estabelecidas no Acordo de Paris, as emissões totais de CO_2 vinculadas ao consumo de fontes de energia cresceram 1,1% em 2023, e a concentração de CO2 atingiu um novo pico de 425,38 ppm em 2024. (NOAA, 2024) (Fig. 1).

Figura 1 - Indicador de emissão de CO_2 desde os anos 1960 até os dias atuais. Observe que no final da década de 80 passamos o nível considerado seguro em emissões de CO_2. Os últimos dados apontam para o nível de CO_2 em aproximadamente 425ppm (dados de 05 de abril de 2024) (NOAA, 2024).

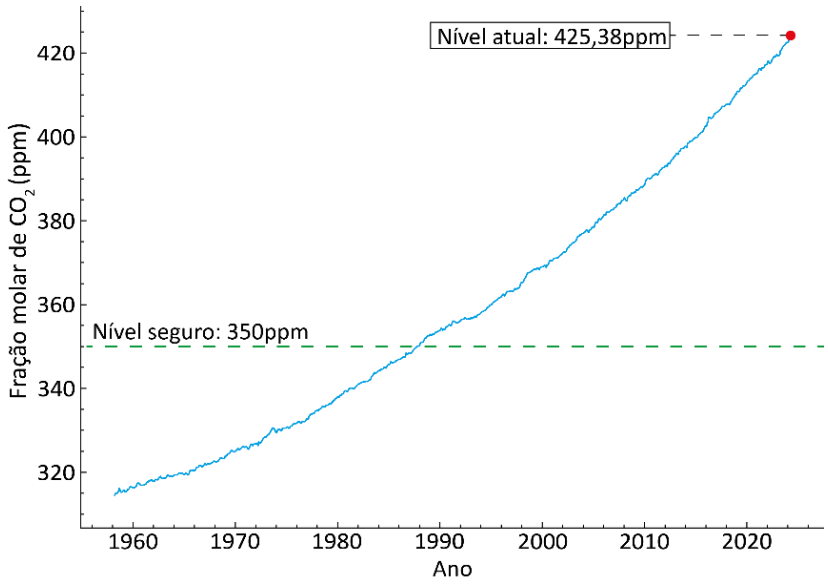

(NOAA, 2024)

De acordo com observações recentes, as concentrações médias globais desse gás de efeito estufa ultrapassaram, em 2022, um patamar crítico, alcançando valores 50% superiores aos registrados antes da Revolução Industrial. Esse cenário reforça a urgência de medidas efetivas

para reduzir as emissões de CO_2 e mitigar os impactos das mudanças climáticas em curso (WMO, 2023).

A matriz energética global ainda se mostra fortemente dependente de fontes fósseis, o que representa um enorme desafio na transição para um sistema mais sustentável e descarbonizado. Dados recentes revelam que os combustíveis fósseis respondem por mais de 80% do suprimento energético mundial (IEA, 2020), com projeções indicando a manutenção dessa participação expressiva até meados deste século. Essa realidade sinaliza as enormes dificuldades inerentes à redução dessa dependência no curto prazo, evidenciando os obstáculos a serem superados na busca por uma efetiva transição energética.

Paralelamente, tecnologias consideradas limpas e renováveis, como a geração solar e eólica, têm ganhado espaço crescente na matriz primária, embora ainda representem uma parcela modesta frente ao volume total de energia produzida globalmente. Apesar dos avanços, seu potencial de expansão esbarra em limitações técnicas e econômicas a serem transpostas para que estas possam desempenhar um papel mais relevante no fornecimento energético sustentável (IEA, 2020).

Ainda no cenário energético atual, o uso de combustíveis fósseis na geração de eletricidade desempenha um papel de destaque nas emissões de gases de efeito estufa. Estimativas apontam que esse setor é responsável por cerca de 40% do total de dióxido de carbono lançado na atmosfera. Esse dado reforça a premência de se buscarem alternativas e soluções inovadoras para uma matriz elétrica mais limpa e sustentável (IEA, 2019).

Diante do desafio das mudanças climáticas, a indústria se depara com a necessidade iminente de gerenciar volumes crescentes de emissões de dióxido de carbono, que correspondem a bilhões de toneladas nas próximas décadas (Martin-Roberts et al., 2021). Uma opção que parece viável em termos técnicos e econômicos é realizar a captura de CO2 nas fontes estacionárias, e realizar o seu armazenamento definitivo em formações geológicas adequadas, como aquíferos salinos, cavernas artificiais em depósitos de sal, em jazidas de carvão ou em rochas vulcânicas máficas e ultramáficas (Leung et al., 2014; Ajayi et al., 2019; Kelemen et al., 2019, 2020; Snæbjörnsdóttir et al., 2020; Hong, 2022). Neste último método o gás pode ser diluído em água ou comprimido até atingir o estado supercrítico antes do armazenamento.

A injeção de CO_2 em meios geológicos (Geological Carbon Storage - GCS), é apontada como a alternativa viável para o armazenamento artificial em larga escala (IPCC, 2005; Leung et al., 2014). Ao avaliar a viabilidade de injetar CO_2 em subsuperfície, é necessário analisar cuidadosamente uma série de aspectos cruciais para o sucesso do empreendimento. Questões

econômicas, geológicas, químicas, sócio-políticas e ambientais, entre outras, desempenham um papel fundamental nessa decisão (Vulin et al., 2023; Bachu, 2000; Raza et al., 2022).

Dentre as alternativas em termos de meio para o armazenamento geológico de CO2, as rochas vulcânicas máficas apresentam vantagens promissoras em termos de mecanismo de retenção do carbono, e de volumes que podem ser armazenados em formações geológicas (Benson et al., 2005; Oelkers et al., 2008; Gislason & Oelkers, 2014; Snæbjörnsdóttir et al., 2016). Através do processo já conhecido de mineralização do carbono, o CO_2 pode ser aprisionado de forma segura na forma de minerais neoformados na escala do tempo geológico, milhares a milhões de anos (Gislason, et al., 2014). Isso é possível devido à composição química das rochas máficas, como os basaltos. Essas rochas contêm tipicamente cerca de 25% de óxidos de cálcio, magnésio e ferro (Schaef et al., 2011). Quando em contato com solução aquosa ácida, esses minerais reagem prontamente, liberando cátions de Ca, Fe e Mg, e criando condições para a formação de novos minerais (carbonatos principalmente), com a incorporação do carbono nestas estruturas (Raza, 2022; Kelemen, 2019) (Fig. 1).

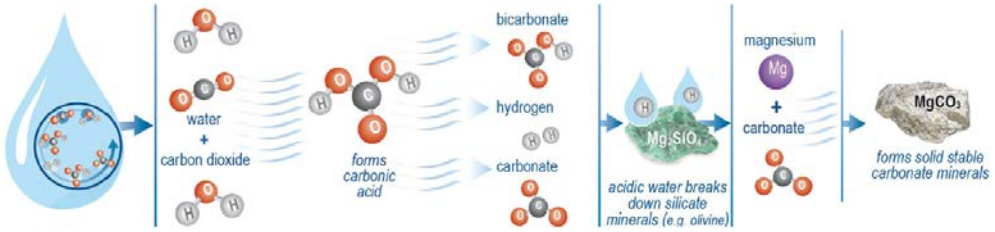

Figura 2 - Processo de mineralização do carbono a partir da injeção de CO2 em rochas basálticas com o mineral olivina (Raza et al., 2022).

Desta forma, estudos e projetos piloto de injeção de CO2 em rochas vulcânicas como basalto têm apontado o mecanismo de mineralização como uma excelente alternativa devido ao processo de mineralização de carbono, devido a sua reatividade e abundância na crosta terrestre. Esse processo tem potencial para fornecer um método seguro e eficaz de armazenamento geológico de CO_2 em larga escala por períodos extremamente longos (Gislason et al., 2010; Schaef et al, 2011; Wolff-Boenisch et al., 2006; Rosenbauer et al., 2012; Gysi & Stefansson, 2012; Galeczka et al., 2014a; Tutolo et al., 2021; Wang & Dreisinger, 2022).

Os projetos piloto desenvolvidos no mundo para verificar a eficácia do método de mineralização de CO2 em basaltos abrangem o projeto CarbFix (Islândia), O Projeto Wallula (Estados Unidos), e o projeto de injeção em Jizan (Arábia Saudita) (Clark et al., 2020; Goldberg, 2010, 2018; McGrail et al, 2006, 2014). Os projetos de Jizan e CarbFix consideraram a injeção de CO2 diluído em água, e o Projeto Walllula realizou a injeção de mil toneladas de

CO2 no estado supercrítico (Clark, 2018, 2020; McGrail et al, 2006, 2014; Oelkers et al., 2022; Fedorik et al., 2023). Todos esses projetos confirmaram por meio de monitoramento multi-métodos que de 70 a 80% do CO2 injetado foi mineralizado no espaço de dois anos (Pogge von Strandmann et al., 2019; Clark et al., 2020; White et al., 2020; Wang & Dreisinger, 2022).

Contudo, os experimentos de mineralização de CO2 em escala de laboratório e de campo em rochas basálticas, revelaram que alguns parâmetros apresentam importância para o fluxo de injeção do gás, a velocidade das reações de dissolução e precipitação de minerais e a quantidade de CO2 que pode ser absorvido por volume poroso de cada reservatório (Cao et al., 2023). Os fatores cruciais na escolha de locais adequados para projetos de GCS baseados em mineralização incluem a alcalinidade da água de formação, superior a 7, temperaturas entre 50°C e aproximadamente 250°C, e valores pressão, entre 0,6 a 50 MPa (Schaef et al., 2011; Kelemen et al., 2020; Raza et al., 2022; Kim et al., 2023). Além disso, aspectos como a profundidade dos estratos, em regiões offshore ou onshore, e a proximidade de grandes volumes de rochas vulcânicas das fontes emissoras são fatores importantes devido aos custos envolvidos na captura, concentração, transporte e injeção (Kelemen et al., 2020; Raza et al., 2022; Kim et al., 2023). Dentre as regiões mais promissoras estão aquelas onde se formaram grandes volumes de rochas vulcânicas devido a formação de LIPs (Large Igneous Provinces), como as do Deccan, na Índia, e a de Paraná-Etendeka, entre a América do Sul e a África (Kelemen et al., 2020; Raza et al., 2022; Singh et al., 2024) (Fig. 2).

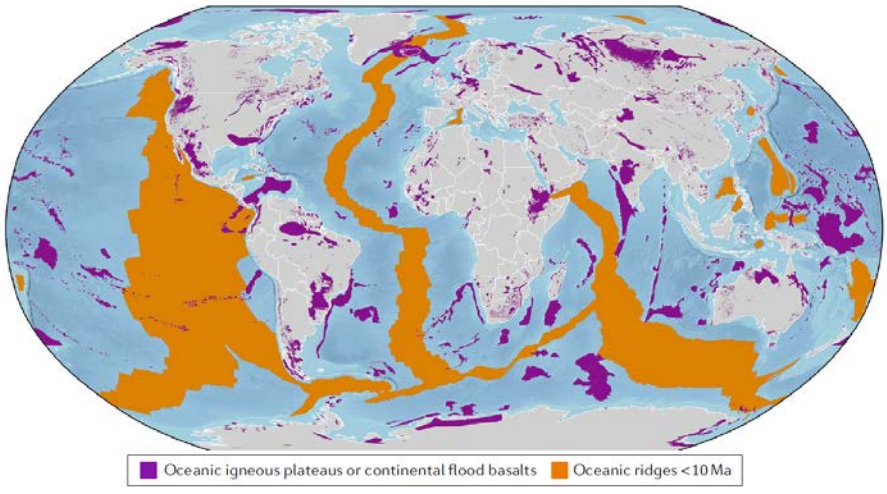

Figura 3 - Localização das regiões, onshore e offshore, consideradas como promissoras para a execução de projetos de GCS via método de mineralização. As dorsais oceânicas (em laranja) com <10 m.a., os platôs vulcânicos e as províncias magmáticas (flood basalts), em roxo (Snæbjörnsdóttir et al., 2020).

A influência de outros aspectos, como a capacidade de injeção e as propriedades de molhabilidade mineral específicas na formação de minerais carbonáticos, ainda não são

totalmente compreendidas. No entanto, os resultados positivos observados nos projetos piloto até então desenvolvidos demonstraram o potencial para armazenar bilhões de toneladas anualmente (Matter et al., 2014; Gislason et al., 2014; Snæbjörnsdóttir et al., 2020; Raza et al., 2022; Tutolo et al., 2022). Dois países em especial planejam construir hubs de injeção de CO2 em regiões de placa oceânica, a Islândia, com a expansão do Projeto CarbFix, e os Estados Unidos através do Projeto CarbSafe (Goldberg, 2018; Snæbjörnsdóttir et al., 2014, 2020).

No Brasil, os estudos com foco na definição de formações geológicas e regiões viáveis para projetos de GCS têm aumentado. Existem estudo que já discutiram o desafio criado pelas concentrações de CO2 nos fluidos dos reservatórios do pré-sal (De Freitas; Kaneko, 2011; Gamboa et al., 2019; Ramos et al., 2023; Oliveira et al., 2024), observando que estes volumes vão crescer com a expansão da produção de óleo e de gás nas bacias de Santos e Campos, e não podem ser liberados para a atmosfera (IPCC, 2018, EPE, 2021). Alguns estudos já apontaram a possibilidade de armazenar CO2 em cavernas artificiais de sal nas camadas de evaporitos que campeiam os reservatórios na região de águas profundas destas bacias (Goulart et al., 2020), e também já propuseram uma estimativa de armazenamento em formações sedimentares do intervalo pós-sal (Rockett et al., 2010). Entretanto, a escavação e manutenção de cavernas de sal em águas profundas requer um investimento elevado (Maia da Costa et al., 2018; Vieira et al., 2020), e em ambos os casos, o CO2 permanecerá bom um período grande de tempo (centenas a milhares de anos) na forma livre, e isto implica no risco de vazamento através das camadas sedimentares, através de falhas e fraturas, e na eventual falha dos poços utilizados para realizar a injeção (Berest et al., 2019).

A segurança dos projetos, o que requer monitoramento, durante a injeção, e após o encerramento do projeto, impactam diretamente os custos do armazenamento geológico (Friedmann et al., 2006; Stenhouse et al., 2009; Ajayi et al., 2019; Aydin et al., 2019; Cao et al., 2020). O monitoramento pode representar mais de 50% dos custos totais do projeto em determinadas circunstâncias (Takagi et al., 2013). Como proposto para efetivar a mitigação das emissões, a injeção de bilhões de toneladas de CO_2 em áreas offshore apresenta desafios adicionais, provenientes tanto da complexidade logística (Stenhouse et al., 2009; Rubin et al., 2015), quanto das características inerentes dos reservatórios (Takagi et al., 2013; Anderson, 2017; Schmelz et al., 2020; Tutolo et al., 2021). O conhecimento necessário para garantir esta escala de operações ainda está em desenvolvimento (Ali et al., 2022), e os riscos relacionados a problemas como vazamentos e sismicidade induzida ainda são desconhecidos (Raza, 2022; Kelemen, 2019; Celia, 2017). Por isso a tecnologia de mineralização, especialmente a partir da

injeção de CO2 em rochas vulcânicas em regiões offshore, possivelmente representará uma parte importante desta solução (Ajayi et al., 2019; Alcalde et al., 2018).

O sucesso futuro do esforço de redução de emissões, depende enormemente da compreensão mais profunda dos custos e riscos associados aos distintos métodos de GCS, incluindo este promissor método de armazenamento baseado na mineralização, especialmente no que tange às incertezas geológicas (Aydin et al., 2010; Vilarrasa e Carrera, 2015; Alcalde et al., 2018; Aminu et al., 2017; Larkin et al., 2019; Cao et al., 2020; Schmelz et al., 2020).

1.2 MOTIVAÇÃO E OBJETIVOS

Algumas pesquisas tratam do potencial de armazenamento de CO2 em formações geológicas nas bacias da margem leste brasileira (Ciotta, 2020; Ciotta & Tassinari, 2020; Rockett, 2010; Pelissari, 2021; EPE, 2018; Silva, Parente, Dos Santos, 2023). Estes trabalhos focaram na possibilidade de usar reservatórios depletados do intervalo pós-sal, ou aquíferos, para fins de armazenamento, ou a possibilidade de utilizar o CO2 reinjetado em reservatórios para fins de recuperação avançada (EOR), ou recuperação melhorada de Petróleo (IOR), e armazenamento (Hermes, 2017; Marcellos et al., 2011; Fleming & Assis, 2020). Poucos trabalhos trataram o armazenamento definitivo de CO_2 em rochas vulcânicas (Ramos et al., 2023; Guzmán, 2024; Alzate Rubio, 2024; Orita & Cruz, 2023), e quase totalidade destes se concentrou no potencial da Formação Serra Geral, Bacia do Paraná.

Conforme o contexto apresentado, a presente pesquisa buscou tratar do potencial das rochas da Formação Cabiúnas, sucessão de rochas basálticas, com menor participação de rochas vulcanoclásticas, de idade Hauteriviano (Fig. 3) (Mizusaki et al., 1992; Marins et al., 2022; Braga et al., 2023), para a realização de projetos de GCS, considerando que estas apresentam a vantagem de permitir o armazenamento por processo de mineralização. As rochas desta unidade apresentam variado grau de intemperismo causado por exposição subaérea, e recobrem o embasamento das regiões proximais e distais da Bacia de Santos durante a fase pré-rifte e rifte do Atlântico Sul nesta região (Stica et al., 2014) (Fig. 4).

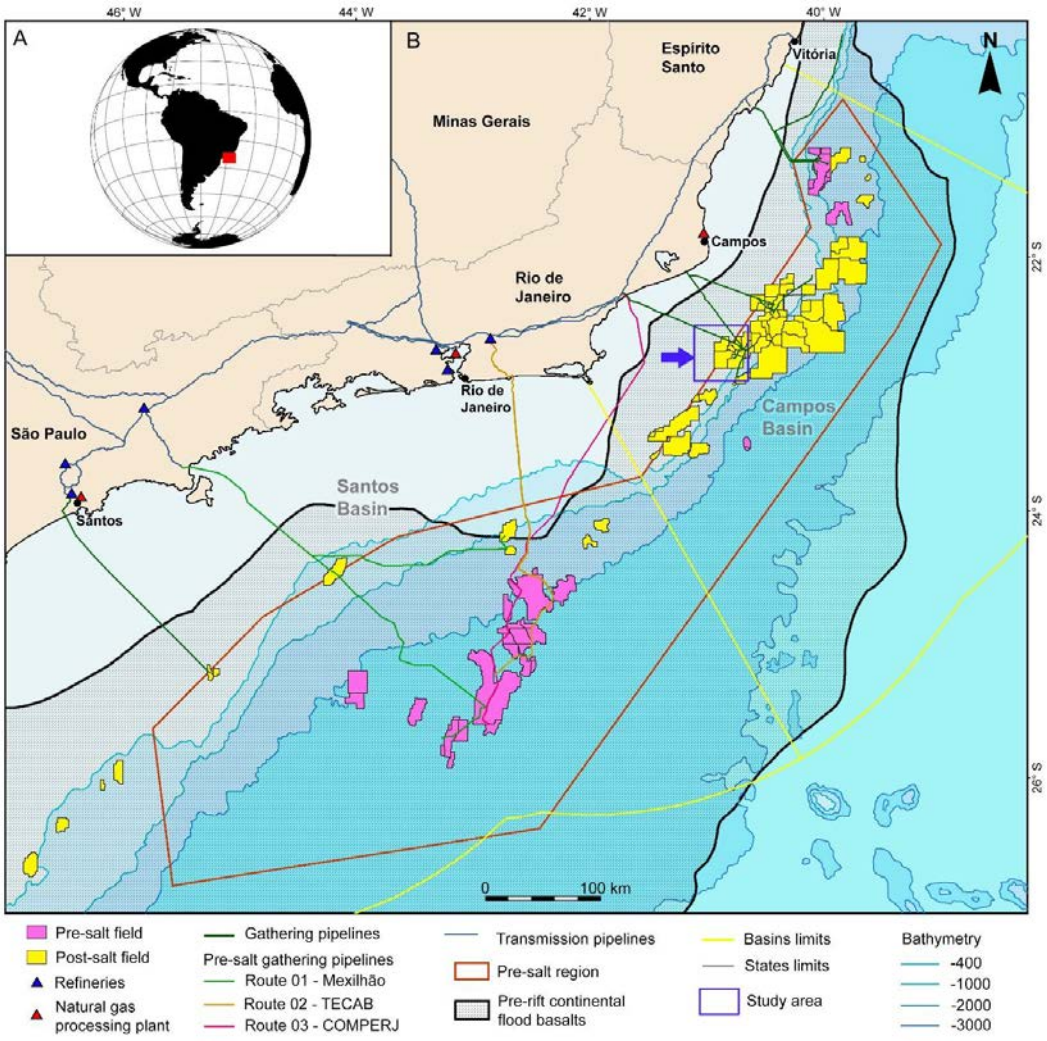

Figura 4 - A) Localização da região das bacias de Santos e Campos na margem leste continental do Brasil (polígono vermelho). B) Distribuição de campos de óleo e gás na região offshore destas bacias (ANP, 2022). O mapa também apresenta a principal infraestrutura de plantas de processamento de gás e derivados, oleodutos e gasodutos, e refinarias (EPE, 2020). O polígono azul na região proximal da Bacia de Campos indica a área onde o estudo foi desenvolvido. A zona hachurada indica a estimativa da cobertura dos estratos basálticos da Formação Cabiúnas (flood basalts) (Stica et al., 2014).

Conforme estudos anteriores (Guardado et al., 1990; Mizusaki et al., 1992; Bruhn et al., 2003), a Formação Cabiúnas possui espessura que varia entre 500 a ~1000 m, e durante a fase exploratório inicial na Bacia de Campos foram descobertas reservas comerciais de óleo em rochas basálticas no Campo de Badejo, e ocorrências não comerciais em basaltos no campo de Linguado (Fig. 4). Desta forma, existe uma quantidade importante de dados sobre estas rochas devido a este interesse inicial por estas acumulações de hidrocarbonetos, que permitiram a produção de óleo e gás até meados dos anos 2000 (Bruhn et al., 2003; Marins et al., 2023). Os reservatórios principais foram encontrados na Formação Lagoa Feia, coquinas e siliciclásticos, e secundariamente foram encontradas acumulações nos basaltos fraturados que estão em

contato por falhas com as geradoras do Grupo Lagoa Feia - Formação Atafona (Guardado, 1990; Bruhn et al., 2003).

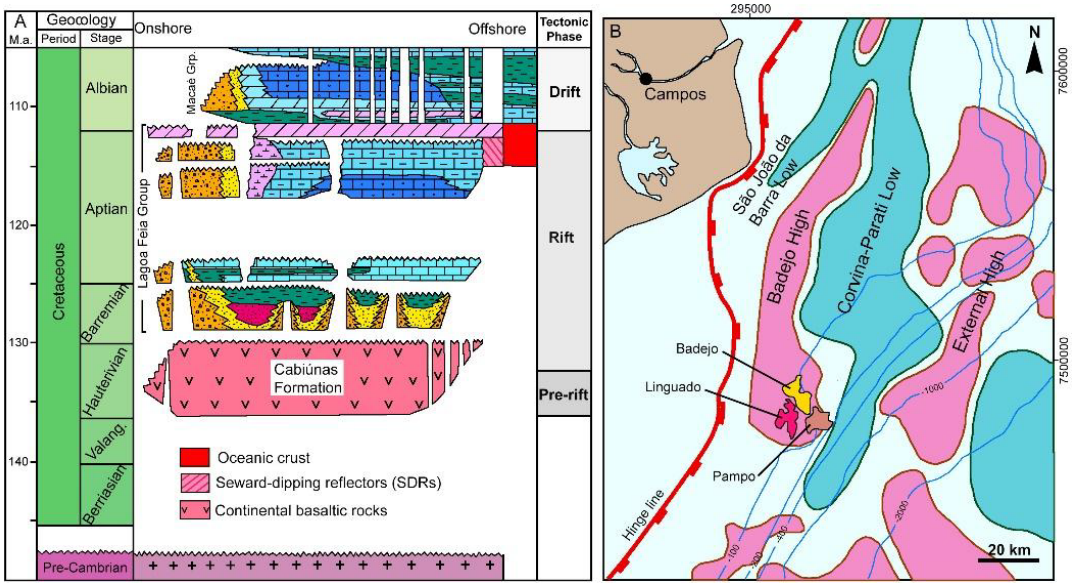

Figura 5 - A) Carta estratigráfica simplificada da sucessão Cretáceo Inferior da Bacia de Campos (adaptado de Stica et al., 2014), B) Compartimentação tectônica da região proximal da Bacia de Campos, mostrando a localização de altos estruturais e do dos campos petrolíferos de Badejo, Linguado e Pampo (de Castro and Picolini, 2015).

A descoberta de óleo nos depósitos vulcânicos do Campo de Badejo revelou uma coluna de rocha fraturada com óleo de cerca de 150 m (Tigre et al., 1983; Guardado et al., 1990; Ren et al., 2020). Conforme Ren et al. (2020), alguns reservatórios basálticos portadores de óleo apresentam porosidades médias similares a rochas do intervalo pré-sal (10 a 15%) (Ma et al., 2011; De Luca et al., 2015). A porosidade dos reservatórios é formada por vesículas e fraturas de resfriamento, além de fraturas e falhas tectônicas e porosidade vugular desenvolvida a partir de dissolução (Tigre et al., 1983; Mizusaki, 1986). Localmente as fraturas apresentam-se abertas, sem cimentação ou preenchimento parcial, e isto permitiu a acumulação dos hidrocarbonetos (Tigre et al., 1983; Guardado et al., 1990; Ren et al., 2020).

Após um ano de produção, em 1982, o volume acumulado do campo de Badejo foi de 213.291 m^3 (1341.6 Mbbl). Conforme Guardado et al (1990) em nove anos de produção este reservatório contribuiu com 8,6 milhões de barris de óleo equivalente (1.176 x 10^6 t), e esta se concentrou em apenas três poços perfurados nestes depósitos (Ren et al., 2020).

Portanto, esta pesquisa procurou utilizar dados legados da indústria de petróleo para avaliar as características destas rochas basálticas da unidade Cabiúnas, na região de águas rasas, plataforma continental, da Bacia de Campos, com foco em dados que foram levantados na

região dos campos de Badejo, Pampo e Linguado (Fig. 4B). Devido ao aspecto de que foram encontradas acumulações comerciais apenas em basaltos fraturados no campo de Badejo, uma parte da pesquisa se concentrou mais nos aspectos de porosidade e fraturamento desta área, porque estes podem servir como um modelo de definição de áreas mais propícias para o desenvolvimento de projetos de GCS nesta unidade, considerando a abrangência proximal de sua ocorrência.

O projeto foi motivado por algumas vantagens que apresentam valor intrínseco para o tema de GCS no país, e em especial para esta região onde se concentra a produção de óleo e gás no presente. Estas vantagens, ou oportunidades seriam: 1 - Existe um grande volume de rochas basálticas na região onde está concentrada a produção do pré-sal, que possui uma demanda, crescente, de armazenamento de CO2 na ordem de centenas de milhares de toneladas por mês; 2 - Uma parte da unidade Cabiúnas recobre a região de plataforma no setor de água rasa da bacia, o que torna o custo de operações de injeção menor, e torna maior a capacidade de armazenamento devido à menor pressão de poro, 3 - Além de servir ao pré-sal, um projeto de GCS poderia atender a fontes estacionárias industriais no continente, como refinarias e petroquímicas, porque já existe uma rede de gasodutos licenciada e operando que poderia incluir carbodutos; 4 Existe também uma rede de dutos conectando a produção do pré-sal entre campos e com o continente, o que reduz o custo de investimento em dutos que poderiam ser utilizados para transportar CO2 para um hub de GCS na região proximal da Bacia de Campos, 5 – Existe uma grande quantidade de dados geológicos e geofísicos legados que recobrem a Bacia de Campos, e que podem ser utilizados para mapear, caracterizar e avaliar as rochas vulcânicas, sem custos de exploração nesta fase inicial de avaliação de prospectos.

Desta forma, a pesquisa foi conduzida no sentido de produzir um estudo de caso com base em todas as informações disponíveis sobre as rochas vulcânicas na região selecionada, considerando o seguinte objetivo principal:

Analisar os dados legados, públicos, da Formação Cabiúnas na região dos campos de Badejo, Pampo e Linguado, visando avaliar o potencial (em termos de parâmetros de reatividade e capacidade de estocagem, de forma comparativa com os experimentos de campo já realizados) para a realização de projetos de armazenamento definitivo de CO2, a partir da injeção do gás nestas rochas.

E os seguintes Objetivos específicos:

1 - Verificar se os parâmetros que influenciam a reatividade e a mineralização (litologia, pressão, temperatura, pH), no caso das rochas da unidade Cabiúnas são compatíveis com os ranges adequados conforme o conhecimento vigente sobre o tema;

2 - Elaborar um modelo hipotético de reservatório considerando a porção perfurada da unidade Cabiúnas para calcular de forma estimada a capacidade de estocagem nestas rochas;

3 - Verificar por meio da modelagem e interpretação de dados de poços e de dados sísmicos a influência dos sistemas de fraturas no controle da porosidade aparente dos depósitos, objetivando demonstrar como os dados legados podem auxiliar de forma expressiva estudos preliminares para a escolha e avaliação inicial de áreas favoráveis para projetos de GCS nesta região;

1.3 ESTRUTURA DA TESE

O produto desta pesquisa foi estruturado na forma de dois artigos científicos com os quais buscou-se alcançar os objetivos propostos acima. O trabalho incluiu uma abrangente revisão da literatura que incluiu todos os aspectos que envolvem o tema de GCS, em especial para o caso do método de mineralização de carbono em rochas máficas. O Primeiro artigo foi publicado no Journal of Greenhouse Gas Control, em 2023, e tratou dos dois primeiros objetivos específicos listados acima. O segundo artigo encontra-se em fase de finalização para efeito de submissão, e este já contém todos os resultados planejados, e algumas conclusões preliminares.

2 METODOLOGIA

2.1 CONJUNTO DE DADOS E PRÉ-PROCESSAMENTO

Para o desenvolvimento desta pesquisa foi obtido junto a Agência Nacional de Petróleo, Gás Natural e Biocombustíveis (ANP), um conjunto de dados referentes a 180 poços, e 5 cubos sísmicos 3D, processados e migrados. Após a análise de todo o material foram efetivamente utilizados 64 poços e 2 cubos sísmicos 3D de mesma origem (uma versão PSTM, e outra versão de volume PSDM), que abrangem a área dos campos de Pampo, Badejo e Linguado (Fig. 5). Todos os 64 poços selecionados penetraram a Formação Cabiúnas, e foram a base para a modelagem e a interpretação necessárias para os objetivos da pesquisa. Os dados sísmicos foram utilizados para definir aspectos importantes como a espessura e a morfologia do topo da unidade Cabiúnas, assim como extrair atributos e estimar propriedades como a porosidade, utilizando também os logs dos poços.

Os dados sísmicos foram empregados para estimar a espessura da sequência Cabiúnas, as falhas regionais delimitando os campos e a posição da camada de sal sobreposta, de idade Aptiano. Diversas técnicas de processamento foram aplicadas aos volumes sísmicos migrados, como a criação de cubos a partir do plugin *dip steering*, o uso de filtros para melhorar a definição de descontinuidades que auxiliam na interpretação de falhas e fraturas (*Median Filter, Fault Enhancement Filter, Ridge Enhancement Filter*). Um total de 11 atributos sísmicos foram extraídos a partir dos dados sísmicos processados com o plugin dip steering: a) Atributos de coerência, *Coherence* e *Similarity*, que são obtidos a partir da comparação da forma dos reflexões nos traços sísmicos, e evidenciam descontinuidades e mudanças abruptas nas interfaces. b) Atributos de frequência, *Spectral Decomposition* e *Instantaneous Frequency*, que também são utilizados para caracterizar regiões afetadas por falhas e fraturas. c) Atributos de geometria, *Most positive Curvature*, *Most Negative Curvature*, *Maximum Curvature*, que evidenciam a variação da geometria das reflexões ao longo de planos e são importante ferramentas para o estudo e modelagem de planos de fraturas e falhas, d) atributos baseados na orientação espacial dos refletores que podem indicar o mergulho e a orientação de planos associados a falhas e fraturas, *polar dip* e *dip-azimuth*, e, e) dois meta-atributos que se baseiam nos atributos de geometria, neste caso o volume de Most Positive Curvature, para calcular a densidade de fraturas, *fracture density*, e a proximidade de fraturas, *fracture intensity* (Kumar & Mandal, 2018; Ismail et al., 2023; Bailey et. al., 2014; Chopra & Marfurt, 2007; Barnes, 2000; Taner et. al., 1994). O software utilizado nos procedimentos de interpretação sísmica das superfícies, melhoria na qualidade dos dados com a aplicação de filtros e no rastreamento das falhas que compõem a geologia estrutural da área foi o Opendtect da dGB Earth Sciences.

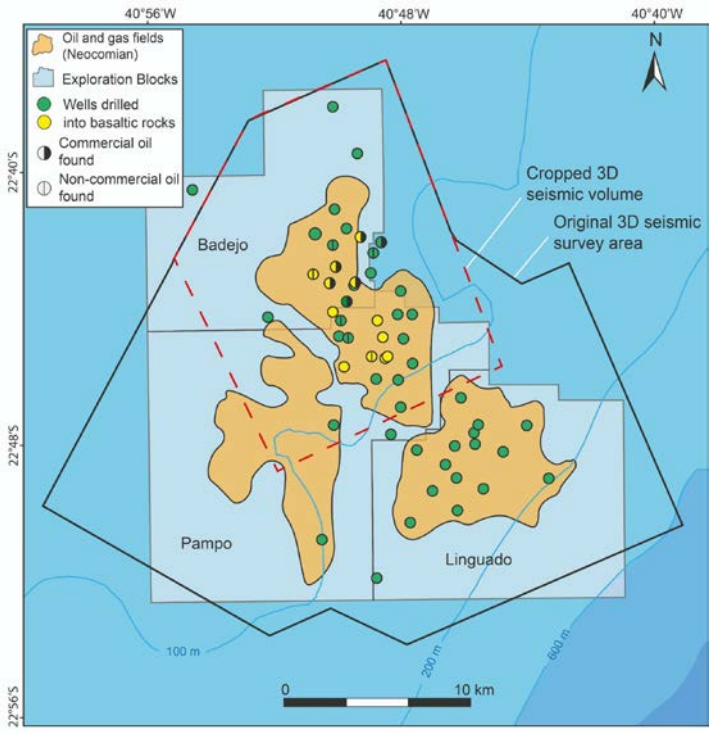

Figura 6 - Mapa da área de estudo com a geometria do cubo sísmico 3D (polígono preto), e dos 64 poços que perfuraram a unidade Cabiúnas e foram utilizados na modelagem e interpretação dos dados. O retângulo de linhas vermelhas tracejadas indica a área do cubo sísmico que foi recortada para o processamento do cubo de porosidade utilizando um plugin de rede neural artificial.

De forma complementar ao estudo do padrão de fraturas encontrado, um dos mapas de atributos de geometria, *most positive curvature*, foi processado no software Arcgis por meio do plugin NetworkGT, para a definição do padrão de intensidade de fraturamento (P21 - quantidade de fraturas por unidade de área), com o objetivo de comparar esta informação com outras propriedades identificadas como a distribuição da porosidade.

2.2 ANÁLISE DE POÇOS E CARACTERÍSTICAS DO RESERVATÓRIO

As informações de logs e de aspectos litofaciológicos dos 64 poços que penetraram a sucessão vulcânica foram utilizados para analisar as propriedades intrínsecas de reservatório e estimar o potencial para armazenamento, considerando outros parâmetros como pressão e temperatura. Os parâmetros da Formação Cabiúnas foram comparados com as condições de reservatório das rochas utilizadas em projetos-piloto de armazenamento de CO_2 (Clark et al., 2020; McGrail et al, 2014; Oelkers et al., 2022).

Embora as rochas basálticas vesiculares exibam elevados valores de porosidade, sua permeabilidade matricial tende a ser reduzida (Lamur et al., 2017; Macente et al., 2019; Tang et al., 2022). Nesse contexto, a permeabilidade é majoritariamente influenciada pela presença

de sistemas de micro e macrofraturas. Contudo, a insuficiência de dados no presente estudo impossibilitou a modelagem da permeabilidade das rochas vulcânicas analisadas. Consequentemente, o foco das investigações concentrou-se na estimativa da porosidade, parâmetro que viabiliza a avaliação do potencial de armazenamento de CO2, que pode ser injetado nas formações diluídas em água ou na forma supercrítica (Schaef, et. al., 2011).

A Formação Cabiúnas apresenta espessura que varia de 450 a 1000 m, e esta é menor sobre o *horst* de Badejo, local onde os poços produtores de óleo e gás estão localizados, e a área selecionada para estimar a capacidade de armazenamento de CO_2 englobou os poços produtores e não-comerciais. A migração de fluidos para rochas no *horst* de Badejo indica que estas apresentavam permeabilidade que permitiu o acúmulo de óleo.

2.3 QUANTIFICAÇÃO DA POROSIDADE

Os reservatórios vulcânicos são considerados sistemas fraturados não convencionais, com relações complexas entre porosidade original (vesículas, juntas de resfriamento) e porosidade diagenética (fraturamento, falhas, dissolução e cimentação) (Tang, 2022; Zahasky et al., 2018; Wang et al., 2018; He et al., 2020). A quantificação da porosidade em sequências vulcânicas é frequentemente obtida por meio da modelagem de dados de perfis de poços, o que permite estimar reservas e características de fluxo (Gupta et al., 2012; Navarro et al., 2020; Tang et al., 2022).

Neste estudo, foi utilizado o perfil de densidade (Rhob) para calcular a porosidade aparente das rochas basálticas da Formação Cabiúnas. Essa abordagem permitiu estimar a porosidade *bulk* dos intervalos vulcânicos que incluem todos os tipos de “vazios” como a porosidade primária (vesículas) e à porosidade secundária diagenética, fraturas e falhas. Este tipo de abordagem para a estimativa de porosidade de rochas basálticas também foi utilizado para estimar as propriedades das rochas vulcânicas do projeto Wallula (McGrail et al., 2014).

O cálculo de porosidade foi realizado através do uso da Equação 1, a partir dos dados de perfis de 14 dos 64 poços usados na pesquisa. O cálculo levou em consideração a densidade geral das rochas basálticas (~2,9 gm/cc), a qual foi utilizada para comparação com a densidade aparente fornecida pelos perfis através da seguinte equação:

$$Porosidade = \frac{Rhoma - Rhob}{Rhoma - Rhof} \qquad \text{Eq.1}$$

Onde *Rhoma* é a densidade da matriz, *Rhob* é a densidade bulk (aparente), e *Rhof* é a densidade do fluido. Para a matriz de referência, considerou-se o basalto inalterado com

porosidade zero. O valor de densidade assumido para a matriz (*Rhoma*) foi 2,98 g/cm³, e o valor de densidade do fluido (*Rhof*) foi 1 g/cm³ (Gupta et al., 2012).

2.4 ESTIMATIVA DA CAPACIDADE DE ARMAZENAMENTO

A estimativa da capacidade de sequestro de CO_2, em termos de volume, foi realizada de acordo com propostas discutidas para outras sequências vulcânicas fraturadas (Koukouzas et al., 2019; Raza et al., 2022). Como existem limitações para a definição do volume de fluidos produzidos em reservatórios depletados, como é o caso das rochas vulcânicas do campo de Badejo, adotou-se um método volumétrico simplificado para estimar a capacidade de armazenamento. Este, é adotado pelo Departamento de Energia dos EUA (DOE), que estudou a remediação de aquíferos utilizados para o armazenamento de rejeitos em rochas basálticas (Raza et al., 2022). Ele permite o uso da espessura média, porosidade média e pressão média da formação rochosa tratada para injeção, que permite definir uma estimativa para a capacidade de armazenamento de CO_2. Esta abordagem também foi utilizada em outros estudos sobre a capacidade de formações vulcânicas (Anthonsen et al., 2014).

Conforme descrito por Koukousas et al. (2019), que investigou o potencial de armazenamento de CO_2 em rochas basálticas na Grécia, foi realizada a estimativa da capacidade em termos de volume de gás CO2 dissolvido em água que poderia ser injetado em um reservatório hipotético modelado a partir dos dados geológicos dos basaltos na região do Campo Badejo:

$$\text{Capacidade de armazenamento} = \sum (V \times \varphi \times \rho \times \varepsilon) \qquad \text{Eq.2}$$

Onde V representa o volume das rochas vulcânicas, φ denota a porosidade média, ρ simboliza a gravidade específica do CO_2 supercrítico saturado, e ε corresponde à taxa de armazenamento de CO_2 para as rochas basálticas. A taxa de armazenamento expressa a fração percentual de CO_2 presente na massa injetada no reservatório (CO_2 dissolvido na água), fundamentada na experiência adquirida no projeto piloto CarbFix, na Islândia (Ramos et al., 2023). A adoção de 5% de CO_2 no fluido de injeção é em parte limitada pela disponibilidade de água que pode ser utilizada para a operação de injeção nesse empreendimento onshore (Gislason et al., 2014). O valor de 5% também foi adotado por Koukouzas et al. (2019) para a

estimativa do sequestro de CO_2 em rochas basálticas na Grécia. Contudo, em nosso estudo, utilizamos duas proporções para a estimativa - 5% e 10% da massa de fluido injetada. A gravidade específica do CO_2 foi determinada com base no trabalho de Span & Wagner (1996), de 716,55 kg/m³ (considerando os valores médios de 30 MPa e 90°C para as condições de contorno relativas às características da Formação Cabiúnas).

2.5 CRIAÇÃO DE UM CUBO DE POROSIDADE COM O PLUGIN DE REDE NEURAL ARTIFICAL (RNA)

Para demonstrar a aplicabilidade de dados legados que cobrem regiões com rochas vulcânicas para a modelagem e interpretação de reservatórios que podem ser utilizados para operações de GCS, foi utilizado um plugin do software OpenDtect que trabalha com um workflow baseado em rede neural artificial para criar um volume com dados de porosidade. Este cubo de porosidade foi processado para os 100m abaixo do topo da Formação Cabiúnas, devido a limitação de penetração dos poços nesta formação. A aplicação deste plugin requer a criação de horizontes (*HorizonCube*) que guiam a ação de propagação da informação a partir do algoritmo da rede neural a partir do treinamento da rede neural que é executado com amostras de impedância acústica obtidos dos perfis de poços com base nos perfis Dt e RHOB (DGB Beheer, 2022). Para a criação deste cubo de porosidade, utilizando o método inverso da rede neural, foram utilizados os logs de 12 poços e um volume menor recortado do cubo sísmico original (Retângulo de linhas vermelhas na Figura 5). O HorizonCube foi definido entre as superfícies interpretadas no cubo sísmico original do topo do embasamento e do topo da Formação Cabiúnas. O topo desta última apresenta profundidades que variam de 2.800 a 3.100 m (Guardado, 1990). A modelagem e interpretação do cubo sísmico também permitiu definir a tectonoestratigrafia que envolve o embasamento, a Formação Cabiúnas e os depósitos sotopostos a esta pertencentes ao Grupo Lagoa Feia. A deposição das unidades da fase rifte foram em grande parte controladas por falhas segmentadas normais, sintéticas e antitéticas, com orientação NNE-SSW, e falhas normais e oblíquas de transferência com orientação ENE-WSW.

O mapeamento das falhas primárias, resultantes do processo de rifteamento, revelou que elas atuaram como condutos migratórios, deslocando o petróleo e o gás das rochas geradoras lacustres para as camadas superiores. Essa trama de falhas, com orientação principal NNE-SSW, apresenta maior densidade na região central da área de estudo, coincidindo com a posição de um alto estrutural interpretado como um domo de lava, Horst de Badejo.

3 RESULTADOS OBTIDOS

O primeiro artigo apresentado objetivou avaliar as características regionais da Formação Cabiúnas, e as propriedades físicas dos reservatórios e compará-las com as condições interpretadas como adequadas para o processo de mineralização. Além disso, foi estimado a capacidade de armazenamento de CO2 dissolvido em água em um reservatório hipotético de 31km^2 com 300 m de espessura na parte superior da sequência, na região do Campo de Badejo. Os resultados indicaram ótimas condições para efeito de reatividade e mineralização e a capacidade de armazenamento estimada ficou entre 16 a 47 milhões de toneladas de CO_2, considerando distribuições de porosidade e misturas de água-CO_2 diferentes.

O segundo artigo procurou mostrar a importância dos dados legados da indústria de energia, que ao longo de várias décadas adquiriu uma vasta quantidade de dados (sísmicos e não-sísmicos) em regiões *onshore* e *offshore* do planeta, e que serão utilizados para o estudo exploratório e de caracterização preliminar de prospectos geológicos para fins de execução de projetos de GCS. No estudo de caso apresentado, com foco no reservatório vulcânico do Campo de Badejo, objetivou-se mostrar que o uso de procedimentos de rotina para a modelagem e interpretação de dados geológicos e geofísicos permitirá avaliar fatores importantes como a profundidade, espessura e morfologia sísmica de estratos vulcânicos, a distribuição de propriedades intrínsecas como a porosidade, e de heterogeneidades fundamentais para estes tipos de reservatórios como os sistemas de falhas e fraturas. O estudo demonstrou que a partir do conhecimento sobre as propriedades de reservatórios aprendidas com o desenvolvimento de Badejo, é possível avaliar áreas influenciadas por zonas de falhas, e que apresentam maior densidade de fraturamento como potenciais zonas de injeção de CO2 para efeito de armazenamento.

4 ARTIGO 1

Versão/Status: Artigo publicado no International Journal of Greenhouse Gas Control (IJGGG) em setembro de 2023 (https://doi.org/10.1016/j.ijggc.2023.103942)

International Journal of Greenhouse Gas Control 128 (2023) 103942

Contents lists available at ScienceDirect

International Journal of Greenhouse Gas Control

journal homepage: www.elsevier.com/locate/ijggc

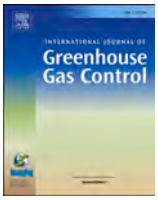

Potential for permanent CO_2 sequestration in depleted volcanic reservoirs in the offshore Campos Basin, Brazil

Germano Mário Silva Ramos *, José Antonio Barbosa, Araly Fabiana Lima de Araújo, Osvaldo José Correia Filho, Carla Joana Santos Barreto, Jefferson Tavares Cruz Oliveira, Roberta Samico de Medeiros

GEOQUANTT Laboratory, Department of Geology, Universidade Federal de Pernambuco, Cidade Universitária, Av. da Arquitetura s/n, Recife 50740-550, Brazil

ARTICLE INFO

Keywords:
Geological sequestration of CO_2
CO_2 mineralization mechanisms
Offshore CCS
Pre-salt CO_2 content
Reservoir modeling

ABSTRACT

The pre-salt oil and gas production in Brazil faces a significant challenge due to the high CO_2 content in these reservoirs. Approximately 600,000 t of CO_2 are reinjected monthly in the reservoirs, but the increased production of CO_2 will demand alternatives for sequestration. Experiments and pilot projects have demonstrated the viability of CO_2 sequestration through the mineralization method in basaltic rocks. Here, we present a study aimed at demonstrating the feasibility of using the volcanic rocks of the Cabiúnas Formation, located at the base of the pre-salt section in shallow waters of the Campos Basin, for CCS projects. We used legacy data to determine the regional characteristics and porosity distribution of the volcanic sequence to assess the feasibility of geological sequestration in this region. Our estimates demonstrated that the Cabiúnas flood basalts have a good to excellent storage capacity. The modeling of a 31km^2 hypothetical reservoir with a thickness of 300 m in the upper part of the sequence above the Badejo Field revealed a storage estimate of 16–47 Mt. The technical aspects discussed in this study provide valuable insights that can help with the development of future CCS projects in the volcanic rocks of this petroleum province.

1. Introduction

According to the IPCC Special Report for policymakers (2018), the global mean surface temperature between 2006 and 2015 was approximately 0.78 °C greater than the average temperature between 1850 and 1900. The report also stated that both past and present anthropogenic emissions are driving global warming at a rate of approximately 0.2 °C per decade. This report has prompted a series of discussions between governments and global oil and gas industry aimed at adopting several initiatives and policies that focus on the reduction of anthropogenic CO_2 emissions. In particular, the industry must address the destination of the hundreds of gigatons of CO_2 emissions that have entered the atmosphere at an increasing pace in the past few decades (Martin-Roberts et al., 2021). The reduction of emissions can be achieved through the reduction of fossil fuel consumption (Bataille et al., 2020; Fuss et al., 2020) and the capture and sequestration (CCS) of the significant amounts of CO_2 produced by industrial processes; this includes the capture and utilization of CO_2 (CCUS) in gas injection projects in oil reservoirs, which is used to increase the recovery factor (Moghanloo et al., 2017; Sampaio et al., 2020). The injection of CO_2 in geological media is the most important method of artificial sequestration (Leung et al., 2014), and involves the injection of CO_2 diluted in water or in a supercritical state into saline aquifers, artificial salt caverns, coal deposits, or volcanic mafic rocks (Leung et al., 2014; Ajayi et al., 2019; Kelemen et al., 2019, 2020; Snæbjörnsdóttir et al., 2020; Hong et al., 2022).

Ringrose and Meckel (2019) state that, to cope with the global demand for the IPCC 2 °C scenario, CCS should support approximately 13% of total cumulative emissions reductions (~120 gigatons) through 2050. For nations with large-scale emissions, offshore geologic sequestration would be the most attractive and effective strategy due to its reservoir quality, safety, and cost-effectiveness (Ringrose and Meckel, 2019). However, to meet the modest demands laid out by world governments, it would be necessary to construct between 10,000 to 14,000 CO_2 injection wells globally by 2050. This suggests that Brazil, an emerging player in oil and gas with a large CO_2 footprint, must look at all alternatives available for carbon sequestration (conventional reservoirs, artificial salt caves, CCUS reinjection, and subsurface mineralization). Previous works have already highlighted the potential for CO_2

* Corresponding author.
E-mail address: germano.mario@ufpe.br (G.M. Silva Ramos).

https://doi.org/10.1016/j.ijggc.2023.103942
Received 19 January 2023; Received in revised form 27 May 2023; Accepted 18 July 2023
Available online 25 July 2023

sequestration in the oil fields of the Campos Basin, specifically with respect to the siliciclastic reservoirs, which have sequestration capacities of approximately 950 Mt (Rockett et al., 2013).

Some critical aspects of CCS projects include the costs involved in capture and injection operations, transportation, the geology of the site project, and the safety issues associated with the eventual leakage of CO_2 for long periods after sequestration (Anderson, 2017; Mechleri et al., 2017; Alcalde et al., 2018; Schmelz et al., 2020; Gholami et al., 2021). The associated costs of CCS projects include the intrinsic technologies and capacity necessary to capture the CO_2 in the different industrial processes responsible for producing most of the gasses (e.g., oil refining, biofuel production, and the cement industries), transportation options, the localization of viable storage sites, and the availability of previous infrastructure, such as pipelines or injection wells (Rubin et al., 2013, 2015; Grusson et al., 2015; Cao et al., 2020; Smith et al., 2021). Safety issues include the eventual leakage of CO_2, the displacement of brine through shallow aquifers, and increased seismicity (Damen et al., 2006; Amonette et al., 2014; Matter et al., 2014; Vilarrasa and Carrera, 2015; Fawad and Mondol, 2022).

In this context, Brazilian authorities expect CO_2 emissions generated by the oil and gas production in the pre-salt province, comprised of the Santos and Campos basins in southeastern Brazil (Fig. 1), to increase significantly in the coming decades to tens of millions of metric tons per year (Godoi et al., 2021) due to the ramp-up in production of these

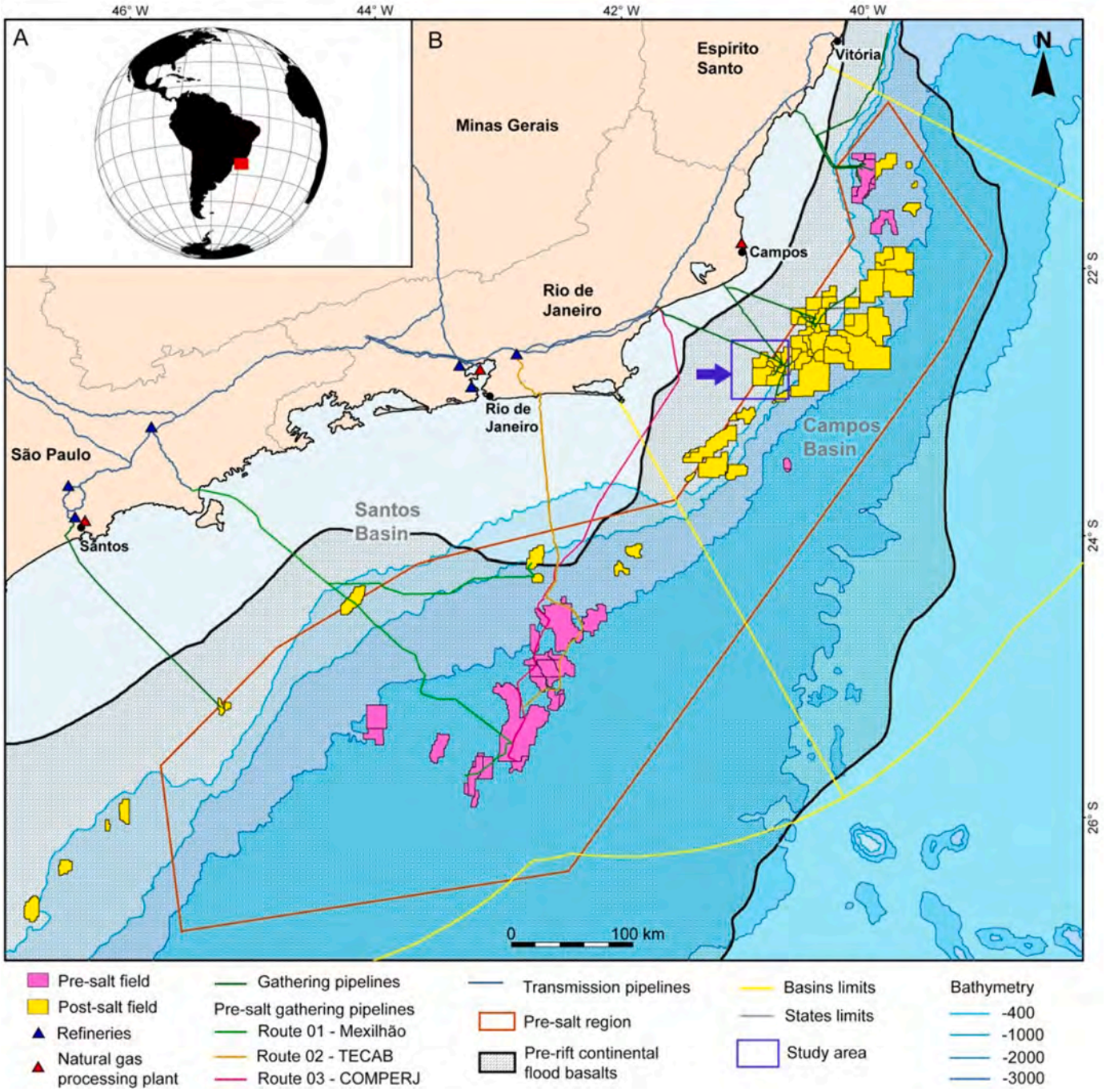

Fig. 1. (A) Location of the pre-salt petroleum province in southeastern Brazil (red polygon). (B) distribution of production oil and gas fields in the Santos and Campos Basin (ANP, 2022). The primary infrastructure, including pipelines, refineries, and natural gas processing plants, are presented (EPE, 2020). The blue arrow indicates the location of the study area. The gray-hatched zone (black polygon) delineates the area covered by continental flood basalts (Stica et al., 2014).

reserves (Fig. 2A and 2B), which possess exceptionally high contents of CO_2 (Fig. 1) (Beltrão et al., 2009; Pizarro e Branco, 2012; Viglio et al., 2017; Lima et al., 2020; Sampaio et al., 2020). In 2021 Brazil produced an average of 2.9 million b/d and 136 million m^3/d of oil and gas, respectively, and it is expected that production will reach 5.2 million b/d of oil and 1.6 million boe/d of natural gas in 2030 (National Company for Energy Studies [EPE], 2021). Indeed, the Campos Basin possesses an average CO_2 concentration of 0.5%, with values of up to 20% near its boundary with the Santos Basin (Fig. 2C) (d'Almeida et al., 2018). Most wells drilled into the pre-salt interval of the Santos Basin report CO_2 concentrations of 5%, with some wells reporting concentrations of up to 50–80% (Fig. 2C) (Santos Neto et al., 2012; Matias et al., 2015; Cornelius, 2021; de Freitas et al., 2022). The higher concentrations of CO_2 in Santos Basin are located in its southeastern,

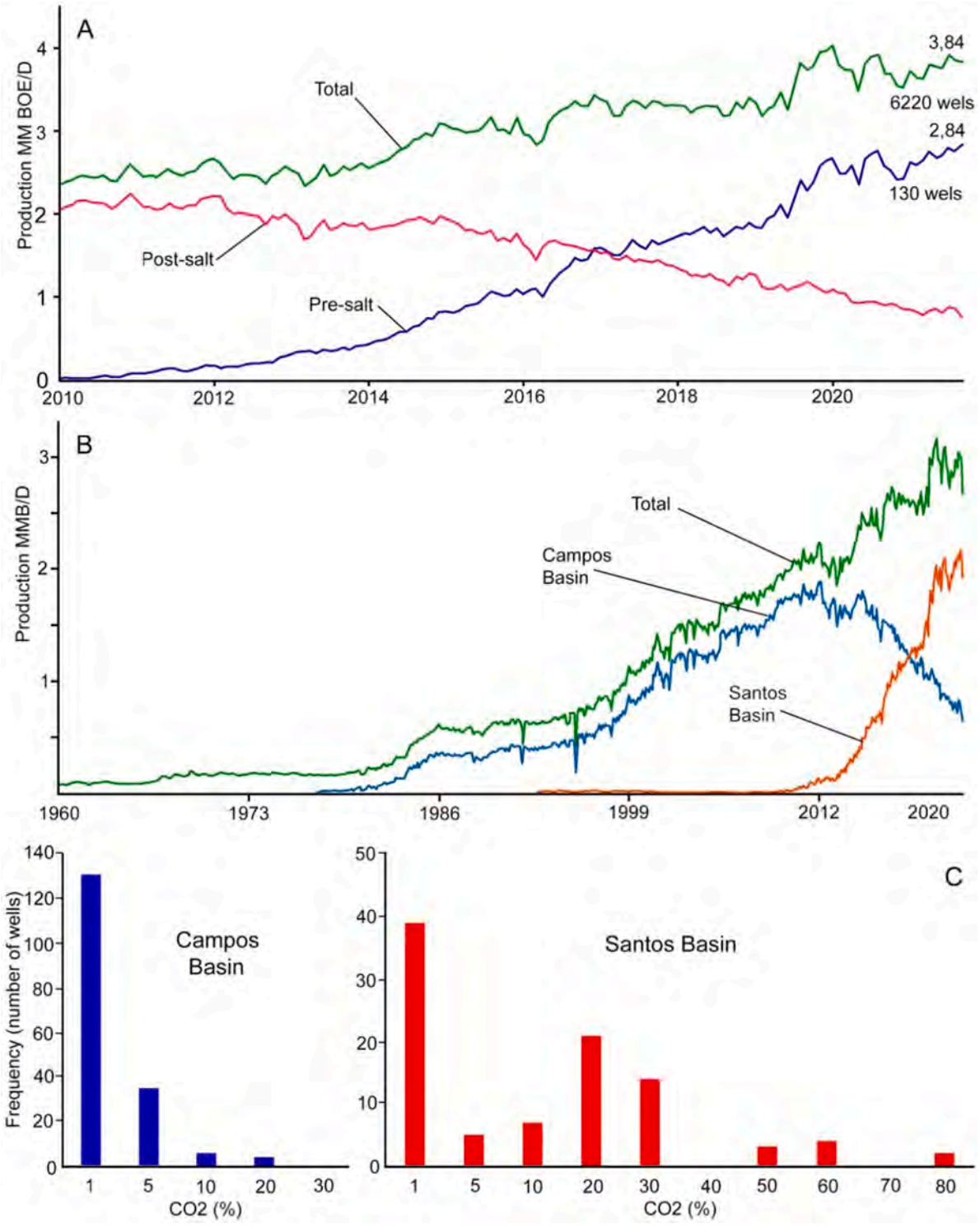

Fig. 2. (A) The contribution of post-salt and pre-salt fields to total Brazil's hydrocarbon production in the last decade (MMO BOE/D - million barrels of oil equivalent per day). (B) The historical contribution of the Santos and Campos basins to Brazil's hydrocarbon production (MMB/D Million barrels per day). It highlights the rapid decline of the Campos fields as well as the increase in Santos Basin production due to the development of operations in the pre-salt interval (adapted from ANP, 2021). (C) A histogram depicting the%-CO_2 content in wells drilled in the pre-salt reservoirs (adapted from Almeida et al., 2018).

ultra-deepwater regions. The CO_2 present in the natural gas produced from the Lula field, the first field to extract natural gas from the pre-salt interval, varies between 8 and 25%, while the natural gas produced from the Iracema accumulation (part of the Lula field; Fig. 2C) contains approximately 1% CO_2 (EPE, 2019, 2020). The origin of CO_2 is likely associated with mantle contamination (Gamboa et al., 2019). Recent data showed that the total CO_2 production from the Brazilian pre-salt intervals reached 630,000 t in July 2021, equivalent to 7 Mt of CO_2 per year (SandP Global, 2021).

Fig. 2A and B show the historical contribution of the Santos and Campos basins to Brazilian hydrocarbon production. The impact of production in the 1980s and the 1990s came from the post-salt reservoirs of the Campos Basin (mainly Cenozoic turbidites) (Guardado et al., 1990; Bruhn et al., 2003), while a majority of the increased production in the last decade came from pre-salt fields found in the Santos Basin (Fig. 2) (National Agency for Petroleum, Natural Gas, and Biofuels [ANP], 2019; 2021). The investment and development of the pre-salt interval in the deep waters of the Campos and Santos Basins continue to evolve rapidly, and current predictions suggest a production of 4 MMboe/d around 2030 (EPE, 2020). The number of wells operating in the post-salt compared to the pre-salt interval (Fig. 2A), highlight the greater productivity of the pre-salt reservoirs. However, the CO_2 content in the hydrocarbon reserves found in pre-salt wells is also considerably higher (Fig. 2C) (ANP, 2021).

One of the CCUS operations in this area is the CO_2 water-alternating-gas (WAG) injection, in which most of the CO_2 produced in the pre-salt fields is reinjected into the reservoirs to increase their recovery factor (IOR/EOR) (Pizarro and Branco, 2012; Lima et al., 2020; Sampaio et al., 2020; Godoi et al., 2021; Pereira et al., 2021). Most of the natural gas that is not transported to the continent and not used in offshore installations is also reinjected into the reservoirs (EPE 2020). However, it is expected that pre-salt production will generate between 200 and 300 million tons of CO_2 in the next three decades, and the capacity of reservoirs to receive the CO_2 may be reduced due to the growing risk of formation damage (e.g., negative influences on the temperature, permeability, and geomechanics of the rocks) (Drexler et al., 2019; Godoi et al., 2021) as well as damage to the equipment caused by CO_2-related problems (e.g., accelerated failures, increasing manutention costs) (Beltrão et al., 2009). Another technology that has been proposed to address the CO_2 sequestration is the utilization of artificial salt caverns in the deep-water evaporites deposits that cover the reservoirs in the distal domains of the Santos and Campos basin (Fig. 1) (Costa et al., 2019; Goulart et al., 2020).

The safety and the effectiveness of keeping CO_2 sequestered in geological media during and after the injection project are the primary issues that affect the cost of the operation (Friedmann et al., 2006; Stenhouse et al., 2009; Aydin et al., 2010; Ajayi et al., 2019; Cao et al., 2020). In some cases, the monitoring required could represent up to >50% of the project costs (Takagi et al., 2013). Injection in saline aquifers, depleted oil and gas reservoirs, and salt caves raise the possibility of long-term leakage due to the mobility of CO_2, seal damage, and well failures (Bérest and Brouard, 2003; Damen et al., 2006; Vilarrasa, 2014; Pawar et al., 2015; Bai et al., 2016; Warren, 2017; Cao et al., 2020; Dinescu et al., 2021; Gholami et al., 2021). Furthermore, the injection of large amounts of CO_2 in offshore areas presents even more challenges due to the logistics involved (Stenhouse et al., 2009; Rubin et al., 2015) as well as the intrinsic characteristics of the reservoir (Takagi et al., 2013; Anderson, 2017; Schmelz et al., 2020). A better understanding of the costs and risks associated with different CCS methods, especially with regard to the various geological uncertainties, is required (Aydin et al., 2010; Vilarrasa and Carrera, 2015; Aminu et al., 2017; Alcalde et al., 2018; Larkin et al., 2019; Cao et al., 2020; Schmelz et al., 2020). The sequestration of CO_2 from pre-salt production will likely demand multiple simultaneous CCS methods focused on offshore solutions due to the remote location of the production infrastructure (Figs. 1 and 2).

The sequestration of CO_2 via mineral carbonation is an emerging technology based on the injection of supercritical or diluted CO_2 into basaltic rocks (Gislason et al., 2014; Matter et al., 2014; Gunnarsson et al., 2018). This method aims to trap free CO_2 molecules within solid composites; specifically, carbonate minerals ($CaCO_3$, $MgCO_3$, $FeCO_3$) (Kelemen et al., 2019; Pogge et al., 2019). The CO_2 injection produces carbonic acid, which reacts with mafic rock, and induces the liberation of cations (e.g., Ca^{2+}, Mg^{2+}, and Fe^{2+}) from the dissolution of Ca- and Mg-bearing silicate and alumino-silicate minerals like olivine, plagioclase, and diopside (Gislason et al., 2014; Kelemen et al., 2020; Snæbjörnsdóttir et al., 2020; Ali et al., 2022; Raza et al., 2022). The reactions are mediated by the partial CO_2 pressure, temperature, and pH of the solution.

The criteria used to identify appropriate sites for mineralization-based CCS projects in volcanic mafic rocks include alkaline water (pH $>$ 7), temperatures ranging from 50 to 250 °C, and pressure ranging from 0.6 to 50 MPa (Kelemen et al., 2020; Raza et al., 2022); these represent the key parameters of the chemical reactions. The influence of other factors, such as injectivity and specific mineral wettability in carbonate mineral formations, is still not completely understood. However, the success of CO_2 sequestration through injection in mafic rocks represents the potential to remove billions of tons of CO_2 per year (Gislason et al., 2014; Snæbjörnsdóttir et al., 2020; Tutolo et al., 2021; Raza et al., 2022).

This study focuses on the Neocomian flood basalt sequence of the Cabiúnas Formation (Sin-rift phase) that covers the Precambrian basement of the Campos Basin, southeastern Brazil (Mizusaki et al., 1988; Guardado et al., 1990; Oreiro, 2006). During the 1980s and the 1990s, the oil-bearing fractured basalts of the Cabiúnas Formation found in the Badejo Field were developed as unconventional reservoirs (Bruhn et al., 2003; Lobo et al., 2007) (Fig. 2). Based on the availability of legacy data (2D and 3D seismic surveys, potential field data, and well data), physical infrastructure, and the proximity of the pre-salt fields, we report an evaluation of the potential of establishing large offshore CO_2 sequestration hubs in these basaltic deposits (Fig. 2). This article aims to investigate the feasibility of CO_2 sequestration in the Cabiúnas basaltic rocks based on their theoretical suitability concerning the mineralization trapping process (Raza et al., 2022) and their capacity in terms of storage volume. We have considered the method based on the injection of water-charged (dissolved) CO_2 (Snæbjörnsdóttir et al., 2020) to estimate the storage volume, however the injection of supercritical CO_2 could also be used due to the characteristics of the sedimentary succession.

Injection of water-dissolved (CarbFix pilot) and supercritical (Wallula pilot) CO_2 was tested for the geological sequestration of CO_2 in basaltic rocks (McGrail et al., 2014; Snæbjörnsdóttir et al., 2018). The feasibility of the reactive effects and mineral formation with the CO_2 trapping has been proved for both alternatives (Macgrail et al., 2009, Kelemen et al., 2019; Raza et al., 2020; Tutolo et al., 2021). Due to the buoyancy of the free phase plume formed by the injection of supercritical CO_2, the project needs to consider a seal cap rock, which is not the case for the water-dissolved injection method (Snæbjörnsdóttir et al., 2020; Tutolo et al., 2021). In the case presented, seal rocks occur over the basaltic succession, which also allow the injection of supercritical CO_2 as another option in terms of method. The main advantage of the supercritical injection is the larger amount of gas that could be injected. Tutolo et al. (2021) pointed out some advantages of injecting supercritical CO_2 in basaltic rocks, markedly the per-well capacity of injection, which will imply a lesser number of wells needed to accomplish large sequestration volumes. However, as discussed by Snæbjörnsdóttir et al. (2020), available water is not a limitation in offshore projects. The energy-consuming process of the water-gas mixture before injection could be less costly than the need to execute WAG (water-gas alternating injection) operations which could be needed to increase the supercritical injection, as discussed by Tutolo et al. (2021). The most crucial consideration for adopting the water-dissolved method is that the free-phase injection will increase the costs of monitoring. The lack of

reliable data about the results of long-term injection of large amounts of CO_2 in both forms will lead to the initial adoption of more conservative options initially, and possibly the water-dissolved form could be tested with fewer risks.

There are two main advantages to utilizing these basaltic rocks: 1) the proximity between the CO_2 emission sources (the pre-salt production facilities) and the basaltic reservoirs (Figs. 1 and 3) and 2) the reliable trapping mechanism, ensured by the mineralization process, and the overlying seal rocks (shales, carbonates, and evaporites from the rift and transitional phases), which will also allow the injection of supercritical

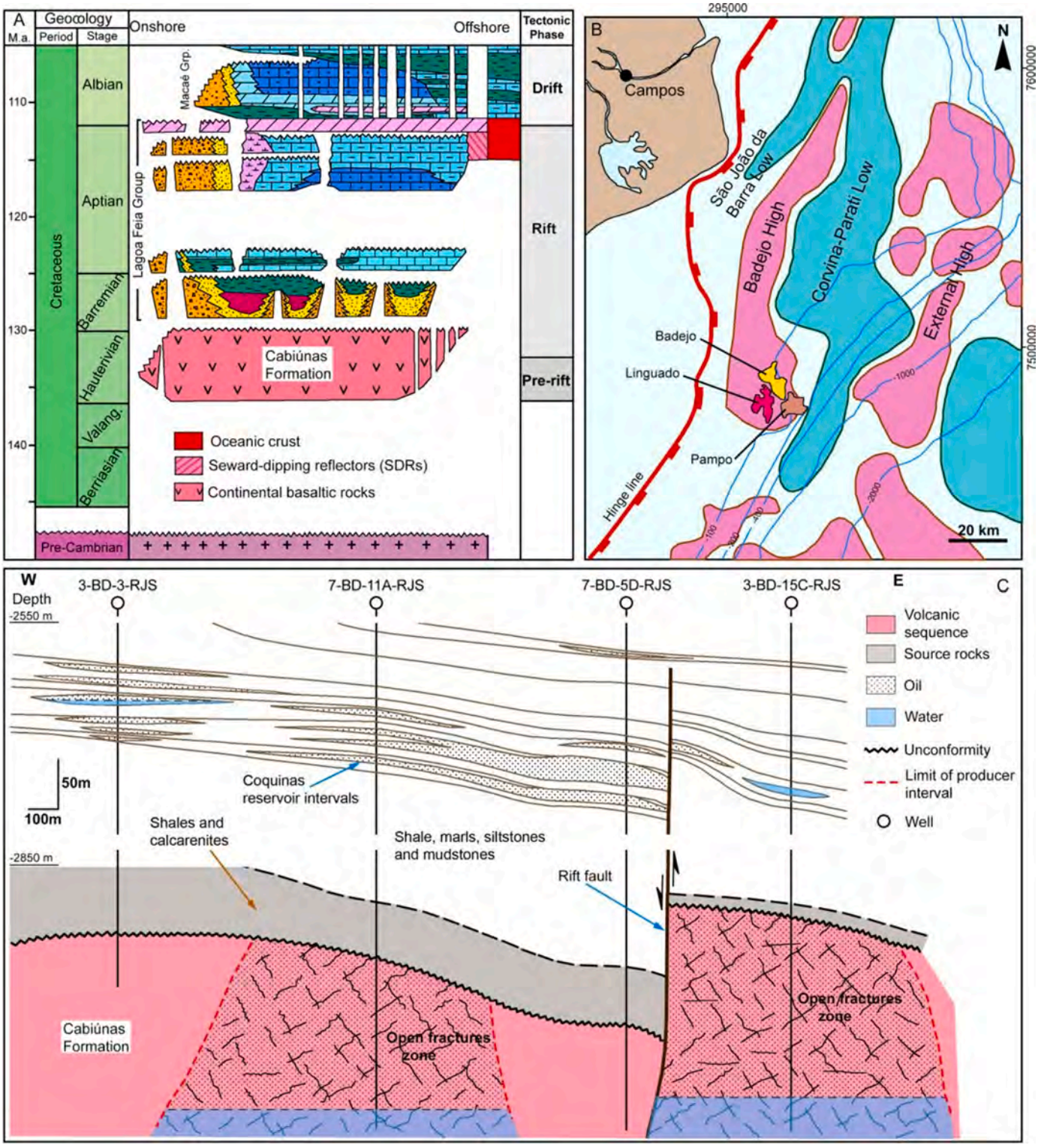

Fig. 3. (A) A simplified stratigraphic column of the Campos Basin that shows the Hauterivian-Albian succession (adapted from Stica et al., 2014). (B) The regional tectonic compartmentalization of the Campos Basin, highlighting regional highs and the location of the Badejo-Linguado-Pampo fields where oil was produced from the volcanic sequence of Cabiúnas Formation (de Castro and Picolini, 2016). (C) A schematic geological section across Badejo Field showing how the hydrocarbon reservoirs were accumulated in the carbonate rocks (Lagoa Feia Grp.) and in the underlying fractured basaltic rocks (modified from Guardado et al., 1990).

CO_2.

Our analysis showed that this alternative is technically feasible and that the basaltic rocks could store vast quantities of CO_2, and helps the industry to cope with CO_2 issues in the coming decades.

2. Geological setting

The petroleum system of Campos Basin is comprised of good quality source rocks (shales) from the rift phase Lagoa Feia Group (freshwater lacustrine to brackish lacustrine facies from the Coqueiros and Atafona formations), which represent the primary oil-generating intervals (Guardado et al., 2000; Bruhn et al., 2003; de Lima et al., 2022) (Fig. 3). Reservoirs are represented by fractured basalts (Neocomian), Coquinas (Barremian), Early to Middle Albian calcarenites and calcirudites (Fig. 3A), and Late Albian to Early Miocene turbidites (Guardado et al., 1990; Rosa and Vicentelli, 2017). The study area also includes the geological trends formed by the Linguado, Badejo, and Pampo fields, located in the northwestern part of the Campos Basin (Figs. 1 and 3), between 100 and 300 m water depth (Fig. 3B). Wells drilled to explore the carbonate and siliciclastic formations below the salt layer in this region also found oil in the fractured basalts deposited over the Precambrian basement (Guardado et al., 1990, 2000; Mohriak et al., 1990; Bruhn et al., 2003; Ren et al., 2020). The rift phase of the Campos Basin also involved the development of normal (synthetic and antithetic) and transcurrent faults, which controlled the formation of grabens and horsts along the proximal and distal regions of the basin (Guardado et al., 1990; Milani and Thomaz Filho, 2000; de Castro and Picolini, 2016). Siliciclastic and shallow carbonates formations were deposited during the transitional phase, followed by Aptian evaporites, while the drift phase included the deposition of carbonates and siliciclastics from the Albian to the Quaternary (Bruhn et al., 2003; de Lima et al., 2022)

The evaporite interval in the continental platform in this region (Fig. 3B) is thinner than in the distal parts of the Campos and Santos basins. Here, the sedimentary deposition and the petroleum system were primarily controlled by a series of elongated paleo-highs and lows that trend mainly NNE–SSW (Fig. 3). The main accumulations of oil and gas found in pre-salt deposits in the Badejo, Linguado, and Pampo fields (siliciclastics and carbonates) were formed through the fault-controlled migration of hydrocarbons from the source rocks of the rift-phase (Fig. 3C). Reservoirs formed over horsts in the Badejo High (Fig. 3B), including the oil-bearing Hauterivian flood basalts of the Cabiúnas Formation in the Badejo Field (de Castro, 2006; de Castro and Picolini, 2016; Mizuno et al., 2018). The Cabiúnas Formation is comprised of interbedded lava flows, sandstones, breccias, and pyroclastic flow units (Mizusaki et al., 1988). The migration and accumulation of oil to the Cabiúnas unit occurred due to the lateral contact between source rocks and basaltic rocks and were primarily controlled by rift faults (Fig. 3C).

2.1. Reservoir characteristics

The igneous rocks of the Cabiúnas Formation are comprised of a poorly differentiated transitional to sub-alkaline sequence that is continental in origin (Mizusaki, 1986; Mizusaki et al., 1988; Marins et al., 2022). Mizusaki et al. (1988) suggested that the sequence also includes successive cycles of interbedded volcaniclastic and sedimentary rocks (sandstones containing clasts of volcanic rocks) (Fig. 4). Each of these cycles was subdivided into 1) lava flows, which exhibit different textures (vitreous basalts, microcrystalline basalts, and vesicular basalts) due to the effect of cooling and their interaction with surface fluids; 2) pyroclastic (hydrovolcanic) breccias; 3) tuffs, commonly altered due to subaerial exposure; and 4) sandstones containing volcanic clasts (Fig. 4B) (Guardado et al., 1990). They argued that this cycle is incomplete in most wells, with the tuffs and sedimentary rocks missing (Fig. 4) (Mizusaki et al., 1988; Guardado et al., 1990; Marins et al., 2022). The individual basalt flows cover large areas, tend to have planar morphologies, and have thicknesses between 3 and 4 m that eventually reach up to 10 m (Mizusaki et al., 1988). Other than the basalts, some diabase and rocks with trachytic textures were found, but their relative volume is very small (Mizusaki, 1986; Mizusaki et al., 1988). Marins et al. (2022) have also described the peperites and the complex interaction between volcanic and sedimentary deposits in this region.

The depth of the Cabiúnas Formation ranges from 2800–3,000 m, but no wells have reached the continental basement below this unit, and its thickness remains unknown. Mizusaki et al. (1988) also identified a regional system that involved subaerial and subaqueous volcanism that described the distribution of volcanic, pyroclastic, and volcaniclastic rocks. Marins et al. (2022) also recognized the continental and subaqueous influences on deposition based on microfossils. The distribution of depositional environments proposed by Mizusaki et al. (1988) is shown in Fig. 5A and is represented by zones named A to E going from north to south, which cover the three fields studied (Fig. 5). Zone A is characterized by successions formed by basalts/auto-breccias,

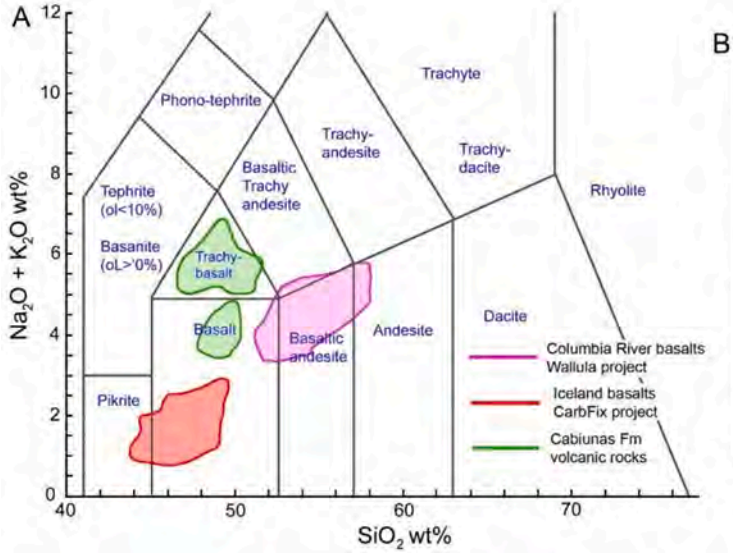

B

Lithofacies	Porosity type: Macro-fracture	Micro-fracture	Vesicle	Micro-porosity	Reservoir quality
Sandstone				—	Poor
Pyroclastic				—	Poor
Breccia	—				Fair
Vesicular basalt		—	—		Good
Microcrystalline basalt	—				Good
Vitreous basalt	—				Fair

Fig. 4. (A) Classification of the basaltic rocks of the Cabiúnas Formation as well as the rocks used in the injection projects based on the relationship between their silica and alkali contents (TAS Diagram) (Mizusaki, 1986; Mizusaki et al., 1988; Alfredsson et al., 2013; Fox, 2022). (B) General correlation between the lithofacies in a cycle formed by volcanic, pyroclastic, and sedimentary rocks of the Cabiúnas Formation as well as their reservoir quality (Modified from Guardado et al., 1990).

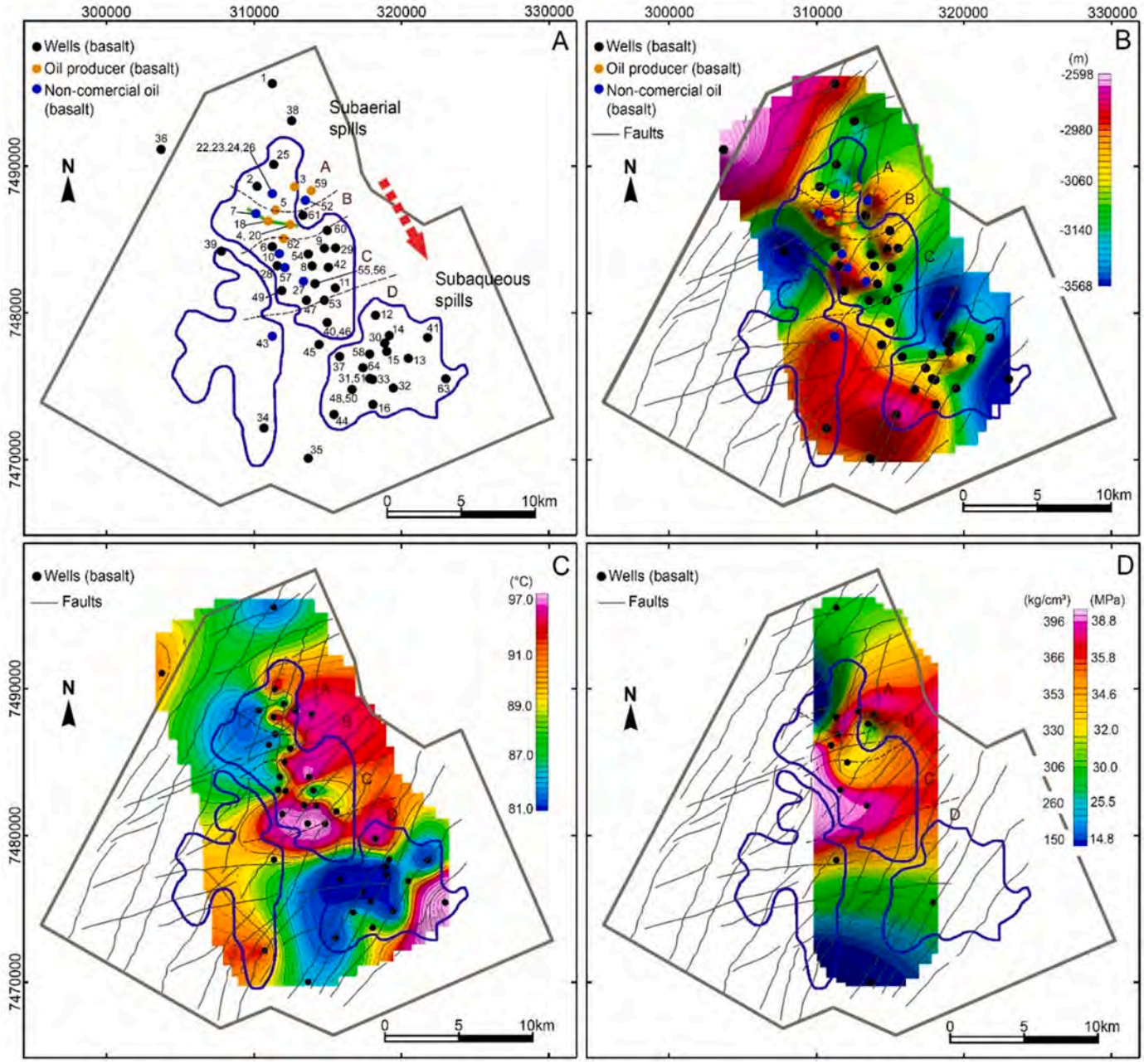

Fig. 5. (A) Outline of the 3D seismic data (PSTM and PSDM volumes) used to study the regional characteristics of the volcanic sequence (Cabiúnas Formation). The locations of the 64 wells used in this study are indicated by black dots. The red arrow highlights the change in the depositional trend (dashed lines) from subaerial (zone A) to subaqueous conditions (zones C and D) that prevailed during the formation of the basaltic and volcaniclastic rocks (Mizusaki, 1986; Mizusaki et al., 1988). (B) A contour map describing the depth to the top of the Cabiúnas formation based on well data (gray thin lines represent regional faults mapped on the seismic data). (C) A map of the interpolated temperature values within the Cabiúnas deposits based on data acquired from the wells. D) A map of the interpolated formation pressure values obtained from tests conducted on the wells. The extent of the Badejo, Linguado, and Pampo fields are shown using blue polygons.

basalts/tuffs, and subaerial conditions (evidenced by oxidation and pedogenetic features). Zone B is characterized by successions formed by basalts/sandstones and basalt/volcaniclastics/hydrovolcanic breccias. Sediments in this zone indicate a coastal environment, with hydrovolcanic breccias also indicating subaqueous volcanism. Zone C is characterized by successions composed of basalts/auto-breccias and basalt/volcaniclastics/hydrovolcanic breccias, with evidence that they were formed in a subaqueous environment. Zone D is also characterized by successions of basalts/tuffs, and there is evidence to suggest that the tuffs formed in this zone were formed subaqueously in a lacustrine environment (Mizusaki, 1986; Mizusaki et al., 1988; Guardado et al., 1990) (Fig. 5A). According to Mizusaki et al. (1988), the lava flows in the Linguado Field are gray, rarely possess vesicles, and have fewer fractures compared to basalts from the Badejo Field (Fig. 5).

The basalts of the Cabiúnas Formation are aphanitic and can be classified into three groups: 1) hyaline, composed of plagioclase, clinopyroxene, and magnetite; 2) hemicrystalline, composed of plagioclase, clinopyroxene, olivine, and magnetite; and 3) holocrystalline, composed of plagioclase, clinopyroxene, olivine, and magnetite. Volcanic glass is abundant, frequent and rare in hyaline, hemycristalline, and holocrystalline basalts, respectively. Vesicles are abundant in the hyaline basalts and rare in the other textures. The alteration of these basalts resulted in the formation of smectite and chlorite which are found filling the vesicles and fractures (Mizusaki, 1986; Mizusaki et al.,

1988). Igneous rocks of the Cabiúnas Formation are represented by potassic and sodic trachybasalts, basalts, secondary mugearites, and continental tephrites (Fig. 4A). Of the samples analyzed by Mizusaki (1986), 66% were supersaturated, 24% were lightly sub-saturated with olivine, 5% were sub-saturated with olivine and nepheline, and 5% were sub-saturated with nepheline (Fig. 4A). Fig. 4A shows the comparison between the Cabiúnas basalts properties and other basaltic formations used for CO_2 mineralization projects.

Mizusaki et al. (1988) also suggested that the sedimentary and volcaniclastic rocks did not represent any reservoir potential; this was corroborated by an analysis performed by Marins et al. (2022). The oil production was related to the wells drilled in the Badejo Field (oil; 31° API), and few oil discoveries were made in the basaltic sequence of Linguado Field (oil; 28° API), but they were non-commercial.

According to Bruhn et al. (2003), oil was discovered in the Badejo Field in 1975, and production started in 1981. The estimated volume of original oil in place (OOIP) in the fractured basalts was 45 million barrels. At the end of the 1980s, the field was producing approximately 6800 bbl of oil/day with a cumulative production of 13 million bbl. Two-thirds of the total production came from three wells that drained the fractured basalts of the Badejo Field.

The reservoir zones were represented by intensely fractured rocks with sub-vertical fractures that cut several basaltic flows. These fractures were attributed to a late tectonic event (Mizusaki, 1986). Data obtained from the testing of core samples showed that the matrix porosity of the igneous rocks of the Cabiúnas Formation was dominated by microporosity (<1 μm) and varied between 0.69–7.5%. The higher porosity values were commonly associated with altered rocks. Matrix permeability varied from 0.7 to 1.0 mD (Mizusaki, 1986). Tests performed in core samples by Marins et al. (2022) were consistent with these findings, reporting matrix permeabilities of 0.1–1.0 mD in the volcanic rocks.

Guardado et al. (1990) reported that the crude oil in the Badejo Field primarily occurred in fractures, microfractures, and vesicles. Vertical fractures were found to be abundant in the top and base of each volcanic-sedimentary cycle, and horizontal fractures were common in the central sections of the cycles, which increases the permeability of the rocks. The porosity and permeability of the breccia zones were similarly influenced by fracturing and were increased by acidic injections that dissolved calcite cement. According to Mizusaki (1986), vesicles are common in the upper sections of the lava flows and are filled with calcite, zeolites, and authigenic clay minerals. In core samples taken from the drilled wells, the aperture of the microfractures varied from 10 to 50 μm, and the aperture of vertical to sub-vertical fractures ranged from a few millimeters up to 2 cm. Some fractures were found filled or partially filled with calcite, chlorite, zeolites, iron oxides, and pyrite. Authigenic minerals, listed according to their abundance, are calcite, chlorite, smectite, micro-crystalline quartz, chalcedony, zeolites, and serpentines (Mizusaki, 1986).

Recently, Marins et al. (2022) studied the volcanic and volcaniclastic rocks sampled from the Badejo and Linguado fields, focusing on the characterization of the lithofacies and their reservoir properties. These authors suggested that these volcanic, volcaniclastic, and sedimentary rocks were primarily formed subaerially and divided their occurrence into four units comprised of interbedded volcanic and sedimentary rocks. Units 1 and 3 were dominated by pahoehoe lava flows, while units 2 and 4 were dominated by rubbly pahoehoe lava flows. Subaerial weathering controlled the porosity and permeability of the rocks. Intense alteration led to the infilling of vesicles and fractures with clay minerals as well as the formation of non-reservoir zones. Marins et al. (2022) also reported the secondary filling of fractures and vesicles with quartz, chlorite, magnesian smectite, chlorite/smectite, and calcite, in that order. These authors also suggested that the top of rubbly lava flows exhibited greater porosities. In addition to the occurrence of cooling joints, the authors also recognized the occurrence of tectonic fractures and fault damage zones, as previously reported by Mizusaki (1986) and Mizusaki et al. (1988). Their analysis of the permeability and porosity of volcanic and sedimentary rocks corroborated the information reported by Mizusaki et al. (1988). Most of the rocks sampled possessed a matrix permeability of <0.1 mD, and some samples of the rubbly lava and the vesicular basalts exhibited permeabilities between 0.1–1.0 mD, with a few rubbly samples reaching up to 10 mD. The porosity of most rocks ranged from 1 to 15%, while the rubbly lavas, peperites, and vesicular basalts exhibited values between 10 and 15% (Marins et al., 2022).

3. Materials and methods

This study included data from a total of 180 wells as well as a 3D seismic survey that covers the Badejo, Pampo, and Linguado oil fields (Fig. 5A). The datasets were provided by the National Agency for Petroleum, Natural Gas, and Biofuels (ANP). Two versions of the 3D seismic volume were analyzed: a time migrated (PSTM; 8 s TWT depth) and a depth migrated (PSDM) volume (Fig. 5A). The seismic data were used to estimate the thickness of the Cabiúnas sequence, the regional faulting constraining the fields, and the position of the overlying Aptian salt layer (Figs. 3, 5, 6, and 7). The methods included the post-processing of the seismic data to enhance its quality and the interpretation of surfaces and regional faults (Figs. 5, 6, and 7), the analysis of well data for the screening of information regarding the Cabiúnas Formation physical parameters (temperature and pore pressure), and the processing of well logs to estimate porosity values.

3.1. Seismic data post-processing

We used the OpenDtect software for the post-processing of the migrated seismic volumes. A dip-steering median filter (SMF) and the fault enhancement filter (FEF) were applied to enhance the quality of the data. We extracted similarity and most positive attributes from the steered data to create new 3D volumes. In addition, a set of conventional filters were applied over the steered data to support the interpretation; this included bandpass frequency filters (3–7 Hz; 7–15 Hz), instantaneous frequency, instantaneous amplitude, and a Hilbert transform. These attribute volumes helped to identify the top of the volcanic sequence and the top of the Precambrian basement, which allowed for an estimation of the regional thickness of the Cabiúnas Formation. The identification of the top of the Cabiúnas Formation was guided by information provided by wells that penetrated this unit (64 wells) (Fig. 5A).

3.2. Analysis of the formation properties

All available legacy data from the wells were analyzed in this study, and we have used the density (RHOB), gamma ray (GR), sonic (DT), and neutron-porosity (NPHI) logs from the wells in the evaluation of the CO_2 sequestration capacity.

Fig. 5A shows the outline of the 3D seismic survey over the Badejo, Linguado, and Pampo fields (Fig. 5) as well as the location of the 64 wells that penetrated the volcanic sequence. We used data from these 64 wells to analyze some of the reservoir characteristics, temperature and pore pressure, that were subsequently used to evaluate the feasibility of CO_2 carbonation in these basaltic rocks (Fig. 5). Specifically, the characteristics of the Cabiúnas Formation were compared to the conditions present in pilot CO_2 mineralization projects to estimate their suitability (Alfredson et al., 2013; McGrail et al., 2014, 2017; Pogge et al., 2019; Clark et al., 2020; White et al., 2020; Ratouis et al., 2022).

3.3. Estimate of volcanic rocks porosity

As the matrix permeability of volcanic rocks is normally very poor, even in rocks with high porosities like vesicular basalts, the permeability of the rocks is primarily controlled by micro- and macro-fracture systems (Lamur et al., 2017; Macente et al., 2019; Tang et al., 2022).

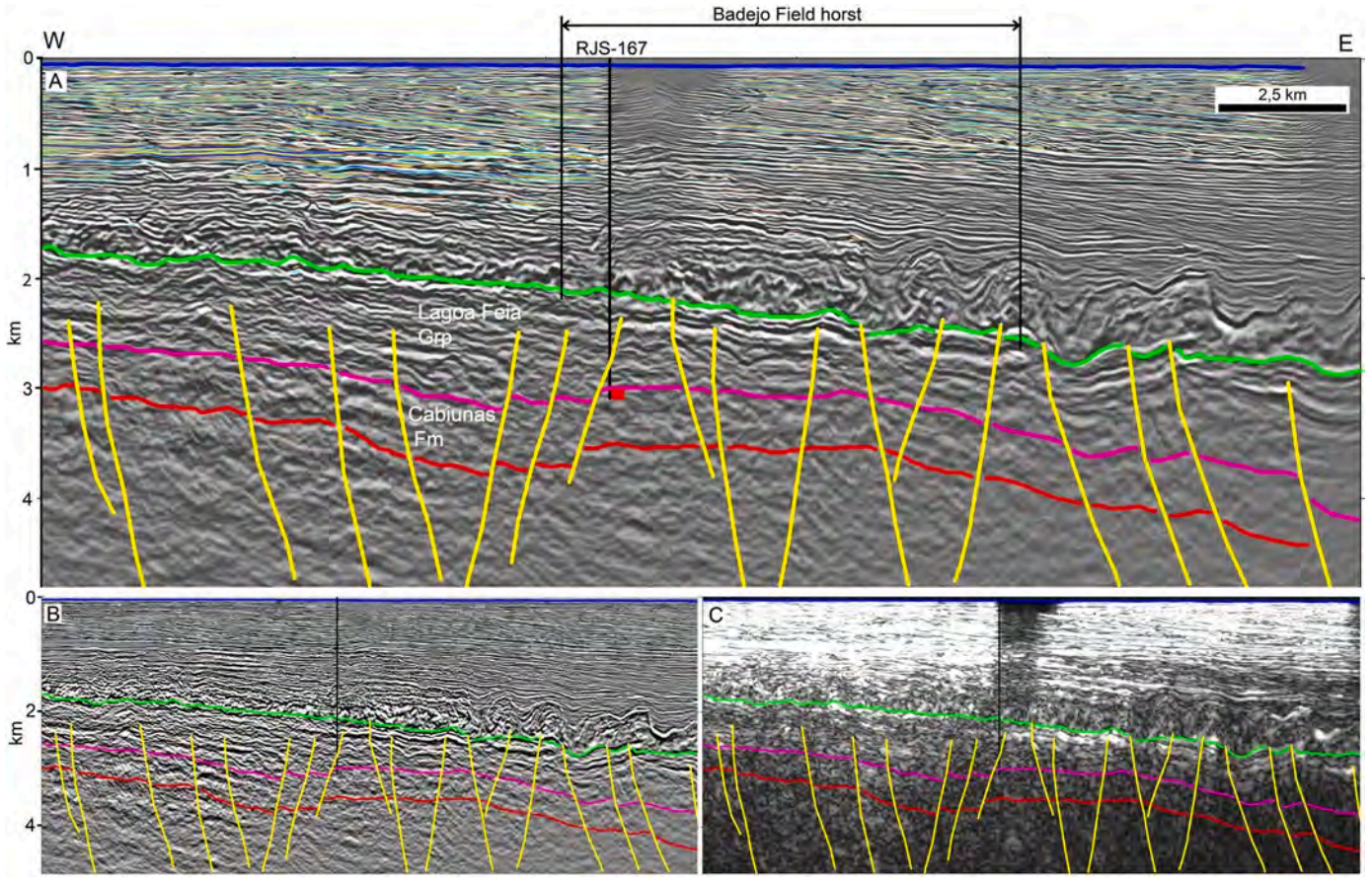

Fig. 6. An arbitrary 2D seismic section extracted from the 3D volume. Interpretation of the top of the Cabiúnas Formation is supported by well data, such as the data from RJS-167 as shown in the section, which penetrated approximately 100 m into the volcanic sequence (see the location of the section and the well in Fig. 8A). The section, oriented E–W, also shows the location of the Badejo horst. (A) dip-steered median filter, (B) fault enhancement filter, (C) instantaneous amplitude over steered data. Red horizon – top basement; pink horizon – top of the Cabiúnas Formation; green horizon – base of the salt layer; yellow lines – faults.

Calculation of permeability in reservoirs formed by volcanic rocks is very difficult due to the interaction between the original features like vesicles and amygdales, and later diagenetic features (Zakharova et al., 2012). Both Mizusaki (1986) and Marins et al. (2022) found that the available data was insufficient to assess the permeability associated with the fracture systems of the Cabiúnas Formation. Thus, we focused on estimating porosity as it allows for an estimation of the CO_2 storage capacity.

Volcanic reservoirs are generally considered unconventional fractured systems (Gupta et al., 2012; Chaudhary et al., 2022), often possessing complex relationships between original porosity (vesicles, cooling joints) and diagenetic porosity (dissolution and fracturing) (Zahasky et al., 2018; Wang et al., 2018; He et al., 2020). The quantification of porosity in volcanic sequences is often obtained through the modeling of well-log data (Ning et al., 2009; Zakharova et al., 2012; Tang et al., 2022), which allows for an estimation of reserves and flow characteristics. Porosity estimates of basaltic rocks can be obtained through the use of resistivity, acoustic velocity, and density logs (Slagle et al., 2011; Gupta et al., 2012; Asfahani, 2017; Navarro et al., 2020). We used density logs (RHOB) to calculate the apparent porosity of the basaltic rocks of the Cabiúnas Formation. This approach allowed us to estimate the bulk porosity of the volcanic intervals, which is related to both primary porosity (vesicles) and diagenetic-related secondary porosity caused by fractures and faults. Gupta et al. (2012) used this technique to estimate the porosity of fractured basalts in onshore and offshore regions of India (Gupta et al., 2012; Chaudhary et al., 2022). McGrail et al. (2011) used a similar approach to define the reservoir intervals in the volcanic sequences of the Columbia River basalts in the Boise Mill site, which was used for the development of the Wallula CO_2 injection project in Washington, USA (McGrail et al., 2014).

We selected density logs from 14 of the 64 wells investigated in our study (Fig. 5A) to obtain the distribution of the average porosity values across the area sampled by the wells. The calculation also accounts for the general density of basaltic rocks (~2.9 gm/cm^3), which was compared to the apparent density taken from the logs using the following equation:

$$\text{Porosity} = \frac{Rhoma - Rhob}{Rhoma - Rhof} \quad (1)$$

where *Rhoma* is the matrix density, *Rhob* is the bulk density, and *Rhof* is the fluid density. A fresh basalt with zero porosity was used as the reference matrix. The assumed density of the matrix (*Rhoma*) was 2.98 gm/cm^3, and the fluid density (*Rhof*) was assumed to be 1 gm/cm^3 (Gupta et al., 2012; Chaudhary et al., 2022).

The sequestration capacity, in terms of the potential volume of CO_2 able to be sequestered, was accomplished following recent methods used in other volcanic sequences that also represent fractured reservoirs (Koukouzas et al., 2019; Raza et al., 2022). The sequestration capacity of sedimentary rocks via injection methods is dependent on many parameters (depth, pore pressure, temperature, mineralogy, and formation fluids) (Ajayi et al., 2019). For depleted oil and gas reservoirs, a simple method to estimate the storage capacity is based on the calculation of the volume of fluids produced as well as the water and gas injected during the recovery stages (Rockett et al., 2013; Raza et al., 2022). The volume of fluids produced can be used to estimate the injection capacity of compressed CO_2. The limit of injectable supercritical CO_2, in

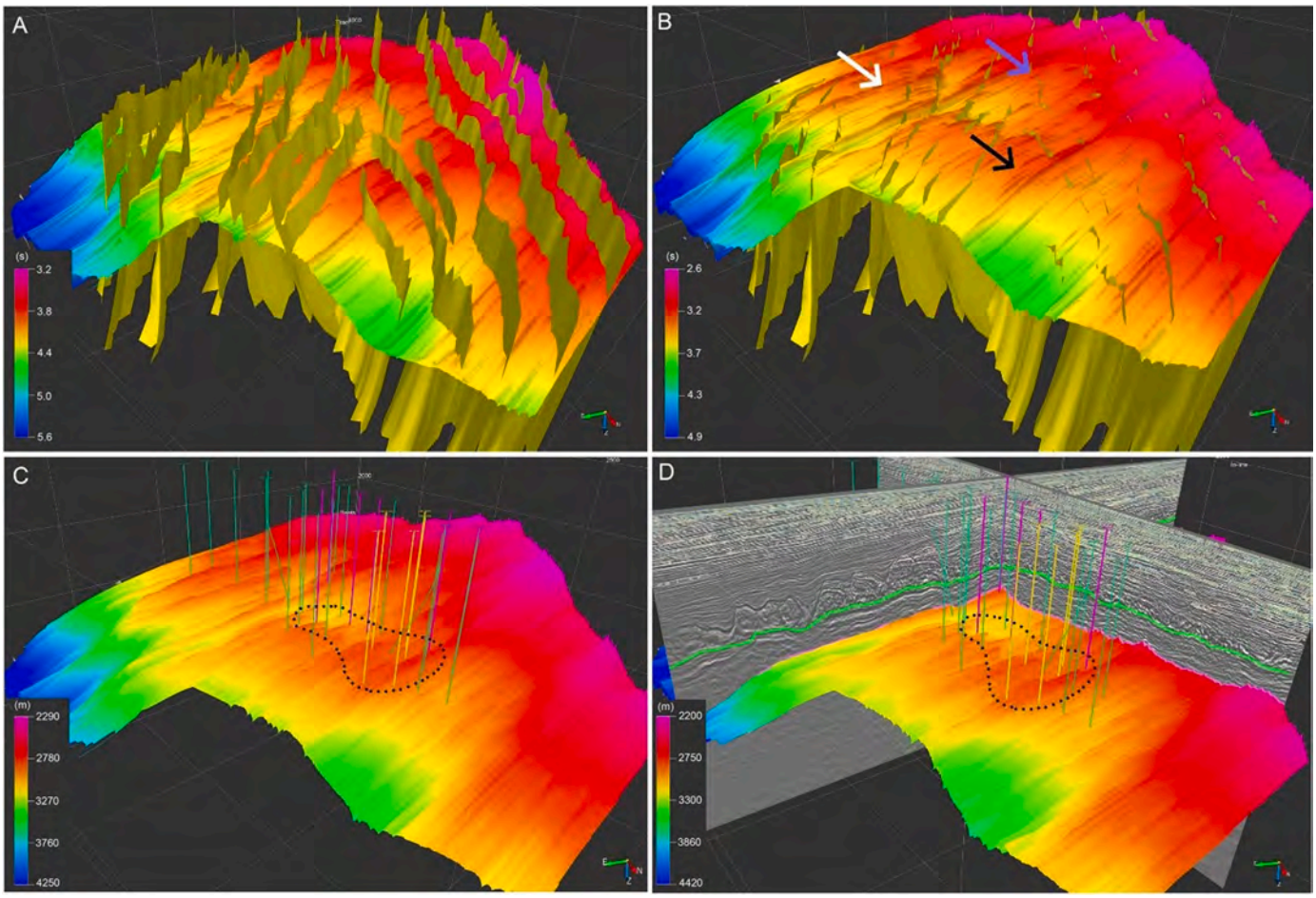

Fig. 7. Interpretations of the surfaces of the (A) top of the basement (depth in time) and the (B) top of the Cabiúnas Formation (depth in time) were mapped onto the 3D seismic survey. The yellow 2D planes represent the main rift fault zones. The black, blue, and white arrows show the location of the Badejo, Linguado, and Pampo horsts, respectively. (C) The surface of the top of the Cabiúnas Formation and the wells used for the estimation of the CO_2 storage capacity (depth in meters). The polygon delineated by the black dotted line indicates the target zone chosen for the estimation of the storage capacity (yellow vertical lines – oil well producers from basalt; purple vertical lines – the non-commercial discovery of oil in basalts; green vertical lines – other wells used to estimate storage capacity in this study). (D) Surface of the top of the Cabiúnas Formation as well as 2D seismic sections showing the position of the base of the regional salt layer atop the Lagoa Feia Group (green horizon).

conventional reservoirs composed of sedimentary rocks is also constrained by the hydrostatic pressure because the seal capacity may be compromised due to overpressure (Alcalde et al., 2018; Zappone et al., 2021).

However, it is difficult to make assumptions about the produced volume in volcanic reservoirs composed of crystalline rocks (Raza et al., 2022). Thus, we adopted a simplified volumetric method to estimate the storage capacity of the rocks, which utilizes the porosity parameter obtained through density logs, as described above. The volumetric approach was adopted by McGrail et al. (2006) to calculate the CO_2 storage capacity for the Columbia River basalt, and it provided a tentative approach for this estimate. This method is based on the experience provided by the US Department of Energy, which studied the remediation of aquifers in basaltic rocks, and it involves the average thickness, average porosity, and average formation pressure of the rock mass treated for injection to obtain a reliable estimate for CO_2 storage (Raza et al., 2022). This technique was also used by Anthonsen et al. (2014) to estimate storage capacity in volcanic rocks in Iceland. We adopted the volumetric method approach described by Koukousas et al. (2019), who studied the CO_2 storage potential of basaltic rocks in Greece, to estimate the volume capacity of an area of the Badejo Field:

$$\text{CapacityStorage} = \sum(\text{V} \times \varphi \times \rho \times \varepsilon) \quad (2))$$

where V is the volume of the basaltic rocks, φ is the average porosity, ρ is the specific gravity of the saturated CO_2, and ε is the CO_2 storage ratio for the basaltic rocks. The storage ratio refers to the percentage of CO_2 in the mass injected into the reservoir (%-CO_2 dissolved in the water) based on the results of the CarbFix pilot project in Iceland (Gislason et al., 2014). This ratio was defined based on the limitations associated with the volume of water available for injection in this onshore project (Gislason et al., 2014). Koukouzas et al. (2019) also adopted a value of 5% for the estimation of CO_2 sequestration in basaltic rocks in Greece. However, we adopted two ratios for our estimate: 5% and 10% of the injected mass because in offshore projects the availability of water for the CO_2 dissolution is not limited. The specific gravity of CO_2 (716.55 kg/m^3) was defined based on the work of Span and Wagner (1996), based on average values of parameters of the Cabiúnas such as depth of the hypothetical reservoir interval, 30 MPa for the formation pressure, and 90 °C for the reservoir temperature.

Our calculation of storage capacity did not consider the time for the injection process. Some works have addressed the possible effect of porosity reduction due to the cumulative injection of CO_2 on the reservoir and the secondary mineralization. A decrease in the porosity during the development will impact the previous calculation of the porosity that can be used to store the gas. Many aspects need to be considered to predict the effect of mineral dissolution and secondary mineral phases

formation (Gunnarson et al., 218) – the complex reactive transport framework (Tutolo et al., 2021) and even aspects like the natural fracture topology could impact the flow of the CO_2 and the mineralization (Wu et al., 2021). Laboratory experiments demonstrated that process like micro fracture-induced mineralization plays an important role in the self-sustainability of the reactions (Xing et al., 2018), and flow-through experiments in basalt samples demonstrated that the porosity decreases slightly (~0.7 to 0.8%) and it could even increase in some cases (Luhmann et al., 2017). As stated by Gunnarson et al. (2018), we just dont have sufficient data at present to completely understand the long-term effects of these complex interactions on the reservoir regarding large injection projects. In this context, we have considered a conservative approach for the calculation of the volume that could be injected in the studied rocks.

4. Results

Of the 64 wells studied, seven wells recorded the occurrence of non-commercial oil, and five wells were oil producers (Guardado et al., 2000). Fig. 5A shows the four zones (A–D) proposed by Mizusaki et al. (1988). They are oriented NNE–SSE and represent the dominant subaerial to subaqueous conditions that were present during the formation of the Cabiúnas deposits. The oil producers were found in the sectors associated with subaerial deposition. The interpolation of the Cabiúnas depth record in the 64 wells studied allowed us to obtain a regional configuration of the depth to the top of the volcanic sequence (Fig. 5B). The contour map of the top of the Cabiúnas also showed that the oil fields (Badejo, Linguado, and Pampo) formed above three horsts on the southeastern border of the Badejo High (Fig. 3). The depth to the top of the Cabiúnas Formation in the production wells in the Badejo Field ranges from 2800–3,100 m, and the three horsts are bounded by primary faults trending NE–SW and secondary faults trending ENE–WSW (Fig. 5B). Temperatures recorded within the Cabiúnas Formation range between ~80–110 °C. Temperatures were found to be higher in the Badejo Field region, and the temperature patterns show two zones with higher values trending N–S and E–W (Fig. 5C). The regional faults interpreted in the 3D seismic data are shown in the maps of Fig. 5, and the relationship between the variations in the studied parameter values and the orientation of the faults suggests the structural compartmentalization of these properties. This is mainly observed for the temperature values in the Badejo Field. Data collected on formation pressure showed that the Badejo horst also exhibited higher values, ranging from ~15–37 MPa. The formation pressure exhibited compartmentalized patterns similar to those observed in the temperature profiles, reinforcing the possibility of a tectonic control on the compartmentalization observed in the temperature values (Fig. 5D).

4.1. Storage capacity modeling using seismic and well data

Fig. 6 shows an interpretation of an arbitrary 2D seismic section extracted from the 3D volume, supported by the information recorded in well RJS-167. The interpretation of the top of the Precambrian basement is shown based on three different representations of the original seismic data, obtained through the use of filters and attributes (Fig. 6). The Badejo horst, located on the eastern border of the Badejo High (Fig. 3), is also highlighted.

Fig. 7 shows the interpreted surface of the top of the basement and the surface of the top of the Cabiúnas Formation. The seismic data interpretation constrained the morphological configuration of the three horsts associated with the Badejo, Linguado, and Pampo oil fields (Fig. 7). The black, blue, and white arrows in Fig. 7B indicate the locations of the Badejo, Linguado, and Pampo horsts, respectively. The main faults formed by the rift event that cut the Cabiúnas Formation were mapped. These faults were paths by which the oil and gas migrated from the lacustrine source rocks of the rift sequence to the upper sequences (Guardado et al., 1990; 2000). The yellow planes in Fig. 7A and 7B indicates the rift faults that cut the Cabiúnas sequence. The lateral contact of the Cabiúnas rocks with the overlying source rocks due to the rifting process was the primary mechanism by which the oil migrated to the volcanic sequence of the Badejo horst (Guardado et al., 1990; 2000) (Figs. 3 and 6). The fluid charging of the Badejo horst also suggests that these rocks possessed some level of permeability that allowed the oil to accumulate. Taking this into account, we defined an arbitrary area around the oil-producing wells in the Badejo horst within which we built a hypothetical model for the estimation of the CO_2 injection storage capacity (polygon indicated using dotted black line) (Fig. 7C and 7D). Fig. 7D shows that the Cabiúnas deposits in the selected area in the Badejo horst is capped by the Lagoa Feia Group deposits (Fig. 3), including interbedded shales and the upper salt layer (green horizon), all of which represent regional seals (Fig. 6). The Fig. 7 shows that selection of target zones for CO_2 injection will need to model tectono-stratigraphic aspects like the location of horsts and the fault compartmentalization.

Fig. 8 shows the regional characteristics of the Cabiúnas Formation in the study region. Fig. 8A shows a time slice positioned at 4000 ms in the 3D seismic survey. Due to the gentle dipping of the basement that underlies the Cabiúnas Formation and Lagoa Feia Group succession, the seismic facies of these three lithosequences are shown by the horizontal cut of the time slice from west to east. It shows that the regional distribution of the Cabiúnas rocks covers the platform of the Campos Basin. Fig. 8B shows the interpreted surface of the top of the Cabiúnas Formation with the most positive curvature attribute, which helped to map the fault zones which controlled the compartmentalization of the reservoirs found in this region (black lines). Rift faults extend from the basement through the Cabiúnas succession to the base of the Lagoa Feia Group (Fig. 6). The darker areas indicate zones with more occurrence of natural fractures, which are critical for flow modeling of possible CCS projects. Fig. 8C and 8D show 2D shaded relief contour maps of the top of the basement and the Cabiúnas Formation. The three horsts related to the three oil fields are positioned on the border of Badejo High. The Badejo horst exhibits a more prominent basement topography, which could have been a key reason for the accumulation of oil in the volcanic rocks in this region. Fig. 8E and 8F show the tentative estimation of the thickness of the Cabiúnas Formation in the study area, which varies between 450 and 1000 m. The formation thickness will be a controlling factor for CCS projects' site selection and the volumes which could be injected into the basaltic rocks. In the arbitrary area defined Over the Badejo horst, the Cabiúnas Thickness varies between ~500–700 m (Fig. 8E and 8F). The production wells are located in the sector that was subject to subaerial conditions during deposition (Zones A–B) (Mizusaki et al., 1988), while the wells drilled through the Linguado and Pampo sectors either found non-commercial oil or were dry. The Badejo horst appears to be the sector that is most compartmentalized by faults (Fig. 8B). The arbitrary zone used for the calculation of the storage capacity is shown in Fig. 8E and 8F (polygon delineated by white lines) and includes both the production wells and the non-commercial findings (Fig. 8E and 8F). Fig. 8F shows the section (brown line) formed by the 14 wells chosen for the estimation of porosity distribution within the volcanic sequence, which allowed for a reliable calculation of the storage capacity. This is the same sequence of wells that Mizusaki et al. (1988) used to describe the geological characteristics of the rocks sampled in the Cabiúnas Formation. The section trends with NNW–SSE and includes wells from the Badejo, Linguado, and Pampo fields.

The results showed above demonstrated that the site selection for CO_2 storage should consider regional structural control and paleogeography, which controlled environmental conditions during the formation of the Cabiúnas deposits.

4.2. Estimation of storage capacity

Fig. 9 shows the section constructed from the profiles of 14 wells, including boreholes from the Badejo, Linguado, and Pampo fields.

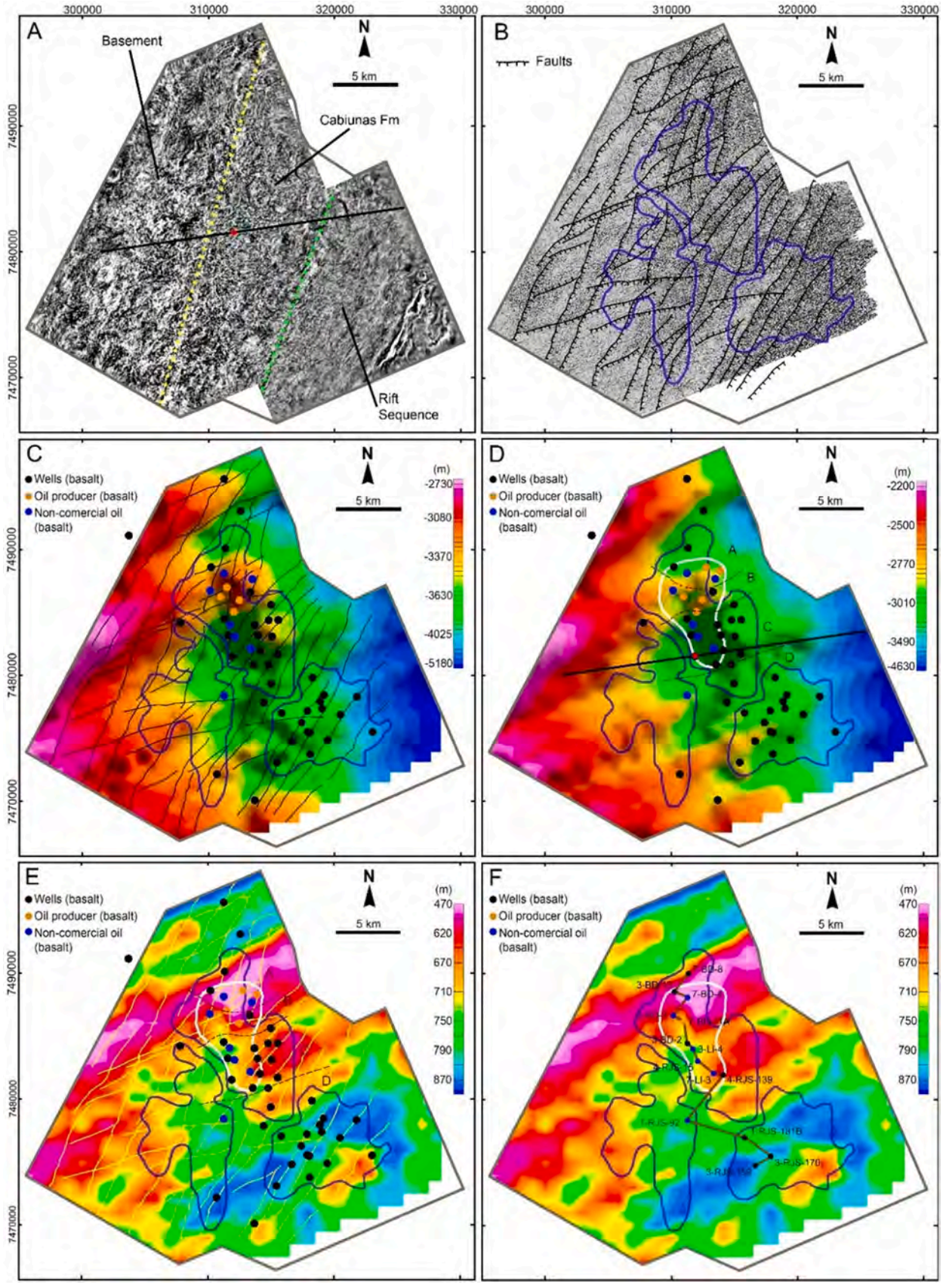

(caption on next page)

Fig. 8. (A) Time slice at 4000 ms of the 3D seismic survey (FEF volume). The yellow and green dotted lines mark the separation between the basement rocks, the Cabiúnas Formation, and the Lagoa Feia Group, characterized by different patterns of seismic facies. The black line and the red dot indicate the position of the arbitrary 2D seismic section and the location of the RJS-167 well shown in Fig. 6. (B) The interpreted surface of the top of Cabiúnas Formation shows the most positive curvature attribute, which helped to map the faults and indicates the intensely fractured zones (darker areas). The black lines show the projection of the rift fault planes trending primarily NE–SW and secondarily ENE–WSW. (C) Basement depth contour map (meters) of the rift faults. (D) Contour map of the depth to the Cabiúnas Formation (meters). The white polygon indicates the area selected around some wells across the Badejo horst used to constrain the hypothetical model used to estimate the CO_2 storage capacity. (E and F) Estimated Cabiúnas Formation isopach maps. The brown line indicates the location of the section that connects the 14 wells used to calculate the porosity logs presented in Fig. 9.

RHOB logs were used to create a new porosity log for the rocks of the Cabiúnas Formation. The wells correlation section trends roughly from NNW–SSE (Fig. 9). The profile of the wells also contained the gamma-ray and the NPHI logs, which are presented together with the porosity log. The section allows us to observe the variation in the depth to the top of the volcanic sequence across the three fields, which is associated with the basement horsts bounded by the faults that cut the overlying Cabiúnas Formation (Figs. 3 and 6).

We also integrated the lithofacies description provided by Mizusaki et al. (1988) into four wells in this section. Their descriptions were based on an analysis of the cores sampled (Fig. 10), allowing us to investigate the correlation between the apparent porosity results and the distribution of lithofacies as previously interpreted by these authors, which can aid future work on reservoir characterization.

There were several interesting positive and negative correlations between the porosity logs and the other logs (GR. NPHI and DT) showed in Fig. 9, possibly caused not only by the lithological variation and diagenesis but also by deposition conditions and early alteration (Mizusaki et al., 1988; Marins et al., 2022). Intervals with porosities ranging between 10 and 20% are widely distributed (Fig. 9). In some wells, these intervals are tens of meters thick; this is important with regard to the reservoir interval volume, especially in the Badejo wells. Wells RJS-181B and RJS-170 in the Pampo Field showed the worst cases of porosity distribution, with many intervals ranging between 0 and 10%. In the Badejo field, some wells (7-BD4 and 3BD-3) possessed thin intervals of volcanic rocks with apparent porosities between 30 and 40% (Fig. 9).

In general, low gamma ray values were correlated with higher density values and, consequently, with lower porosity. However, there were local examples of low gamma ray values that were associated with low-density values and high apparent porosity ranges (RJS-92; Fig. 9). The NPHI log shows that there is a minor positive correlation between high neutronic counts and low-density intervals that potentially contain more fluids (fractures, vesicles, and vugs), especially in the wells drilled in the Badejo field. However, in the wells at the southeastern end of the section (Pampo Field), higher NPHI values are also locally related to intervals with low porosity (RJS-170 and RJS-159 wells). The sonic (DT) log shows that there is a positive correlation between lower Δt values, higher Rhob values, and lower apparent porosity ranges (0–10%). Higher sonic log values are generally associated with low-density rocks and normally indicate higher porosity intervals (Fig. 9). Some of the punctual contradictory patterns can be associated with problems related to the original borehole data acquisition.

The porosity logs reveal the high vertical compartmentalization of the porous intervals. High porous intervals are more frequent in the Badejo Field, compared to the porosity distribution of the Linguado and the Pampo fields. Some sectors show an incipient cyclicity that may be associated with successive lava flows produced by the effusive processes that built the succession. The intercalation of thick intervals with greater porosities with intervals with low porosity values in the wells of the Badejo and Linguado fields highlight the complexity of the relationship between the porosity and lithofacies distributions (Fig. 9). There is no discernible pattern in the vertical variation between the wells regarding the continuity of possible reservoir intervals or flow units.

Fig. 10 shows four well profiles from the geological section shown in Fig. 9, including the GR, RHOB, and porosity logs, as well as a color bar representing an interpretation of lithofacies provided by Mizusaki et al. (1988). This lithofacies description covers each of the cored intervals, and these four wells were chosen because they represent the larger cored intervals across the sampled boreholes. The most representative lithologies are basalt flows that can be classified into two categories: 1) gray lavas, which were less affected by subaerial exposure and 2) red lavas, which show evidence of weathering, such as oxidation and meteoric diagenesis, before burial (Mizusaki, 1986; Mizusaki et al., 1988). The correlation between the porosity estimates and the lithologies showed that sedimentary rocks, volcaniclastic rocks, and breccias generally represent low porosity intervals, with few exceptions such as in well BD-11A.

As reported by Mizusaki et al. (1988), red lava flows were generally correlated to high porosity intervals, especially in the Badejo Field wells. However, they were less represented in the sampled intervals in terms of thickness. Gray lava flows were correlated with low to medium porosity intervals; a good example of this was a thick vertical interval in the BD-11A well, which exhibited low porosity values (Fig. 10). Apparent porosity values are influenced by both primary features, such as vesicles, and late diagenetic structures, such as faults, fractures, and dissolution cavities. Since there was no specific relationship between the porosity and the lithologies described in the sampled intervals, this suggests the strong influence of diagenetic factors.

The six wells with the greatest penetration depths into the Cabiúnas Formation were used to define the vertical range of porosity values (Table 1). This allows for the estimation of the vertical section of a hypothetical interval for a given average porosity. The hypothetical scenario was comprised of a 3D volume formed by the perimeter shown in Fig. 8D, representing an area of 31 km^2 that covers the Badejo Field and a total reservoir thickness of 300 m for fluid injection. We calculated the probable interval thickness with isotropic porosities of 10%, 15%, and 20% using the mean values extracted from the porosity logs from the six wells (Table 1). The scenarios assumed were very conservative based on the ranges adopted, considering that porosity values in basaltic formations normally ranges from 10% to >60% (Andrews, 2022; Chaudhary et al., 2022). For example, the total sampled thickness used to estimate mean values is approximately 678 m. Using a threshold value of 10%, we found that 440 m of the vertical rock sequence exceeded this value, representing ~73% of the total thickness; i.e., the interval containing porosity values equal to or higher than 10% based on the porosity logs. Thus, we adopted a thickness of 231 m for the first scenario (10% porosity) because it represents approximately 73% of the 300 m thickness of the general hypothetical reservoir (Table 2). In reality, the interval would exhibit a higher total porosity than we assumed in the isotropic scenario with an isotropic value. Table 2 shows the injection scenarios based on the estimated thickness calculated from the threshold porosity values of 10%, 15%, and 20%. Based on the assumed compressibility limits and the%-CO_2 in the injected water (5% and 10%), we calculated storage capacity values ranging from 15.8 to 23.4 Mt and 31.7–47 Mt for 5% and 10% diluted CO_2, respectively (Table 2). These results indicates that the sequestration capacity could be even higher if the real range of porosity values is considered. This is especially important because higher porosity will potentially imply better injectivity conditions. In addition, as observed in the Wallula project, the selection of intervals with greater porosity values (15–25%) (injection zones) should be done while taking into account the occurrence of intervals with much lower porosity that can act as cap rocks (McGrail et al., 2011; White et al., 2020).

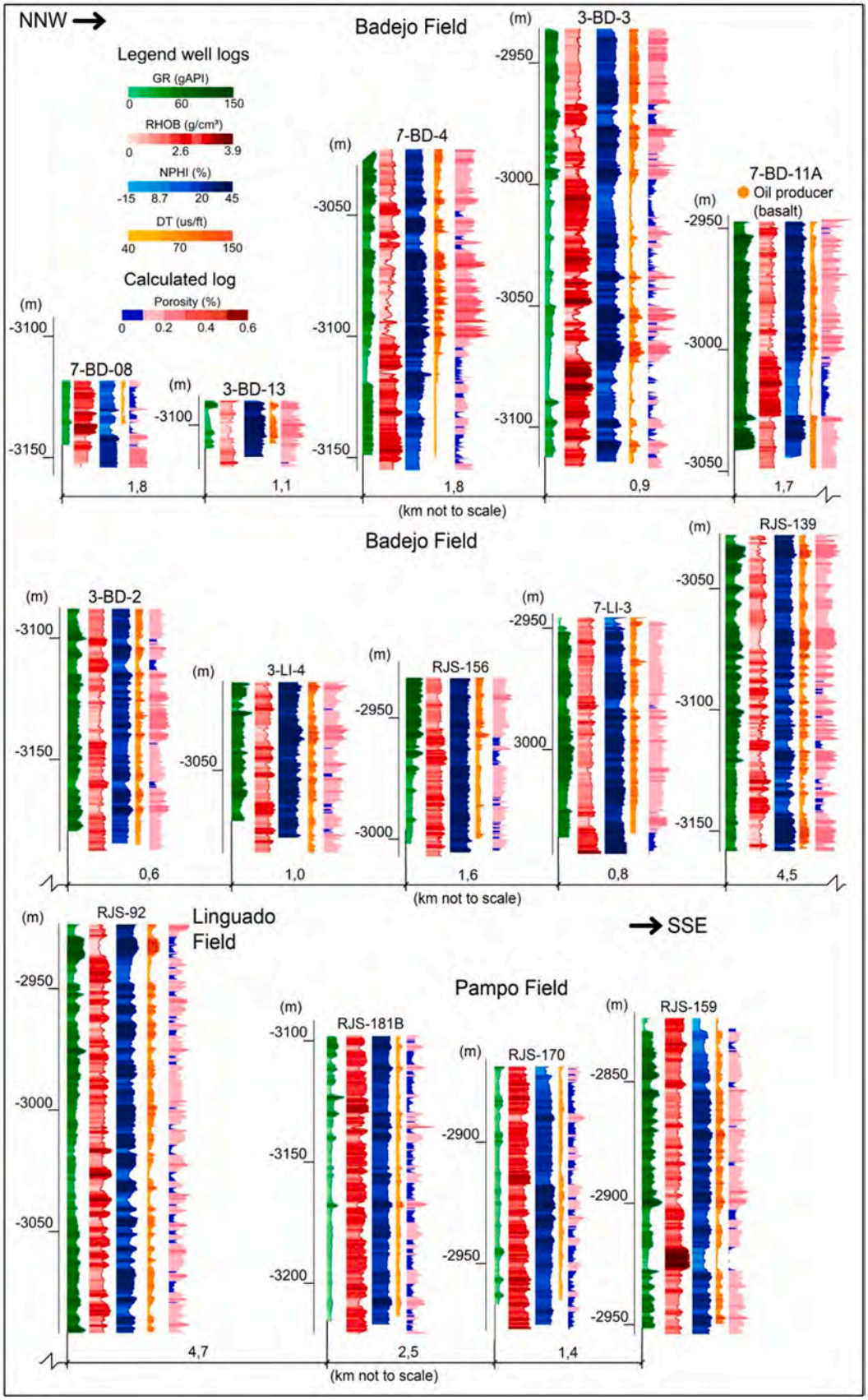

Fig. 9. Geologic section of 14 wells across the Badejo, Linguado, and Pampo fields (see Fig. 8F for the location of these wells). (A) Well profiles show the GR, RHOB, NPHI, DT, and porosity logs. The depth to the top of the Cabiúnas Formation was obtained from borehole records. Well 7-BD-11A was an oil producer from basalts in the Badejo field.

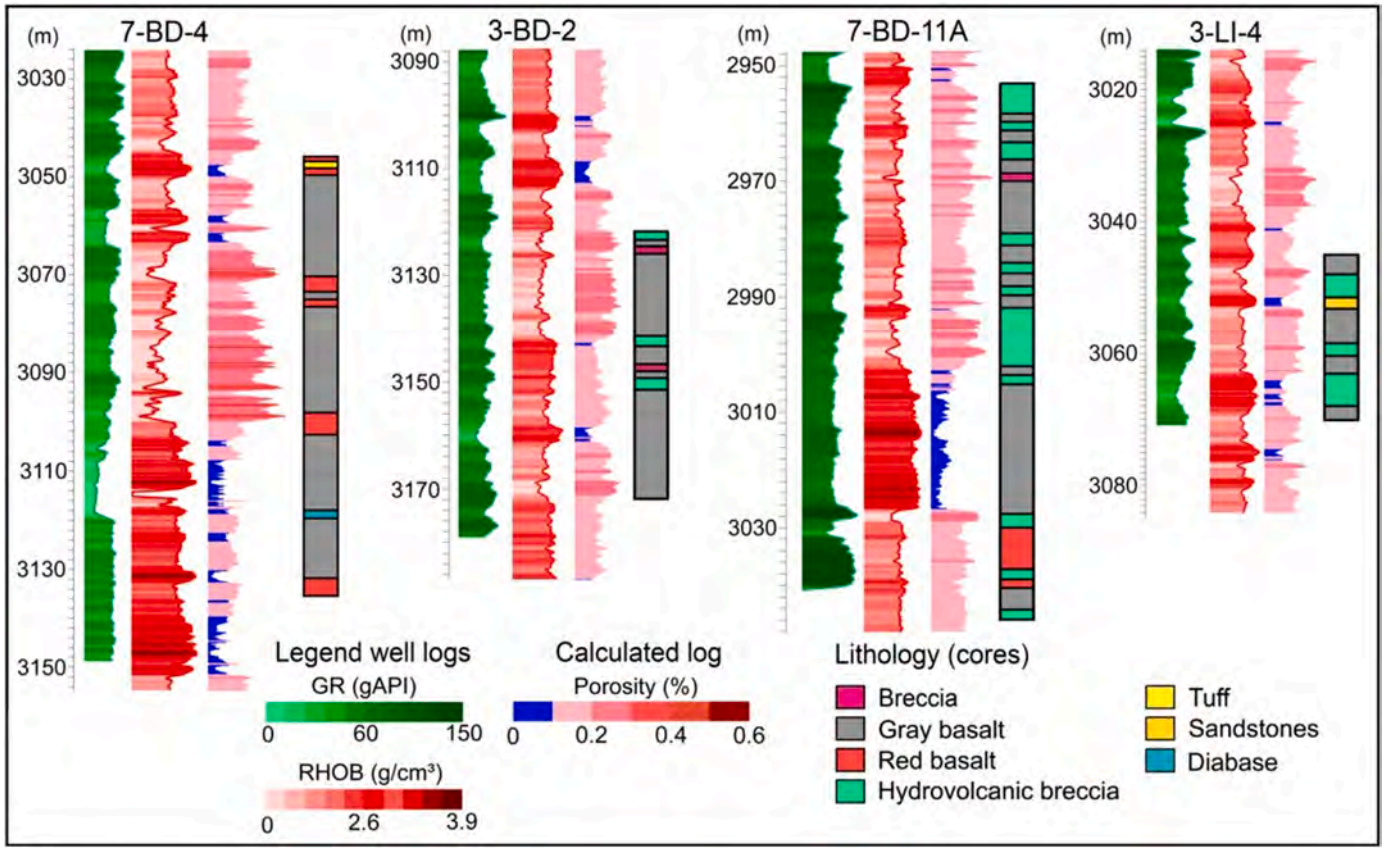

Fig. 10. Details of four wells shown in Fig. 9 and how they relate to the lithofacies distribution proposed by Mizusaki et al. (1988) from core analysis. The gray basalt and reddish basalts (with subaerial alteration) exhibit good porosity values.

5. Discussion

Data provided by the wells which penetrated the Cabiúnas Formation showed that the temperature and pressure zones within the basaltic sequence are compartmentalized by faults (Fig. 5). The temperature of the Cabiúnas rocks at the Badejo Field (Fig. 5) ranged from 75 to 108 °C. According to Gadikota et al. (2021), experimental evidence suggests the complete conversion of calcium silicate ($CaSiO_3$) and the >80% conversion of magnesium silicate (Mg_2SiO_4) to their respective carbonates occur at temperatures between 150 and 200 °C. Tutolo et al. (2021) argued that many of the experiments developed so far provided valuable data on the conditions and reaction effects of silicate minerals in basaltic rocks. However, the controlled alkalinity budget through the high content of NaHCO3 or KHCO3 used in the experiments is orders of magnitude different from the real-world subsurface operations. The authors also argued that some experiments using deionized water also showed that the mineralization is feasible, but the differences between controlled experiments and the field-scale projects using diluted or supercritical CO_2 need to be reconsidered.

Also based on experiments and field studies, Gadikota et al. (2021) suggested that the optimal conditions for mineralization in basaltic formations occur at high temperatures between 100 and 220 °C and at partial CO_2 pressures between 5 and 20 MPa. The olivine is highly reactive and its optimal temperature for carbon mineralization is ~180 °C (Raza et al., 2022). Marieni et al. (2021) showed that the most efficient temperature range for carbonation in seawater systems was 25–170 °C and that the optimal limit was below 260 °C. In addition, pilot projects in Iceland and Washington, USA have shown that the ideal temperature range for carbonation lies between 25 and 250 °C and that temperatures higher than 100 °C accelerate the process (Clark et al., 2020; Marieni et al., 2021; Raza et al., 2022). Higher temperatures also limit any biological activity that might harm the injectivity and the carbonation reactions (Gunnarson et al., 2018). According to these latter authors, CO_2 is 15% less soluble in seawater than in freshwater, but seawater accelerates the dissolution process in these rocks. Thus, the use of seawater for injection is feasible. The availability of seawater in the context of offshore projects also reduces storage costs.

The formation pressure of the volcanic rocks in the Badejo Field also appears to be compartmentalized, with significant changes of pressure values marked by faults, suggesting that fault zones controlled the fluid migration and the trapping of fluids in the syn-rift reservoir, consistent with the model described by Guardado et al. (1990). Analysis of well data showed that formation fluid pressure ranged from 25 to 38 MPa, with an average value of 30–32 MPa. Successful mineral carbonation projects (onshore) were conducted in geological formations with hydrostatic pressures ranging from 2.5 to ~16 MPa (Table 3). Mineralization processes in mafic rocks are still not completely understood (Raza et al., 2022). However, experimental studies with controlled temperatures, CO_2 saturations, and fluid pressures have shown that high pressures increase the solubility of CO_2 in water as well as the dissolution rate of volcanic glass and minerals (Kelemen et al., 2019; Raza et al., 2022). Experiments have shown that temperatures greater than 50 °C and CO_2 partial pressure greater than ~20 MPa resulted in the more rapid dissolution of minerals and higher rates of mineralization (Gíslason et al., 2018; Clark et al., 2020; Raza et al., 2022). Indeed, greater reservoir depths, temperatures, and hydrostatic pressures mean that less water is required to achieve CO_2 dissolution and the expected reactive effects for the carbonation process. According to Gunnarson et al. (2018), at a pressure of 25 bars and a temperature of 25 °C, approximately 27 tons of pure water is required to dissolve a ton of CO_2 gas either before or during the injection. This showcases the advantage of higher hydrostatic pressures during injections with respect to the

Table 1
Porosity estimates from the 14 wells selected for storage capacity estimation. Porosity estimates of the wells marked in red were used to define the thickness of the intervals possessing the threshold porosity values outlined by the three hypothetical scenarios.

Well ID	Cabiunas Drilled thickness (m)	Interval thickness with ≥10% Porosity	Interval thickness with ≥15% Porosity	Interval thickness with ≥20% Porosity
7 BD 8 RJS	37	20.5 (40%)	13.2 (14.3%)	11.5 (8.2%)
3 BD 13 RJS	48	42.5 (85%)	37 (71.7%)	23.7 (37.6%)
7 BD 4 RJS	133	109.8 (79.7%)	83.6 (60.6%)	48.2 (35%)
3 BD 3 RJS	196	123.1 (59.6%)	93.5 (43.3%)	54.9 (22%)
7 BD 11A RJS	101	79.1 (78.2%)	61 (60.3%)	18.2 (17.8%)
3 BD 2 RJS	104	97.2 (93.2%)	71.5 (67.5%)	31.4 (27.3%)
3 LI 4 RJS	76	70.6 (92.7%)	54.6 (71%)	21.4 (26%)
4 RJS 156 RJS	69	57.2 (81.7%)	39.8 (54.6%)	12.6 (12.4%)
7 LI 3 RJS	97	87.8 (90.5%)	68.7 (70.8%)	16.1 (16.5%)
4 RJS 139 RJS	137	124 (90.5%)	62.6 (45.5%)	60.2 (43.8%)
1 RJS 92 RJS	195	155 (78.6%)	114.8 (57%)	55.7 (25.3%)
1 RJS 181B RJS	126	63.6 (49.6%)	30.3 (33.6%)	13.5 (9%)
3 RJS 170 RJS	108	46.2 (42.8%)	12.6 (11.6%)	2.5 (2.2%)
3 RJS 159 RJS	126	103 (81.7%)	67 (53.1%)	13.6 (10.6%)
Total	1553	1179.6 (76%)	810.2 (52%)	383.5 (24.6%)

Table 2
Storage capacity estimations of the hypothetical zone. The hypothetical interval has a thickness of 300 m and an area of 31 km^2. The probable thickness of the intervals that exhibit a porosity of 10%, 15%, and 20% were calculated based on the proportion of the selected wells that exhibited values equal to or greater than the stated thresholds. In each scenario, the estimated storage capacity is presented Mt.

	Probable thickness with porosity ≥ 10%	Probable thickness with porosity ≥ 15%	Probable thickness with porosity ≥ 20%
Drilling interval 300 m	213	138	72
Storage Capacity Mton (5% diluted CO2)	23,4	22,8	15,8
Storage Capacity Mton (10% diluted CO2)	47	45,6	31,7

solubility of CO_2.

A main concern regarding the injection process is the possibility of pressure buildup due to the permeability of the reservoir, and the infiltration rate will control the rock dissolution and define the viability of the mineralization (Gíslason et al., 2014; Clark et al., 2020; Raza et al., 2022). However, the available data in the Cabiúnas Formation is insufficient to conduct any detailed investigations; these factors should be investigated in future experimental or numerical studies and new drilling operations.

Table 3
Physical characteristics of the geological systems of basaltic rocks used for CO_2 mineral carbonation of pilot projects compared with properties of the Cabiúnas Formation (Gislason et al., 2010; Zakharova et al., 2012; Lavalleur and Colwell, 2013; McGrail et al., 2017; Clark et al., 2018; Gunnarsson et al., 2018; Schwartz, 2018; Marieni et al., 2021).

Projects	Avg. Temp (°C)	Avg pH	Avg Pressure (MPa)	Depth (m)	Porosity (%)
CarbFix 1	35 (20–50)	10 (9–11)	2.5 (350 m)	530	5 - 40
CarbFix 2	~250 (220 - 260)	7.17	16.7 (2000 m)	1900 - 2200	8 - 10
Wallula	45.5 (37–54)	9.55 (9–10.1)	7.5 (7–8)	830 - 890	15 - 45
Cabiunas	90	7.14	32.46	2930 - 3260	10 - 40

The pH of the solution in the reservoir is a key factor that affects the dissolution rate of the rocks (glass and minerals) (Kelemen et al., 2020; Raza et al., 2022). Besides the partial pressure of CO_2 and the temperature, alkalinity and salinity of the water are also primary drivers (Gíslason et al., 2010). According to these authors, ultramafic and basaltic rocks such as gabbros and basaltic glass, which are rich in divalent cations and poor in silica, have relatively quick dissolution rates, with cation release rates that are approximately two orders of magnitude greater than that of granite and rhyolite. Dissolution of glassy rocks release Ca^{2+} results in an increase in pH of formation fluids from as low as 4–6 to values as high as 7–9. Thus, water in contact with basaltic glasses and ultramafic rocks, sealed off from atmospheric CO_2 or other CO_2 sources, exhibits high pH values ranging from 9 to 11 (Gíslason et al., 2010) (Table 3). Available data about the Cabiúnas Formation suggest that the water has pH values of ~7, which is favorable for CO_2 mineralization as discussed above (Table 3) (Supplementary material). Table 3 shows a comparison between the chemical and physical parameters of basaltic formations were CO_2 carbonation projects were developed and the parameters of the Cabiúnas Formation.

The interpretation of seismic data allowed for the estimation of the thickness of the Cabiúnas Formation (Figs. 6, 7, and 8), which varies between 1000 m in some grabens to 400–500 m over the basement horsts that form the Badejo Field (Fig. 8). This allowed us to understand the effects of the compartmentalization produced by the rift faults that cut through the volcanic succession and showed that the thickness of the Cabiúnas deposits is capable of hosting injection projects with multiple injection intervals. This interpretation, in conjunction with well data, also showed that the regions above horsts bounded by faults (Figs. 6 and 8) represent the best option for injection projects. Evidence of previous fluid migration into these zones indicates that they have more ideal reservoir qualities (porosity and permeability). This is also consistent with the oil-producing wells in the basalts above the horst that form the Badejo Field (Figs. 6 and 8). Based on these conditions, we estimated the storage capacity of this region for carbon sequestration (white polygon; Fig. 8D and 8E). The apparent porosity extracted from the RHOB log was useful in understanding the general relationship between porosity and lithofacies distribution (Fig. 9) and the analysis of the porosity of the 14 wells across the three fields allowed us to gain a rough understanding of the porosity distribution in the Cabiúnas deposits (Fig. 9). The estimated porosity accounts for features such as primary vesicles, explosive fractures, shrinkage fractures, as well as secondary pores and fractures (Tang et al., 2022). Recent work on the characteristics of basaltic oil reservoirs has suggested that fractures and late dissolution play an important role in fluid flow (Tang et al., 2022). Since the permeability of rock matrix of basaltic rocks are low, secondary fracturing and diagenetic aspects play an important role in reservoir permeability (Barreto et al., 2017; Tang et al., 2022). In terms of porosity, the location of the best reservoir zones is influenced by primary fractures related to the

architecture of the successions, which includes lava flows and other lithologies. The processes of cooling, gas release, and primary fracturing forms zones of high porosity at specific intervals within the lava flow (Mizusaki et al., 1988; Guardado et al., 1990; Reis et al., 2013; Barreto et al., 2017; Tang et al., 2022). Explosive fracturing and auto-brecciation also are important factors; however, the authigenic formation of minerals and compaction tends to reduce the porosity in these types of lithologies, especially in burial depths above 3 km (Tang et al., 2022).

The analysis of the porosity logs showed that the basaltic sequence in the Badejo and Linguado fields were the most ideal, with thick vertical zones with higher porosity (Fig. 9). Mizusaki et al. (1988) suggested that the reservoir conditions were controlled by aspects associated with their deposition across four distinct environments. This is consistent with our analysis of the porosity logs. However, the influence of diagenetic processes should be considered in future studies (Marins et al., 2022). Mizusaki et al. (1988) suggested that reddened lavas possessed higher porosities because they were formed in subaerial conditions, where early alteration before burial resulted in their erosion, dissolution, and oxidation (reddish deposits). In contrast, the gray lavas were formed in subaqueous conditions and were not exposed to weathering, resulting in lower porosities (Mizusaki et al., 1988). We compared the interpretation of the core samples by Mizusaki et al. (1988) (Fig. 10) with the porosity logs and agree with their interpretation of the relationship between the reddened lavas and high porosity. However, we found that gray lavas exhibited both low and high porosity values, implying that the porosity of the lithology was controlled by mechanisms besides the early weathering (Fig. 10).

Marins et al. (2022) studied core samples from five wells from the Badejo and Linguado fields (3-BD-13-RJS, 7-BD-11A-RJS, 3-BD-15C-RJS, 3-LI-04-RJS, and 7-LI-03-RJS) and observed that, in some intervals, weathering resulted in early pore filling and a reduction in porosity; this phenomenon was also observed by Mizusaki et al. (1988). Marins et al. (2022) also noted that less weathered lava flows preserved the high porosity associated with primary structures (such as vesicles and cooling fractures), which represent higher reservoir quality. They also showed how petrophysical properties varied between lava flows (volcanic intra-facies) and that the best values of porosity matrix were associated with vesicular basalts and intra-zones of rubbly pahoehoe lava bodies (Marins et al., 2022). Studies on analog onshore lava flows of the Paraná Basin had similar findings regarding primary structures in fractured, vesicular, rubbly pahoehoe lava intervals (Barreto et al., 2017; Rossetti et al., 2018).

Despite the lack of detailed data on the fracture system, the approach adopted was successful in allowing us to create a model for the estimation of the storage capacity of the basaltic formation for the purposes of fluid injection (Liu et al., 2019; Chaudhary et al., 2022; Ratouis et al., 2022). This volumetric method represents a conservative and reasonable estimate of the sequestration capacity of the hypothetical model. The estimated storage capacity of the hypothetical interval presented here highlights the feasibility of the Cabiúnas Formation for CO_2 sequestration projects. The model suggests that the CO_2 injections into the upper 300 m of the basaltic sequence in the selected zones in the Badejo Field would be capable of storing 15.8–47 Mt of CO_2 (Fig. 8). The calculation was conducted for the range of viable thicknesses associated with a specific isotropic porosity (10%, 15%, 20%) as well as two%-CO_2 dilutions (5% and 10%).

Volcanic rocks are widely distributed in the Campos and Santos basins, in both the post-salt and pre-salt intervals (Neves et al., 2019; Ren et al., 2020; Magee et al., 2021). Mineralization-based storage solution using diluted CO2 do not require cap rocks because the CO_2 does not form a buoyant plume, and most of the CO2 reacts with the rocks within a short period (2–3 years) (Alfredsson et al., 2013; Gislason and Oelkers, 2014; Snæbjörnsdóttir et al., 2014). Furthermore, the water needed for the CO_2 injection process will not be an issue due to the availability of seawater. Another advantage of using the Cabiúnas Formation for injection operations is the presence of overlying deposits of the Lagoa Feia Group that can act as cap rocks (Fig. 4), which will allow also to use the option for the injection of supercritical CO_2.

In summary, the main advantages of CCS projects utilizing mineral carbonation techniques in the basaltic sequence of the Campos Basin for the sequestration of CO_2 emissions from pre-salt production are 1) the suitability of the Cabiúnas volcanic sequence for mineralization-based CO_2 sequestration; 2) the vast volumes of basaltic rocks located in the shallow water pre-salt section of Campos Basin, which reduce the cost of operation; 3) its geographic proximity to the source of the emissions; 4) its proximity existing infrastructure for the transportation of CO_2 from emission sources to future injection hubs (pipeline systems are already installed and are currently used for natural gas transportation); 5) additional sealing capabilities provided by fine-grained rocks and salt deposits positioned above the volcanic sequence, which allows the injection of supercritical CO_2 besides the diluted CO_2 option treated here.

However, this study presents some limitations regarding legacy data and assumptions made to achieve a conservative estimate of the sequestration capacity of the basaltic formation. Thus, additional work must be conducted to fully evaluate the viability of these projects, such as the sophisticated experimental and numerical modeling of factors such as their reactivity, geomechanics, the detailed definition of fluids and reservoir conditions, rock–fluid interactions during injection, and injectivity versus equivalent permeability relationship (McGrail et al., 2014; Snæbjörnsdóttir et al., 2018; Jayne et al., 2019; White et al., 2020; Xing et al., 2022).

6. Conclusions

This study presents a comprehensive evaluation of the storage capacity of the pre-salt volcanic sequence located in shallow waters of the Campos Basin for the purposes of CO_2 sequestration. We have shown that the geological sequestration of CO_2 via mineralization processes is feasible considering the regional and local characteristics of these rocks, which were previously developed as oil reservoirs. Based on the available legacy data, we evaluated the tectono-stratigraphic characteristics and thickness of the volcanic unit and conducted an updated investigation into the distribution of the porosity of the rocks by processing well log data. The study also presents a review of the main aspects that control various intrinsic reservoir parameters, such as temperature, pressure, and pH, which are essential for the future development of CO_2 injection operations. A comparison of the main boundary conditions of the reservoirs showed that they were suitable for the mineralization-based geological sequestration of CO_2. The results also showed that the tectonic control of late fluid migrations is an important mechanism that must be considered in potential injection projects. We used the hypothetical model of a 31 km^2 hypothetical reservoir with a thickness of 300 m based on a selected area located in the Badejo Field to estimate the storage capacity of Cabiúnas basaltic rocks, assuming a CO_2 injection into porous zones with three different porosity thresholds (10%, 15%, and 20%) and two levels of CO_2 concentration and obtained storage estimates ranging from 15.8 to 47.0 Mt. Thus, this could represent another alternative for the safe geological sequestration of CO_2 over the next few decades, especially considering the growing demand for geological storage for gasses produced by the pre-salt operations in the region. The occurrence of vast amounts of volcanic rocks in this region also represents cost-related advantages due to its potential CO_2-trapping mechanism and its geographical proximity to emission sources and pre-existing infrastructure for gas transportation in the pre-salt province. Future studies are required to address issues that were not discussed here, such as the option of injecting supercritical CO_2, equivalent permeability/injectivity relationship, geomechanics, reactive transport, and the impact of fluid characteristics of the reservoirs for carbonation techniques.

Author statement

G.M.S.R, J.A.B, and A.F.L.A conceived the idea and the potential of contribution. J.A.B, G.M.S.R and J.C.T.O. processing of the geophysical surveys and borehole data. Interpretation and modeling of seismic data. Estimate of the storage capacity. G.M.S.R and J.A.B wrote the manuscript and prepared the figures with support from A.F.L.A, O.J.C.F, C.J. B, and R.SM. J.AB. and C.J.B discussed the results and commented on the final version of the manuscript.

Declaration of Competing Interest

The authors declare that they have no known competing financial interests or personal relationships that could have appeared to influence the work reported in this paper.

Data availability

No data was used for the research described in the article.

Acknowledgments

We thank the National Agency for Petroleum, Natural Gas, and Biofuels for providing the geological and geophysical data used in this research and the DGB Earth Sciences for academic support. JAB also thanks the grant provided by Council for Scientific and Technological Development - CNPq (315343/2020–6). We thank Professor Benjamin M. Tutolo and the anonymous reviewer for their excellent and constructive suggestions that helped significantly improve this manuscript.

References

Alcalde, J., Flude, S., Wilkinson, M., Johnson, G., Edlmann, K., Bond, C.E., Scott, V., Gilfillan, S.M.V., Ogaya, X., Haszeldine, R.S., 2018. Estimating geological CO_2 storage security to deliver on climate mitigation. Nat. Commun. 9 (1), 1–13. https://doi.org/10.1038/s41467-018-04423-1.

Alfredsson, H.A., Oelkers, E.H., Hardarsson, B.S., Franzson, H., Gunnlaugsson, E., Gislason, S.R., 2013. The geology and water chemistry of the Hellisheidi, SW-Iceland carbon storage site. Int. J. Greenhouse Gas Control 12, 399–418. https://doi.org/10.1016/j.ijggc.2012.11.019.

Ali, M., Jha, N.K., Pal, N., Keshavarz, A., Hoteit, H., Sarmadivaleh, M., 2022. Recent advances in carbon dioxide geological storage, experimental procedures, influencing parameters, and future outlook. Earth Sci. Rev. 225, 103895 https://doi.org/10.1016/j.earscirev.2021.103895.

Anderson, S.T., 2017. Risk, liability, and economic issues with long-term CO_2 storage—a review. Nat. Resour. Res. 26 (1), 89–112. https://doi.org/10.1007/s11053-016-9303-6.

Ajayi, T., Gomes, J.S., Bera, A., 2019. A review of CO_2 storage in geological formations emphasizing modeling, monitoring and capacity estimation approaches. Pet. Sci. 16 (5), 1028–1063. https://doi.org/10.1007/s12182-019-0340-8.

Aminu, M.D., Nabavi, S.A., Rochelle, C.A., Manovic, V., 2017. A review of developments in carbon dioxide storage. Appl. Energy 208, 1389–1419. https://doi.org/10.1016/j.apenergy.2017.09.015.

Amonette, J.E., Johnson, T.A., Spencer, C.F., Zhong, L., Szecsody, J.E., Vermeul, V.R., 2014. Geochemical monitoring considerations for the FutureGen 2.0 project. Energy Procedia 63, 4095–4111. https://doi.org/10.1016/j.egypro.2014.11.441.

Andrews, G. 2022. Geological Carbon Storage in Northern Irish Basalts: prospectivity and Potential. Available At SSRN: 10.2139/ssrn.4157443.

ANP. 2019. Boletim Mensal da Produção de Petróleo e Gás Natural.

ANP. 2021. Panorama Exploratório das Bacias de Santos e Campos: gigantes Nacionais.

ANP. 2022. Polígono do Pré-Sal.

Anthonsen, K.L., Aagaard, P., Bergamo, P.E.S., Gislason, S.R., Lothe, A.E., Mortensen, G. M., Snæbjörnsdóttir, S.Ó., 2014. Characterisation and selection of the most prospective CO_2 storage sites in the Nordic region. Energy Procedia 63, 4884–4896. https://doi.org/10.1016/j.egypro.2014.11.519.

Asfahani, J., 2017. Porosity and hydraulic conductivity estimation of the basaltic aquifer in Southern Syria by using nuclear and electrical well logging techniques. Acta Geophys. 65 (4), 765–775. https://doi.org/10.1007/s11600-017-0056-3.

Aydin, G., Karakurt, I., Aydiner, K., 2010. Evaluation of geologic storage options of CO_2: applicability, cost, storage capacity and safety. Energy Policy 38 (9), 5072–5080. https://doi.org/10.1016/j.enpol.2010.04.035.

Bai, M., Zhang, Z., Fu, X., 2016. A review on well integrity issues for CO_2 geological storage and enhanced gas recovery. Renew. Sustain. Energy Rev. 59, 920–926. https://doi.org/10.1016/j.rser.2016.01.043.

Barreto, C.J.S., de Lima, E.F., Goldberg, K., 2017. Primary vesicles, vesicle-rich segregation structures and recognition of primary and secondary porosities in lava flows from the Paraná igneous province, southern Brazil. Bull. Volcanol. 79 (4), 1–17. https://doi.org/10.1007/s00445-017-1116-x.

Bataille, C., Waisman, H., Briand, Y., Svensson, J., Vogt-Schilb, A., Jaramillo, M., Delgado, R., Arguello, R., Clarke, L., Wild, T., Lallana, F., Bravo, G., Nadal, G., Le Treut, G., Godinez, G., Quiros-Tortos, J., Pereira, E., Howells, M., Buira, D., Tovilla, J., Farbes, J., Ryan, J., Ugarte, D.D.L.T., Requejo, F., Gomez, X., Soria, R., Villamar, D., Rochedo, P., Imperio, M., 2020. Net-zero deep decarbonization pathways in Latin America: challenges and opportunities. Energy Strategy Rev. 30, 100510 https://doi.org/10.1016/j.esr.2020.100510.

Beltrão, R.L.C., Sombra, C.L., Lage, A.C.V., Netto, J.R.F., Henriques, C.C.D., 2009. SS: pre-salt Santos basin-challenges and new technologies for the development of the pre-salt cluster, Santos basin, Brazil. Day 1 Mon. In: Proceedings of the Offshore Technology Conference. https://doi.org/10.4043/19880-MS. May 04 2009,.

Bérest, P., Brouard, B., 2003. Safety of salt caverns used for underground storage blow out; mechanical instability; seepage; cavern abandonment. Oil Gas Sci. Technol. 58 (3), 361–384. https://doi.org/10.2516/ogst:2003023.

Bruhn, C.H., Gomes, J.A.T., Del Lucchese Jr, C., Johann, P.R., 2003. Campos basin: reservoir characterization and management-Historical overview and future challenges. In: Proceedings of the Offshore Technology Conference. Offshore Technology Conference.

Cao, C., Liu, H., Hou, Z., Mehmood, F., Liao, J., Feng, W., 2020. A review of CO_2 storage in view of safety and cost-effectiveness. Energies 13 (3), 600. https://doi.org/10.3390/en13030600.

Chaudhary, M., Sharma, R., Kapoor, D., Sadiq, M., 2022. Formation evaluation of Deccan (basalt) trap basement of Kutch Offshore basin, Gulf of Kutch, India. J. Pet. Sci. Eng. 217, 110854 https://doi.org/10.1016/j.petrol.2022.110854.

Clark, D.E., Gunnarsson, I., Aradóttir, E.S., Arnarson, M.Þ., Þorgeirsson, Þ.A., Sigurðardóttir, S.S., Sigfússon, B., Snæbjörnsdóttir, S., Oelkers, E.H., Gíslason, S.R., 2018. The chemistry and potential reactivity of the CO_2-H_2S charged injected waters at the basaltic CarbFix2 site, Iceland. Energy Procedia 146, 121–128. https://doi.org/10.1016/j.egypro.2018.07.016.

Clark, D.E., Oelkers, E.H., Gunnarsson, I., Sigfússon, B., Snæbjörnsdóttir, S.Ó., Aradottir, E.S., Gíslason, S.R., 2020. CarbFix2: CO_2 and H_2S mineralization during 3.5 years of continuous injection into basaltic rocks at more than 250°C. Geochim. Cosmochim. Acta 279, 45–66. https://doi.org/10.1016/j.gca.2020.03.039.

Cornelius, S., 2021. Geological sources of CO_2 in the Pre-Salt Reservoirs of Santos, Campos and Espirito Santo Basins, Brazilian SE Atlantic Margin. In: Proceedings of the 3rd HGS and EAGE Conference on Latin America, 2021. European Association of Geoscientists & Engineers, pp. 1–4. https://doi.org/10.3997/2214-4609.202188008.

Costa, A.M., Costa, P.V., Miranda, A.C., Goulart, M.B., Udebhulu, O.D., Ebecken, N.F., Azevedo, R.C., de Eston, S.M., de Tomi, G., Mendes, A.B., Meneghini, J.R., Nishimoto, K., Sampaio, C.M., Brandão, C., Breda, A., 2019. Experimental salt cavern in offshore ultra-deep water and well design evaluation for CO_2 abatement. Int. J. Min. Sci. Technol. 29 (5), 641–656. https://doi.org/10.1016/j.ijmst.2019.05.002.

d'Almeida, K.S., Vilela, P.C., Cardoso, R.A., Fernandes, R.F., Souza, M.F.F, 2018. Ocorrência de CO_2 em campos petrolíferos na margem leste brasileira. Empresa de Pesquisa Energética.

Damen, K., Faaij, A., Turkenburg, W., 2006. Health, safety and environmental risks of underground CO_2 storage–overview of mechanisms and current knowledge. Clim. Change 74 (1), 289–318. https://doi.org/10.1007/s10584-005-0425-9.

de Castro, J.C., 2006. Evolução dos conhecimentos sobre as coquinas-reservatório da Formação Lagoa Feia no trend Badejo-Linguado-Pampo, Bacia de Campos. Geociências 25 (2), 175–186.

de Castro, R.D., Picolini, J.P., 2016. Main features of the Campos Basin regional geology. Geol. Geomorphol. 1, 1–12. https://doi.org/10.1016/B978-85-352-8444-7.50008-1 v.

de Freitas, V.A., dos Santos Vital, J.C., Rodrigues, B.R., Rodrigues, R., 2022. Source rock potential, main depocenters, and CO_2 occurrence in the pre-salt section of Santos Basin, southeast Brazil. J. South Am. Earth Sci. 115, 103760 https://doi.org/10.1016/j.jsames.2022.103760.

de Lima, A.L.B., da Silva, T.F., González, M.B., Peralba, M.D.C.R., Jural, P.A., Lenz, R.L., Barrionuevo, S., Dubois, D.S., Spigolon, A.L.D., 2022. Characterization of heavy oils from the Campos Basin, Brazil: free biomarkers in oils, adsorbed and occluded in asphaltene structures. J. Pet. Sci. Eng. 215, 110542 https://doi.org/10.1016/j.jsames.2022.103760.

Dinescu, S., Radu, S.M., Florea, A., Danciu, C., Tomuș, O.B., Popescu, S., 2021. Possible Risks of CO_2 Storage in Underground Salt Caverns. Ann. Univ. Petroşani 23, 27–36.

Drexler, S., Correia, E.L., Jerdy, A.C., Cavadas, L.A., Couto, P., 2019. Effect of CO_2 injection on the interfacial tension for a Brazilian Pre-Salt field. In: Proceedings of the Offshore Technology Conference Brasil. OnePetro. https://doi.org/10.4043/29769-MS.

EPE, 2020. Estudo sobre o aproveitamento do gás natural do pré-sal.

EPE, 2021. Brazilian oil and gas report 2020/2021.

Fawad, M., Mondol, N.H., 2022. Monitoring geological storage of CO_2 using a new rock physics model. Sci. Rep. 12 (1), 1–11. https://doi.org/10.1038/s41598-021-04400-7.

Fox, L.M., .2022. Stratigraphic and Geochemical Evaluation of Distal Flows of the Columbia River Flood Basalts in the Greater Vale Area, Southeastern Oregon.

Friedmann, S.J., Dooley, J.J., Held, H., Edenhofer, O., 2006. The low cost of geological assessment for underground CO_2 storage: policy and economic implications. Energy Convers. Manage. 47 (13–14), 1894–1901. https://doi.org/10.1016/j.enconman.2005.09.006.

Fuss, S., Canadell, J.G., Ciais, P., Jackson, R.B., Jones, C.D., Lyngfelt, A., Peters, G.P., Van Vuuren, D.P., 2020. Moving toward net-zero emissions requires new alliances for carbon dioxide removal. One Earth 3 (2), 145–149. https://doi.org/10.1016/j.oneear.2020.08.002.

Gadikota, G., 2021. Carbon mineralization pathways for carbon capture, storage and utilization. Commun. Chem. 4 (1), 23.

Gamboa, L., Ferraz, A., Baptista, R., Neto, E.V.S., 2019. Geotectonic controls on CO_2 formation and distribution processes in the Brazilian pre-salt basins. Geosciences 9 (6), 252. https://doi.org/10.3390/geosciences9060252 (Basel).

Gholami, R., Raza, A., Iglauer, S., 2021. Leakage risk assessment of a CO_2 storage site: a review. Earth Sci. Rev. 223, 103849 https://doi.org/10.1016/j.earscirev.2021.103849.

Gislason, S.R., Wolff-Boenisch, D., Stefansson, A., Oelkers, E.H., Gunnlaugsson, E., Sigurdardottir, H., Sigfusson, B., Broecker, W.S., Matter, J.M., Martin, S., Gudni, A., Fridriksson, T., 2010. Mineral sequestration of carbon dioxide in basalt: a pre-injection overview of the CarbFix project. Int. J. Greenhouse Gas Control 4 (3), 537–545. https://doi.org/10.1016/j.ijggc.2009.11.013.

Gislason, S.R., Broecker, W.S., Gunnlaugsson, E., Snæbjörnsdóttir, S., Mesfin, K.G., Alfredsson, H.A., Aradottir, E.S., Sigfusson, B., Gunnarsson, I., Stute, M., Matter, J. M., Arnarson, M.Th., Galeczka, I.M., Gudbrandsson, S., Stockman, G., Wolff-Boenisch, D., Stefansson, A., Ragnheidardottir, E., Flaathen, T., Gysi, A.P., Olssen, J., Didriksen, K., Stipp, S., Menez, B., Oelkers, E.H., 2014. Rapid solubility and mineral storage of CO_2 in basalt. Energy Procedia 63, 4561–4574. https://doi.org/10.1016/j.egypro.2014.11.489.

Gislason, S.R., Oelkers, E.H., 2014. Carbon storage in basalt. Science 344 (6182), 373–374. https://doi.org/10.1126/science.1250828.

Gislason, S.R., Sigurdardóttir, H., Aradóttir, E.S., Oelkers, E.H., 2018. A brief history of CarbFix: challenges and victories of the project's pilot phase. Energy Procedia 146, 103–114. https://doi.org/10.1016/j.egypro.2018.07.014.

Godoi, J.M.A., dos Santos Matai, P.H.L., 2021. Enhanced oil recovery with carbon dioxide geosequestration: first steps at Pre-salt in Brazil. J. Pet. Explor. Prod. 11 (3), 1429–1441. https://doi.org/10.1007/s13202-021-01102-8.

Goulart, M.B.R., da Costa, P.V.M., da Costa, A.M., Miranda, A.C., Mendes, A.B., Ebecken, N.F., Meneghini, J.R., Nishimoto, K., Assi, G.R., 2020. Technology readiness assessment of ultra-deep salt caverns for carbon capture and storage in Brazil. Int. J. Greenhouse Gas Control 99, 103083. https://doi.org/10.1016/j.ijggc.2020.103083.

Grusson, Y., Sun, X., Gascoin, S., Sauvage, S., Raghavan, S., Anctil, F., Sáchez-Pérez, J.M., 2015. Assessing the capability of the SWAT model to simulate snow, snow melt and streamflow dynamics over an alpine watershed. J. Hydrol. 531, 574–588. https://doi.org/10.1016/j.jhydrol.2015.10.070 (Amst).

Guardado, L.R., Gamboa, L.A.P., Lucchesi, C.F., 1990. Petroleum geology of the Campos Basin, Brazil, a model for a producing Atlantic type basin. Divergent/passive Margin Basins.

Guardado, L.R., Spadini, A.R., Brandão, J.S.L., Mello, M.R., 2000. Petroleum System of the Campos Basin, Brazil. AAPG Memoir 73, 317–324. Chapter 22.

Gunnarsson, I., Aradóttir, E.S., Oelkers, E.H., Clark, D.E., Arnarson, M.Þ., Sigfússon, B., Snæbjörnsdóttir, S., Matter, J.M., Stute, M., Júlíusson, B.M., Gíslason, S.R., 2018. The rapid and cost-effective capture and subsurface mineral storage of carbon and sulfur at the CarbFix2 site. Int. J. Greenhouse Gas Control 79, 117–126. https://doi.org/10.1016/j.ijggc.2018.08.014.

Gupta, S.D., Chatterjee, R., Farooqui, M.Y., 2012. Formation evaluation of fractured basement, Cambay Basin, India. J. Geophys. Eng. 9 (2), 162–175. https://doi.org/10.1088/1742-2132/9/2/162.

He, H., Li, S., Liu, C., Kong, C., Jiang, Q., Chang, T., 2020. Characteristics and quantitative evaluation of volcanic effective reservoirs: a case study from Junggar Basin, China. J. Pet. Sci. Eng. 195, 107723 https://doi.org/10.1016/j.petrol.2020.107723.

Hong, S., Moon, S., Cho, J., Park, A.H.A., Park, Y., 2022. Effects of Mg ions on the structural transformation of calcium carbonate and their implication for the tailor-synthesized carbon mineralization process. J. CO_2 Util. 60, 101999 https://doi.org/10.1016/j.jcou.2022.101999.

Jayne, R.S., Wu, H., Pollyea, R.M., 2019. A probabilistic assessment of geomechanical reservoir integrity during CO_2 sequestration in flood basalt formations. Greenhouse Gases Sci. Technol. 9 (5), 979–998. https://doi.org/10.1002/ghg.1914.

Kelemen, P.B., McQueen, N., Wilcox, J., Renforth, P., Dipple, G., Vankeuren, A.P., 2020. Engineered carbon mineralization in ultramafic rocks for CO_2 removal from air: review and new insights. Chem. Geol. 550, 119628 https://doi.org/10.1016/j.chemgeo.2020.119628.

Kelemen, P., Benson, S.M., Pilorgé, H., Psarras, P., Wilcox, J., 2019. An overview of the status and challenges of CO_2 storage in minerals and geological formations. Front. Clim. 1 (9) https://doi.org/10.3389/fclim.2019.00009.

Koukouzas, N., Koutsovitis, P., Tyrologou, P., Karkalis, C., Arvanitis, A., 2019. Potential for mineral carbonation of CO_2 in Pleistocene basaltic rocks in Volos region (central Greece). Minerals, 9 (10), 627. https://doi.org/10.3390/min9100627.

Lamur, A., Kendrick, J.E., Eggertsson, G.H., Wall, R.J., Ashworth, J.D., Lavallée, Y., 2017. The permeability of fractured rocks in pressurized volcanic and geothermal systems. Sci. Rep. 7 (1), 1–9. https://doi.org/10.1038/s41598-017-05460-4.

Larkin, P., Gracie, R., Shafiei, A., Dusseault, M., Sarkarfarshi, M., Aspinall, W., Krewski, D., 2019. Uncertainty in risk issues for carbon capture and geological storage: findings from a structured expert elicitation. 10.1504/IJRAM.2019.103335.

Lavalleur, H.J., Colwell, F.S., 2013. Microbial characterization of basalt formation waters targeted for geological carbon sequestration. FEMS Microbiol. Ecol. 85 (1), 62–73. https://doi.org/10.1111/1574-6941.12098.

Leung, D.Y., Caramanna, G., Maroto-Valer, M.M., 2014. An overview of current status of carbon dioxide capture and storage technologies. Renew. Sustain. Energy Rev. 39, 426–443. https://doi.org/10.1016/j.rser.2014.07.093.

Lima, R.O., de L Cunha, A., Santos, J.A.O., Garcia, A.J.V., dos Santos, J.P.L., 2020. Assessment of continuous and alternating CO_2 injection under Brazilian-pre-salt-like conditions. J. Pet. Explor. Prod. Technol. 10 (7), 2947–2956. https://doi.org/10.1007/s13202-020-00968-4.

Liu, D., Agarwal, R., Li, Y., Yang, S., 2019. Reactive transport modeling of mineral carbonation in unaltered and altered basalts during CO_2 sequestration. Int. J. Greenhouse Gas Control 85, 109–120. https://doi.org/10.1016/j.ijggc.2019.04.006.

Lobo, J.T., Duarte, B.P., Szatmari, P., de Castro Valente, S., 2007. Basaltos continentais do Cretáceo Inferior da bacia de Campos, SE do Brasil: compilação de dados e petrogênese. Braz. J. Geol. 37 (2), 224–236.

Luhmann, A.J., Tutolo, B.M., Bagley, B.C., Mildner, D.F., Seyfried Jr, W.E., Saar, M.O, 2017. Permeability, porosity, and mineral surface area changes in basalt cores induced by reactive transport of CO_2-rich brine. Water Resour. Res. 53 (3), 1908–1927. https://doi.org/10.1002/2016WR019216.

Macente, A., Vanorio, T., Miller, K.J., Fusseis, F., Butler, I.B., 2019. Dynamic evolution of permeability in response to chemo-mechanical compaction. J. Geophys. Res. Solid Earth 124 (11), 11204–11217. https://doi.org/10.1029/2019JB017750.

Magee, C., Pichel, L.M., Madden-Nadeau, A.L., Jackson, C.A.L., Mohriak, W., 2021. Salt–magma interactions influence intrusion distribution and salt tectonics in the Santos Basin, offshore Brazil. Basin Res. 33 (3), 1820–1843. https://doi.org/10.1111/bre.12537.

Marieni, C., Voigt, M., Clark, D.E., Gíslason, S.R., Oelkers, E.H., 2021. Mineralization potential of water-dissolved CO_2 and H_2S injected into basalts as function of temperature: freshwater versus Seawater. Int. J. Greenhouse Gas Control 109, 103357. https://doi.org/10.1016/j.ijggc.2021.103357.

Marins, G.M., Parizek-Silva, Y., Millett, J.M., Jerram, D.A., Rossetti, L.M., e Souza, A.D. J., Planke, S., Bevilaqua, L.A., Carmo, I.D.O., 2022. Characterization of volcanic reservoirs; insights from the Badejo and Linguado oil field, Campos Basin, Brazil. Mar. Pet. Geol., 105950 https://doi.org/10.1016/j.marpetgeo.2022.105950.

Martin-Roberts, E., Scott, V., Flude, S., Johnson, G., Haszeldine, R.S., Gilfillan, S., 2021. Carbon capture and storage at the end of a lost decade. One Earth 4 (11), 1569–1584. https://doi.org/10.1016/j.oneear.2021.10.002.

Matias, H.C., Ninci, B., Guangsheng, X., Pessoa, M.C., Mattos, F., Margem, R., Carballo, J., Esteban, M., Tritlla, R., Loma, R., Pimentel, G., 2015. Unlocking Pandora-Insights from Pre-salt Reservoirs in Campos and Santos Basins (Offshore Brazil). In: Proceedings of the 77th EAGE Conference and Exhibition 2015, 2015. European Association of Geoscientists & Engineers, pp. 1–5. https://doi.org/10.3997/2214-4609.201412891.

Matter, J.M., Stute, M., Hall, J., Mesfin, K., Snæbjörnsdóttir, S.Ó., Gislason, S.R., Oelkers, E.H., Sigfusson, B., Gunnarsson, I., Aradottir, E.S., Alfredsson, H.A., Gunnlaugsson, E., Broecker, W.S., 2014. Monitoring permanent CO_2 storage by in situ mineral carbonation using a reactive tracer technique. Energy Procedia 63, 4180–4185. https://doi.org/10.1016/j.egypro.2014.11.450.

McGrail, B.P., Schaef, H.T., Ho, A.M., Chien, Y.J., Dooley, J.J., Davidson, C.L., 2006. Potential for carbon dioxide sequestration in flood basalts. J. Geophys. Res. Solid Earth 111 (B12). https://doi.org/10.1029/2005JB004169.

McGrail, B.P., Spane, F.A., Amonette, J.E., Thompson, C.R., Brown, C.F., 2014. Injection and monitoring at the Wallula basalt pilot project. Energy Procedia 63, 2939–2948. https://doi.org/10.1016/j.egypro.2014.11.316.

McGrail, B.P., Schaef, H.T., Spane, F.A., Horner, J.A., Owen, A.T., Cliff, J.B., Qafoku, O., Thompson, C.J., Sullivan, E.C., 2017. Wallula basalt pilot demonstration project: post-injection results and conclusions. Energy Procedia 114, 5783–5790. https://doi.org/10.1016/j.egypro.2017.03.1716.

Mechleri, E., Brown, S., Fennell, P.S., Mac Dowell, N., 2017. CO_2 capture and storage (CCS) cost reduction via infrastructure right-sizing. Chem. Eng. Res. Des. 119, 130–139. https://doi.org/10.1016/j.cherd.2017.01.016.

Milani, E.J., Thomaz Filho, A., 2000. Sedimentary basins of south America. Tectonic Evol. South Am. 31, 389–449.

Mizuno, T.A., Mizusaki, A.M.P., Lykawka, R., 2018. Facies and paleoenvironments of the Coqueiros Formation (Lower Cretaceous, Campos Basin): a high frequency stratigraphic model to support pre-salt "coquinas" reservoir development in the Brazilian continental margin. J. South Am. Earth Sci. 88, 107–117. https://doi.org/10.1016/j.jsames.2018.07.007.

Mizusaki, A.M.P., Filho, A.T., Valença, J., 1988. Volcano sedimentary sequence of neocomian age in Campos Basin (Brazil). Rev. Bras. Geociências, 18 (3), 247–251.

Mizusaki, A.M.P., 1986. Rochas igneo-básicas do neocomiano da Bacia de Campos: caracterização e comportamento como reservatório de hidrocarbonetos. Anuário do Instituto de Geociências 16, 77–78.

Moghanloo, R.G., Yan, X., Law, G., Roshani, S., Babb, G., Herron, W., 2017. Challenges associated with CO2 sequestration and hydrocarbon recovery. In: Recent Advances in Carbon Capture and Storage. pp. 209.

Mohriak, W.U., Mello, M.R., Dewey, J.F., Maxwell, J.R., 1990. Petroleum geology of the Campos Basin, offshore Brazil. Geol. Soc. 50 (1), 119–141. https://doi.org/10.1144/GSL.SP.1990.050.01.07.

Navarro, J., Teramoto, E.H., Engelbrecht, B.Z., Kiang, C.H., 2020. Assessing hydrofacies and hydraulic properties of basaltic aquifers derived from geophysical logging. Braz. J. Geol. 50 (04) https://doi.org/10.1590/2317-4889202020200013.

Neves, I.D.A., Lupinacci, W.M., Ferreira, D.J.A., Zambrini, J.P.R., Oliveira, L.O.A., Azul, M.O., Ferrari, A.L., Gamboa, L.A.P., 2019. Presalt reservoirs of the Santos Basin: cyclicity, electrofacies, and tectonic-sedimentary evolution. Interpretation 7 (4), SH33–SH43. https://doi.org/10.1190/INT-2018-0237.1.

Ning, L., Dexing, Q., Qingfeng, L., Hongliang, W., Youshen, F., Lixin, D., Qingfu, F., Kewen, W., 2009. Theory on logging interpretation of igneous rocks and its

application. Pet. Explor. Dev. 36 (6), 683–692. https://doi.org/10.1016/S1876-3804(10)60002-X.
Oreiro, S.G., 2006. Interpretação sísmica dos eventos magmáticos pós-aptianos no Alto de Cabo Frio, sudeste do Brasil, gênese e relação com os lineamentos pré-Sal. http://www.bdtd.uerj.br/handle/1/7000.
Pawar, R.J., Bromhal, G.S., Carey, J.W., Foxall, W., Korre, A., Ringrose, P.S., Tucker, O., Watson, M.N., White, J.A., 2015. Recent advances in risk assessment and risk management of geologic CO_2 storage. Int. J. Greenhouse Gas Control 40, 292–311. https://doi.org/10.1016/j.ijggc.2015.06.014.
Pereira, P., Ribeiro, C., Carneiro, J., 2021. Identification and characterization of geological formations with CO_2 storage potential in Portugal. Pet. Geosci. 27 (3) https://doi.org/10.1144/petgeo2020-123.
Pogge von Strandmann, P.A., Burton, K.W., Snæbjörnsdóttir, S.O., Sigfússon, B., Aradóttir, E.S., Gunnarsson, I., Alfredsson, H.A., Mesfin, K.G., Oelkers, E.H., Gislason, S.R., 2019. Rapid CO_2 mineralisation into calcite at the CarbFix storage site quantified using calcium isotopes. Nat. Commun. 10 (1), 1–7. https://doi.org/10.1038/s41467-019-10003-8.
Ratouis, T.M., Snæbjörnsdóttir, S.Ó., Voigt, M.J., Sigfússon, B., Gunnarsson, G., Aradóttir, E.S., Hjörleifsdóttir, V., 2022. CarbFix2: a transport model of long-term CO_2 and H_2S injection into basaltic rocks at Hellisheidi, SW-Iceland. Int. J. Greenhouse Gas Control 114, 103586. https://doi.org/10.1016/j.ijggc.2022.103586.
Raza, A., Glatz, G., Gholami, R., Mahmoud, M., Alafnan, S., 2022. Carbon mineralization and geological storage of CO_2 in basalt: mechanisms and technical challenges. Earth Sci. Rev. 229, 104036 https://doi.org/10.1016/j.earscirev.2022.104036.
Reis, G.D.S., 2013. A formação Serra Geral (cretáceo, bacia do Paraná) como análogo para os reservatórios ígneo-básicos da margem continental brasileira. http://hdl.handle.net/10183/72233.
Ren, K., Zhao, J., Liu, Q., Zhao, J., 2020. Hydrocarbons in igneous rock of Brazil: a review. Pet. Res. 5 (3), 265–275. https://doi.org/10.1016/j.ptlrs.2020.06.001.
Rockett, G.C., Ketzer, J.M.M., Ramírez, A., Van den Broek, M., 2013. CO_2 storage capacity of Campos Basin's oil fields, Brazil. Energy Procedia 37, 5124–5133. https://doi.org/10.1016/j.egypro.2013.06.427.
Rosa, M.C., Vincentelli, M.G.C., 2017. Seismic Attribute Analysis in carbonate reservoir physical properties distribution: neobarremian-Eoaptian coquina reservoir case. In: Proceedings of the 15th International Congress of the Brazilian Geophysical Society & EXPOGEF. Brazilian Geophysical Society, pp. 270–273. https://doi.org/10.1190/sbgf2017-053. Rio de Janeiro, Brazil, 31 July-3 August 2017.
Rossetti, L., Lima, E.F., Waichel, B.L., Hole, M.J., Simões, M.S., Scherer, C.M., 2018. Lithostratigraphy and volcanology of the Serra Geral Group, Paraná-Etendeka Igneous Province in Southern Brazil: towards a formal stratigraphical framework. J. Volcanol. Geotherm. Res. 355, 98–114. https://doi.org/10.1016/j.jvolgeores.2017.05.008.
Rubin, E.S., Davison, J.E., Herzog, H.J., 2015. The cost of CO_2 capture and storage. Int. J. Greenhouse Gas Control 40, 378–400. https://doi.org/10.1016/j.ijggc.2015.05.018.
Rubin, E.S., Short, C., Booras, G., Davison, J., Ekstrom, C., Matuszewski, M., McCoy, S., 2013. A proposed methodology for CO_2 capture and storage cost estimates. Int. J. Greenhouse Gas Control 17, 488–503. https://doi.org/10.1016/j.ijggc.2013.06.004.
Sampaio, M.A., de Mello, S.F., Schiozer, D.J., 2020. Impact of physical phenomena and cyclical reinjection in miscible CO_2-WAG recovery in carbonate reservoirs. J. Pet. Explor. Prod. Technol. 10 (8), 3865–3881. https://doi.org/10.1007/s13202-020-00925-1.
Santos Neto, E.V., Cerqueira, J.R., Prinzhofer, A., 2012. Origin of CO_2 in Brazilian basins. Search Discovery Article 40969.
Schmelz, W.J., Hochman, G., Miller, K.G., 2020. Total cost of carbon capture and storage implemented at a regional scale: northeastern and midwestern United States. Interface Focus 10 (5), 20190065. https://doi.org/10.1098/rsfs.2019.0065.
Schwartz, M.O., 2018. The new Wallula CO_2 project may revive the old Columbia River Basalt (western USA) nuclear-waste repository project. Hydrogeol. J. 26 (1), 3–6. https://doi.org/10.1007/s10040-017-1632-y.
S&P Global, 2021, CCUS in the decarbonization of upstream production in Brazil. https://www.spglobal.com/commodityinsights/en/ci/research-analysis/ccus-in-the-decarbonization-of-upstream-production-in-brazil.html/(Accesed 27 December 2022).
Slagle, A.L., Goldberg, D.S., 2011. Evaluation of ocean crustal Sites 1256 and 504 for long-term CO_2 sequestration. Geophys. Res. Lett. 38 (16) https://doi.org/10.1029/2011GL048613.
Smith, E., Morris, J., Kheshgi, H., Teletzke, G., Herzog, H., Paltsev, S., 2021. The cost of CO_2 transport and storage in global integrated assessment modeling. Int. J. Greenhouse Gas Control 109, 103367. https://doi.org/10.1016/j.ijggc.2021.103367.
Snæbjörnsdóttir, S.Ó., Wiese, F., Fridriksson, T., Ármansson, H., Einarsson, G.M., Gislason, S.R., 2014. CO_2 storage potential of basaltic rocks in Iceland and the oceanic ridges. Energy Procedia 63, 4585–4600. https://doi.org/10.1016/j.egypro.2014.11.491.
Snæbjörnsdóttir, S.Ó., Gislason, S.R., Galeczka, I.M., Oelkers, E.H., 2018. Reaction path modelling of in-situ mineralisation of CO_2 at the CarbFix site at Hellisheidi, SW-Iceland. Geochim. Cosmochim. Acta 220, 348–366. https://doi.org/10.1016/j.gca.2017.09.053.
Snæbjörnsdóttir, S.Ó., Sigfússon, B., Marieni, C., Goldberg, D., Gislason, S.R., Oelkers, E.H., 2020. Carbon dioxide storage through mineral carbonation. Nat. Rev. Earth Environ. 1 (2), 90–102. https://doi.org/10.1038/s43017-019-0011-8.
Span, R., Wagner, W., 1996. A new equation of state for carbon dioxide covering the fluid region from the triple-point temperature to 1100K at pressures up to 800MPa. J. Phys. Chem. Ref. Data 25 (6), 1509–1596. https://doi.org/10.1063/1.555991.
Stenhouse, M.J., Gale, J., Zhou, W., 2009. Current status of risk assessment and regulatory frameworks for geological CO_2 storage. Energy Procedia 1 (1), 2455–2462. https://doi.org/10.1016/j.egypro.2009.02.007.
Stica, J.M., Zalán, P.V., Ferrari, A.L., 2014. The evolution of rifting on the volcanic margin of the Pelotas Basin and the contextualization of the Paraná–Etendeka LIP in the separation of Gondwana in the South Atlantic. Mar. Pet. Geol. 50, 1–21. https://doi.org/10.1016/j.marpetgeo.2013.10.015.
Takagi, M., Koide, K., Shimizu, J., Iwamoto, C., Ohoka, M., Ikeda, S., Azuma, H., 2013. Cost estimates for the CO_2 geological storage in deep saline aquifers offshore Japan: a case study. Energy Procedia 37, 3374–3378. https://doi.org/10.1016/j.egypro.2013.06.225.
Tang, H., Tian, Z., Gao, Y., Dai, X., 2022. Review of volcanic reservoir geology in China. Earth Sci. Rev., 104158
Tutolo, B.M., Awolayo, A., Brown, C., 2021. Alkalinity generation constraints on basalt carbonation for carbon dioxide removal at the gigaton-per-year scale. environmental. Sci. Technol. 55 (17), 11906–11915. https://doi.org/10.1021/acs.est.1c02733.
Viglio, J.E., Giulio, G., Di, M., Ferreira, L.D.C., 2017. Not all glitters in the black gold: uncertainties and environmental threats of the Brazilian pre-salt. Ambiente Soc. 20, 21–38. https://doi.org/10.1590/1809-4422ASOC58R3V2032017.
Vilarrasa, V., 2014. Impact of CO_2 injection through horizontal and vertical wells on the caprock mechanical stability. Int. J. Rock Mech. Min. Sci. 66, 151–159. https://doi.org/10.1016/j.ijrmms.2014.01.001.
Vilarrasa, V., Carrera, J., 2015. Geologic carbon storage is unlikely to trigger large earthquakes and reactivate faults through which CO_2 could leak. Proc. Natl. Acad. Sci. 112 (19), 5938–5943. https://doi.org/10.1073/pnas.1413284112.
Wang, Y., Yang, R., Song, M., Lenhardt, N., Wang, X., Zhang, X., Yang, S., Wang, J., Cao, H., 2018. Characteristics, controls and geological models of hydrocarbon accumulation in the Carboniferous volcanic reservoirs of the Chunfeng Oilfield, Junggar Basin, Northwestern China. Mar. Pet. Geol. 94, 65–79. https://doi.org/10.1016/j.marpetgeo.2018.04.001.
Warren, J.K., 2017. Salt usually seals, but sometimes leaks: implications for mine and cavern stabilities in the short and long term. Earth Sci. Rev. 165, 302–341. https://doi.org/10.1016/j.earscirev.2016.11.008.
White, S.K., Spane, F.A., Schaef, H.T., Miller, Q.R., White, M.D., Horner, J.A., McGrail, B.P., 2020. Quantification of CO_2 mineralization at the Wallula basalt pilot project. Environ. Sci. Technol. 54 (22), 14609–14616. https://doi.org/10.1021/acs.est.0c05142.
Xing, T., Zhu, W., Fusseis, F., Lisabeth, H., 2018. Generating porosity during olivine carbonation via dissolution channels and expansion cracks. Solid Earth 9 (4), 879–896. https://doi.org/10.5194/se-9-879-2018.
Xing, T., Ghaffari, H.O., Mok, U., Pec, M., 2022. Creep of CarbFix basalt: influence of rock–fluid interaction. Solid Earth 13 (1), 137–160. https://doi.org/10.5194/se-13-137-2022.
Zahasky, C., Thomas, D., Matter, J., Maher, K., Benson, S.M., 2018. Multimodal imaging and stochastic percolation simulation for improved quantification of effective porosity and surface area in vesicular basalt. Adv. Water Resour. 121, 235–244. https://doi.org/10.1016/j.advwatres.2018.08.009.
Zakharova, N.V., Goldberg, D.S., Sullivan, E.C., Herron, M.M., Grau, J.A., 2012. Petrophysical and geochemical properties of Columbia River flood basalt: implications for carbon sequestration. Geochem. Geophys. Geosyst. 13 (11) https://doi.org/10.1029/2012GC004305.
Zappone, A., Rinaldi, A.P., Grab, M., Wenning, Q.C., Roques, C., Madonna, C., Obermann, A.C., Bernasconi, S.M., Brennwald, M.S., Kipfer, R., Soom, F., Cook, P., Guglielmi, Y., Nussbaum, C., Giardini, D., Mazzotti, M., Wiemer, S., 2021. Fault sealing and caprock integrity for CO_2 storage: an in situ injection experiment. Solid Earth 12, 319–343. https://doi.org/10.5194/se-12-319-2021.

Journal of South American Earth Sciences

USING LEGACY DATA FROM THE OIL INDUSTRY TO EVALUATE VOLCANIC FORMATIONS FOR GEOLOGICAL CO2 STORAGE: A CASE STUDY FROM THE CAMPOS BASIN, BRAZIL

--Manuscript Draft--

Manuscript Number:	SAMES-D-25-00071
Article Type:	Research Paper
Section/Category:	Geophysics, geochemistry, volcanology, igneous and metamorphic petrology
Keywords:	Geological CO2 Storage (GCS); CO2 mineralization mechanism; Offshore GCS; Artificial neural network; Reservoir modeling
Corresponding Author:	GERMANO MARIO SILVA RAMOS, M.D. Universidade Federal de Pernambuco Centro de Tecnologia e Geociencias Recife, PE BRAZIL
First Author:	GERMANO MARIO SILVA RAMOS, M.D.
Order of Authors:	GERMANO MARIO SILVA RAMOS, M.D.
	José Antonio Barbosa
	Osvaldo José Correia Filho
	Carla Joana Barreto
	Jefferson Tavares Cruz Oliveira
	Tiago Siqueira de Miranda
	Aline Macrina da Silva
	Roberta Samico de Medeiros
	Tallys Celso Mineiro
Abstract:	Geological CO2 storage (GCS) in basaltic/volcanic formations is a promising avenue for mitigating anthropogenic emissions of greenhouse gases because these regions can effectively trap CO2 via mineralization. However, implementing CO2 storage projects in offshore regions demands significant investment due to the requirement to explore vast areas as well as characterize any potential prospects to verify their technical and economic feasibility. Legacy data from the oil industry could be used to provide an initial assessment of potential prospects in sedimentary basins with volcanic formations. In this study, we demonstrate the immense value of legacy products, including seismic and well log data, to identify zones with higher potential for CO2 storage. A case study was conducted on the unconventional, mature volcanic oil reservoir of the Badejo Field in the Campos Basin, Brazil, located within the basaltic Cabiúnas Formation. These flood basalts are located on continental platforms and thus represent promising opportunities for potential GCS projects in shallow water domains. Understanding the mechanism of hydrocarbon migration and accumulation in these reservoirs will provide insights into the factors that control fluid flow in basaltic rocks. We find that the relationship between faults/fractures and the apparent porosity of the volcanic succession is critical for predicting the reservoir response to CO2 injection. This investigation used industry-standard tools, including attribute analysis and porosity estimation based on an acoustic impedance inversion method. The legacy data allowed us to characterize the complex relationships between fractures and aspects such as paleo-topography and the control of fault zones on lateral flow. Understanding these controls on fluid flow can help identify regions with high potential for GCS project development. Legacy data from the oil industry that covers offshore regions that contain volcanic successions thus represents a valuable resource that can help save costs and accelerate the development of GCS projects.
Suggested Reviewers:	Helio Jorge Portugal Severiano Ribeiro State University of Norte Fluminense severian@lenep.uenf.br

	Nick Schofield University of Aberdeen n.schofield@abdn.ac.uk
	Sreedurga Somasundaram Cairn Oil & Gas (Vedanta Limited) sreedurga.somasundaram@cairnindia.com
	Rahman Ashena University of Mining Leoben rahman.ashena.313@gmail.com
	Satinder Chopra Samigeo satinder.chopra@samigeo.com
Opposed Reviewers:	

5 ARTIGO 2

USING LEGACY DATA FROM THE OIL INDUSTRY TO EVALUATE VOLCANIC FORMATIONS FOR CO_2 GEOLOGICAL STORAGE: THE CASE OF CAMPOS BASIN, BRAZIL

Germano Mário da Silva Ramos[1], José Antonio Barbosa[1], Osvaldo José Correia Filho[1,2], Carla Joana Barreto[1], Jefferson Tavares Cruz Oliveira[1], Tiago Siqueira de Miranda[1,2], Aline Macrina da Silva[1], Roberta Samico de Medeiros[1],Tallys Celso Mineiro[1]

[1]GEOQUANTT Research Group, Geology Department, Federal University of Pernambuco. Av. da Arquitetura s/n, Cidade Universitária, Recife, Brazil. 50740-550.

[2]MODLAB, Institute for Petroleum and Energy Research i-LITPEG, Federal University of Pernambuco. Av. da Arquitetura s/n, Cidade Universitária, Recife, Brazil. 50740-550.

Abstract

The CO_2 geological storage (GCS) in basaltic/volcanic formations represents a promising technology to help mitigate greenhouse gas anthropogenic emissions because it improves the definitive CO_2 trapping through the mineralization mechanism. However, implementing CO_2 storage projects in offshore regions will demand investment in exploring vast areas, and the characterization of prospects to confirm their technical and economic feasibility. In this context, legacy data from the oil industry could be used for at least an initial assessment of potential prospects in sedimentary basins with volcanic formations. In this study we demonstrated the immense value of legacy products, seismic and well log data, to identify zones with higher potential for CO_2 storage. It focused on the mature unconventional volcanic oil reservoir of the Badejo Field, in the Campos Basin, Brazil, formed in the basaltic Cabiúnas Formation. These flooding basalts are located in the platform regions, representing a good potential for GCS projects in the shallow water domains. We aimed to study the mechanism of hydrocarbon migration and accumulation in these reservoirs to help understand aspects that will control fluid flow in basaltic rocks. We emphasized the relationship between faults/fractures and the apparent porosity of the volcanic succession because it is critical to predict further aspects of CO_2 injection. The investigation used industry-standard tools including attribute

analysis and porosity estimation based on an acoustic impedance inversion method. The legacy data allowed us to access the complex interplay between fractures and other aspects like the paleo topography, and fault zone control on lateral flow. Understanding these flow-controlling parameters can be used to define prospects with good potential for GCS project development. Thus, legacy data covering offshore regions containing volcanic successions worldwide represents a valuable resource to save costs and improve/accelerate the development of GCS projects.

Keywords: CO_2 Geological Storage (GCS), CO_2 mineralization mechanism, Offshore GCS, Artificial Neural Network, Reservoir modeling

1. Introduction

Geological CO_2 storage (GCS), is a critical part of the measures needed to reduce the global emissions of this greenhouse gas in the next decades (Alcalde et al., 2018; IPCC, 2019; Zahasky and Krevor, 2020; Vitillo et al., 2022). The present CO_2 capture and sequestration projects, which involve geological storage (CCS), or the use and storage (CCUS) like the EOR (Enhanced Oil Recovery) methods, can remove only tens of millions of CO_2 per year (Zhang et al., 2022; Dziejarski et al., 2023; McLaughlin et al., 2023). However, to achieve the ambitious goal of net zero emissions in the next decades we should develop projects capable of storing billions of tons of CO_2 annually (Chen et al., 2022; Fuss et al., 2020). That will demand drilling tens of thousands of wells in continental margins, for example (Ringrose and Meckel, 2019). Zhang et al (2022) suggested that an estimated 29 Mt of CO_2 was stored in 2019, and an estimated 197 Mt was stored in the 1996-2020 period. It demonstrates that the GCS technology is evolving, but to avoid the worst scenarios caused by CO_2 atmospheric concentration, the amount of CO_2 stored in geological reservoirs needs to increase drastically. The IEA (2021) suggests that to achieve the 2°C target of temperature increase by 2050 the volume of cumulative CO_2 mitigation should reach 92 Gt (gigatons), which highly depends on the contribution from the geological storage projects (Wei et al., 2020).

The technologies we can use for geological storage projects involve the injection of CO_2 in siliciclastic aquifers, depleted hydrocarbon reservoirs, coal seam deposits, artificial salt caves, and volcanic mafic rocks (Aydin et al., 2010; Ajayi et al., 2019; Ali et al., 2022; Khandoozi et al., 2023; Albertz et al., 2023; Mwakipunda et al., 2024).

The advantage of storage in volcanic rocks relies on the fact that fast reactive phenomena result in CO_2 trapping in the form of carbonate minerals into the reservoir, which reduces operation risks and monitoring costs (Kelemen et al., 2019; Snæbjörnsdóttir et al., 2020; Raza et al., 2022; Rasool and Ahmad, 2023; Sun et al., 2023; Cao et al., 2024). Mafic rocks formed in magmatic provinces (flood basalts) that are located in onshore and shallow marine regions are important prospects for GCS projects (Goldberg et al., 2010; Zakharova et al., 2012; Kumar & Shrivastava, 2019; Snæbjörnsdóttir et al., 2020; Chaudhary et al., 2022). The three injection pilots developed in basaltic rocks to date showed the success of the operations, and most of the CO_2 was incorporated in minerals in a period that is two orders of magnitude faster than expected for other lithologies (Clark et al., 2020; White et al., 2020; Snæbjörnsdóttir et al., 2020). Following these projects, some countries are planning to develop large projects that aim to inject CO_2 in flood basalt provinces and in the oceanic crust, such regions where the reactive phenomena will allow the permanent storage of billions of tons of CO_2, safely and more cheaply (Slagle et al., 2011; Goldberg et al., 2010; 2018; Snæbjörnsdóttir et al., 2020; Tutolo, et al., 2021; Sun et al., 2023; Nisbet et al., 2024). However, some aspects are still poorly known, like the effective analysis of the storage capacity in onshore and offshore volcanic rocks, and the repeatability of the success of the pilot projects for large commercial projects, which depends on the capacity of injection for long periods (decades) despite the eventual problems generated by the mineral precipitation in the porous network (Kelemen et al., 2019; Tutolo et al., 2021; Raza et al., 2022; Sun et al., 2023; Nisbet et al., 2024).

Ramos et al. (2023) demonstrated the potential of flood basalt formations that covered the basement of the continental platform of Campos Basin (Fig. 1), for the development of GCS projects. These authors proposed that basaltic formations in the shallow waters of the Campos Basin could store the expressive production of CO_2 associated with the production of the Brazil pre-salt hydrocarbon reservoirs (d´Almeida et al., 2018). The basaltic Cabiúnas Formation is related to the magmatism produced during the South Atlantic Ocean opening (Mizusaki et al., 1992; Mohriak et al., 1990; de Castro & Picolini, 2016) (Figs. 1 and 2). The continental lava flood that covered the basement of the continental margin of Campos Basin is related to the regional magmatism of the Paraná-Etendeka Province (Rossetti et al., 2019). This formation includes basaltic lava flows, volcaniclastic deposits, volcanic breccias, and local occurrences of diabase (Mizusaki, 1988; Mizusaki et al., 1992; Guardado et al., 1990; Marins et al., 2022; Braga et al., 2023).

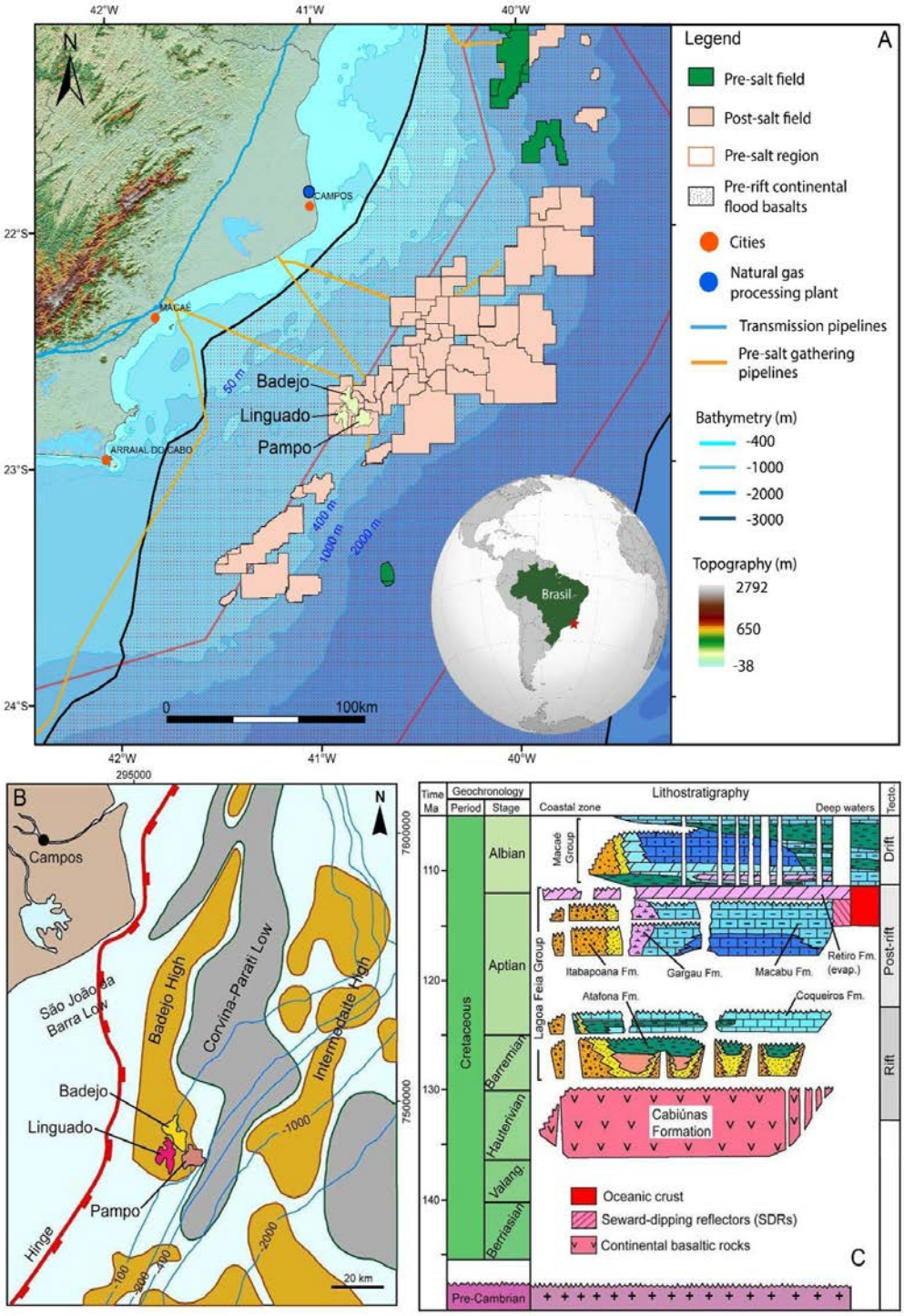

Figure 1 - A) Location of Campos Basin, Southeastern Brazil. Most of the fields found in the 1980s are within the isobath of 400 m, which includes the three fields with oil discoveries in volcanic reservoirs over the Badejo High - Badejo, Linguado, and Pampo (Source - ANP, 2023), B) A) Tectonic compartmentalization of proximal Campos Basin. The rift formed grabens and horsts aligned NE-SW. The regional Badejo High represents an elongated paleohigh that formed hydrocarbon traps, C) Stratigraphic chart of Campos Basin showing the Lower-Upper Cretaceous interval.

Wells drilled in the late 1970s found oil and gas in the Neocomian (120-130 m.y.) basaltic rocks below the pre-salt sequence composed by siliciclastic and carbonate rocks of the Lagoa Feia Group (Figs. 1 and 2) (Guardado et al., 1990; Bruhn et al., 2003). The volcanic reservoirs of the Cabiúnas Formation (Badejo Field) produced oil and gas from 1981 to 1990 (Bruhn et al., 2003; Marins, et al., 2022), with a total of 8.6 MMbbl (1.176 x 10^6 t) (Guardado et al., 1990; Ren et al., 2020). The volcanic reservoir interval of the Badejo Field produced oil and gas related to faults and fracture systems, formed mainly in vesicular basalt and volcanic breccias (Guardado et al., 1990; Bruhn et al., 2003). We argue that the advantage of storing CO_2 in these rocks relies on the fact that the region along the Badejo High is located in shallow waters, which is less costly to operate, and because of the proximity of the large emitter process (pre-salt oil production) and the potential advantage of the trapping mechanism (Figs. 1 and 2)

Ramos et al. (2023) first investigated the hypothetical potential for CO_2 storage in the Badejo volcanic reservoir region based on the analysis of legacy data acquired by the oil companies (Mizusaki et al., 1992; Marins et al., 2022). The available data included 3D seismic volumes and well logs, acquired by the oil industry from 1980 to 1990. The study explored the feasibility of injecting water-diluted CO_2 in the basaltic rocks to achieve safe and economical storage for the large volumes of CO_2 separated from the pre-salt reservoirs production (Fig. 1). Their analysis used reservoir parameters of the Badejo volcanic reservoir (pressure, temperature), and porosity data calculated from well logs (Rhob and DT), to estimate the CO_2 storage capacity in a hypothetical reservoir formed in the top of the basaltic succession. These parameters are critical for a preliminary evaluation of chemical and volumetric storage conditions (Kelemen et al., 2019; Tutolo et al., 2021; Raza et al., 2022). Ramos et al. (2023), showed that the volcanic reservoirs formed in the upper part of the Cabiúnas Formation are strongly bound by fault zones. The areas where the wells found commercial oil showed higher pressure and temperature values about the nearby regions, which suggests the structural control on the migration of hydrocarbons and other fluids through the basaltic successions (Guardado et al., 1990; Ramos et al., 2023).

The study of Ramos et al. (2023) claimed the importance of legacy data to access critical aspects of the volcanic formations for the initial investigation to find potential injection zones (depth, lithofacies, pore pressure, temperature, tectonic features, petrophysics) for developing GCS projects (McGrail et al., 2006, 2014; Zakharova et al., 2012; Snæbjörnsdóttir et al., 2018). Ramos et al., (2023) preliminarily discussed the relationship between fault zones, oil accumulations, and higher porosity zones.

Considering the context discussed above, the objective of the present study was to advance the demonstration of the importance of legacy data like the information available on the Badejo Field to help the industry access undrilled zones for CO_2 storage purposes. We used the publicly available seismic and well legacy data from the Badejo Field to verify the relationship between fracture patterns in the basaltic rocks and the reservoir quality (Walker et al., 2012; Fernández-Ibáñez al., 2022a, 2022b; Mendes et al., 2022). The investigation used commercial software to interpret and model seismic data, including creating a porosity model using an acoustic impedance inversion method (neural network plugin), filtering and seismic attributes extraction. The modeling of the data demonstrated the influence of regional faults and the fracturing forming compartments with higher porosity values (Sun et al., 2018; Jia et al., 2019; Navarro et al., 2020; Fan et al., 2020; Ruz-Ginouves et al., 2021). Results showed that regional faults, fracture intensity, and connectivity are critical factors for the quality of volcanic reservoirs in the context studied, and for the formation/evolution of compartments that would impact injection operations. Also, we showed the influence of fracture intensity, as well as horizontal and vertical fracture connectivity on the fluids flow. By comprehending the mechanism of oil migration in these volcanic reservoirs we potentially access the mechanisms which will influence the CO_2 storage aspects like injectivity and volume capacity, controlled by structural compartmentalization. Thus, legacy data will represent critical resources, saving time and investments in implementing GCS projects. In magmatic provinces, as demonstrated in southeastern Brazil, it can allow the definition of prospective areas in offshore domains, which present large advantages in terms of safety, and vast storage volume.

1.1 Geological Setting

The Campos Basin encompasses part of the coastal zone of the Rio de Janeiro and Espírito Santo States (Fig. 1), Southeast Brazil. It is bounded to the north by the Vitória High, and to the South by the Cabo Frio High, and covers approximately 100,000 km^2. The rift phase of Campos Basin exhibits a series of synthetic and antithetic regional faults that formed a succession of grabens and horsts predominantly aligned in the NE-SW direction (Bruhn et al., 2003; Stanton et al., 2019; Strugale et al., 2021) (Fig. 1). The rift compartmentalization can be divided into two hinge zones (de Castro & Picolini, 2015), the inner edge, that is formed by a fault that controlled the São Tomé low and present expressive reactivation during the Cenozoic, and the outer edge, that is formed by faults that outline the western flank of the external low. These outer edge faults present an NE-SW direction in the central part of the basin and turn to

the NE direction in the northern part of the basin. This outer edge also presents E-W displacements caused by transfer zones (de Castro & Picolini, 2016, Fetter, 2009).

The Badejo paleohigh represents an elongated structure trending NE-SW, which was involved in the formation of oil and gas fields bounded by normal faults that cut the Cabiúnas Formation and the overlying rift strata (Fig. 1). The Badejo, Linguado, and Pampo oil fields are located in the southern termination of this structure. According to Cobbold et al. (2001), during the Late Cretaceous and Cenozoic, this part of the southeastern Brazilian margin was subject to transtensional/transpressional reactivation. Three intervals of tectonic reactivation are recognized: the first during 90-80 M.y, a second in the period 50-40 M.y, and a third phase during 25-0 M.y. During the Paleocene-Eocene, the extensive magmatism that affected the southern region of the basin caused intrusions and reactivation of faults. Another event in the Neogene, mainly mid-Miocene, caused fault reactivation (de Castro & Picolini, 2015).

The sedimentary record of Campos Basin is divided into three major tectono-stratigraphic sequences: **Rift sequence**, which is composed of volcanic-sedimentary rocks spanning the Hauterivian to Early Aptian. The Hauterivian interval includes the Cabiúnas Formation basaltic rocks and minor siliciclastics. The Barremian to Early Aptian interval includes lacustrine carbonates and shales from the Lagoa Feia Group (Fig. 1). These shales represent the main source rock of the basin, and the carbonates of this interval formed good-quality hydrocarbon reservoirs; **The transitional sequence**, which spans the Middle-Late Aptian, is composed of siliciclastic, carbonate and evaporites rocks and forms the upper part of the Lagoa Feia Group (Figs 1 and 2); **Post-rift/Drift Sequence**, is composed of an Albian-Cenomanian interval of carbonate and siliciclastic deposits that forms the Macaé Group. The Campos Group comprises the Turonian-Eocene interval, which is composed of siliciclastics and marls, and a succession of coarse-grained sandstones, platform carbonates and distal mudstones spanning the Eocene-Holocene interval (Fig. 1) (Guardado et al., 1990; Mizusaki et al., 1992; Winter et al., 2007; de Castro & Picolini, 2015; Stanton et al., 2019).

The extensive Early Cretaceous volcanic rocks that covered the basement of Campos Basin are related to the Paraná-Etendeka Magmatism recorded in the Paraná Basin, dated 140-134 M.y (Mizusaki et al., 1992). According to Mizusaki et al. (1992), the Cabiúnas basaltic formation represents an easterly younger extension of the Paraná Province magmatism, which erupted during the early rift stages in this region. This formation includes subalkaline tholeiitic basalts, diabase, volcanic breccias, tuffs, peperites, and volcaniclastic rocks (Mizusaki, 1988; Marins et al., 2022; Braga et al., 2023).

The Badejo-Linguado-Pampo trend comprises a series of oil and gas reservoirs found in the shallow waters of the Campos Basin (80 - 120 m) (Figs. 1 and 2), over the southern part of the Badejo High. The wells drilled in this region found commercial oil reserves in carbonate reservoirs (coquinas) below the evaporite bed in the rift sequence (Lagoa Feia Group) (Figs. 1 and 2). About 64 wells were drilled into the fractured basaltic deposits of the Cabiúnas Formation, which formed the economic basement of Campos Basin, and 6 wells found commercial oil reserves, 7 found non-commercial oil and 51 found no oil (Figs. 2 and 3) (Guardado et al., 1990; Mizusaki et al., 1992; Bruhn et al., 2003). Guardado et al. (1990), observed that the production from the basalts was very dependent on the fracturing system and lithofacies nature of the volcanic rocks. Bruhn et al. (2003) stated that the oil (with 28 - 32° API) is contained in fractures, vugs, and vesicular zones and the accumulation was controlled by extensional faults of the rift phase that connected the fractured volcanic reservoir and source rocks (Fig. 2). These authors also commented that some faults present strike-slip regime and have sealing nature, compartmentalizing the reservoirs.

As observed in the tectono-stratigraphic section shown in Figure 2, the upper part of the thick basaltic sequence is in lateral contact with source rocks of the Lagoa Feia Group, through displacement created by rift faults. This lateral contact allowed the hydrocarbons to migrate into the fractured basaltic beds, which present zones with high porosity and permeability values (Fig. 2) (Guardado et al., 1990). However, the permeability was controlled not only by fracturing but also by syn-formational and diagenetic conditions. Subaerial formation and weathering seem to have a critical role in the quality of these reservoirs (Mizusaki, 1988; Mizusaki et al., 1992; Marins et al., 2022). The commercial oil occurrences are located in the Badejo Field, where the formation of the lava flows was dominated by subaerial conditions. Wells drilled in volcanic rocks formed south of Badejo into Linguado and Pampo fields, which presents evidence of transitional to shallow water conditions, showed that the basaltic rocks present lower porosity values (Ramos et al., 2023), and there was no commercial oil found. Figure 2 highlights that two wells drilled into the basalts forming the horst block of the Badejo Field found commercial oil in permeable rocks, and other near ones found no commercial accumulations, which indicates that the migration/accumulation was strongly controlled by some aspects.

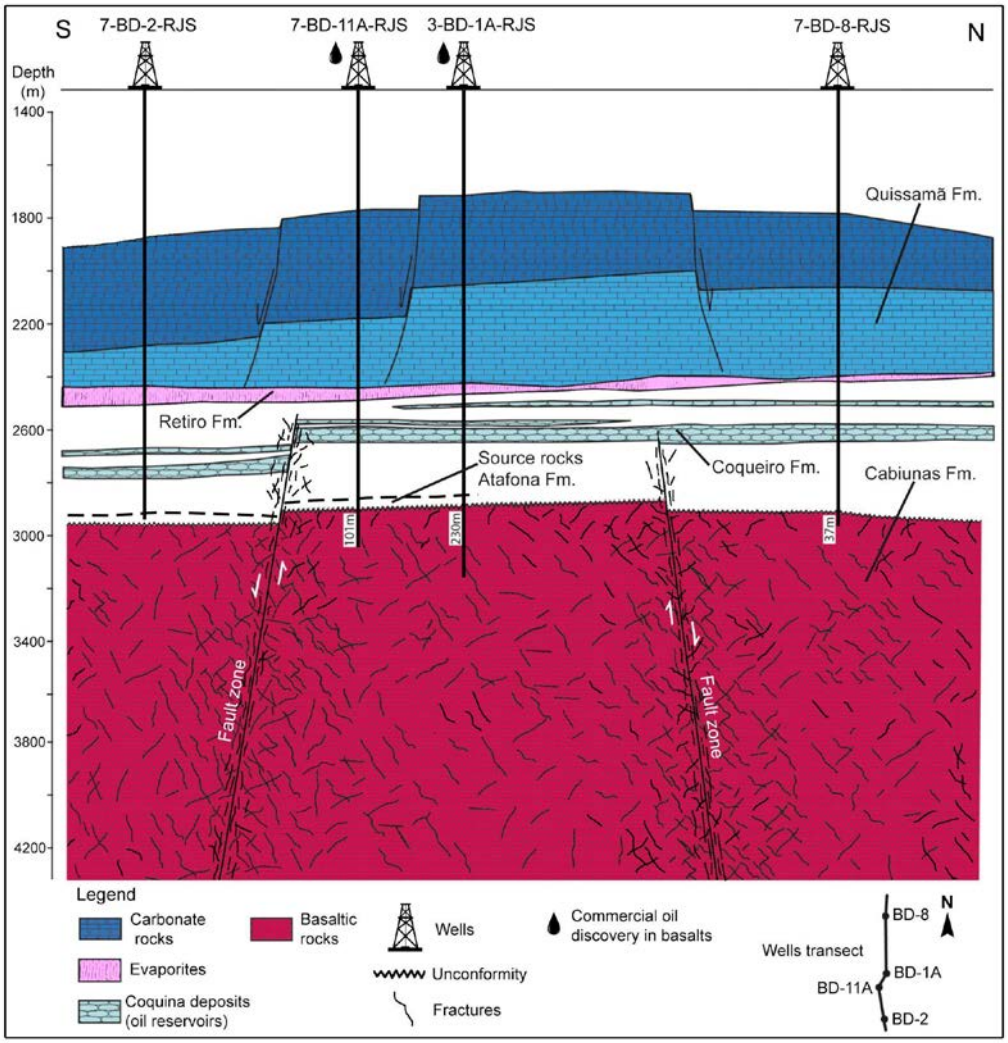

Figure 2 - Schematic structural section showing the relationship between the top of Cabiúnas basaltic rocks and the lower Cretaceous sedimentary succession, including rift and post-rift deposits. This representation shows the occurrence of oil discoveries in wells drilled into the basaltic rocks (Modified from Guardado et al., 1990, and Sampaio, 2012).

2. Materials and Methods

In this research we used a PSTM seismic volume (0307 - 3D PAMPO BADEJO LINGUADO), which covered the region of the three fields in the southern end of the Badejo High (Fig. 3). This survey presents a 6-second depth, and an area of 630 km^2. In the present research, we used the same set of well data used by Ramos et al. (2023) to analyze the characteristics of the basaltic succession and to guide the interpretation and modeling of the seismic volume used in the research (Figs. 3A and 3B).

Regarding the fact that the commercial oil accumulations in the volcanic reservoirs were located in the Badejo oil field (Guardado et al., 1990; Bruhn et al., 2003; Ramos et al., 2023; Marins et al., 2022), and that the volcanic succession showed better porosity values in this area (Ramos et al., 2023), we focused the study in a reduced block encompassing the Badejo Field region by cropping the original seismic volume (Fig. 3). The cropped time migrated volume comprises 13 x 17 km (235 km^2) and a depth of 4,5 seconds (Fig. 4). We used this volume for the calculation of the porosity cube using an inversion method based on the acoustic impedance data. Figure 3B exhibits the 3D visualization of the cropped seismic volume with the position of 6 wells that produced oil from the basaltic formation (Fig. 3A). The well data guided the interpretation of the seismic volume and creation of stratigraphic surfaces for the top of the volcanic succession. No well in this region reached the Precambrian basement, and the interpretation of this surface was based on the seismic features, and the other analysis by the literature (Fig. 3B). The thickness of the Cabiúnas Formation over the continental platform reaches maximum values between 800 and 1000 m (Mizusaki et al., 1992; Bruhn et al., 2003)

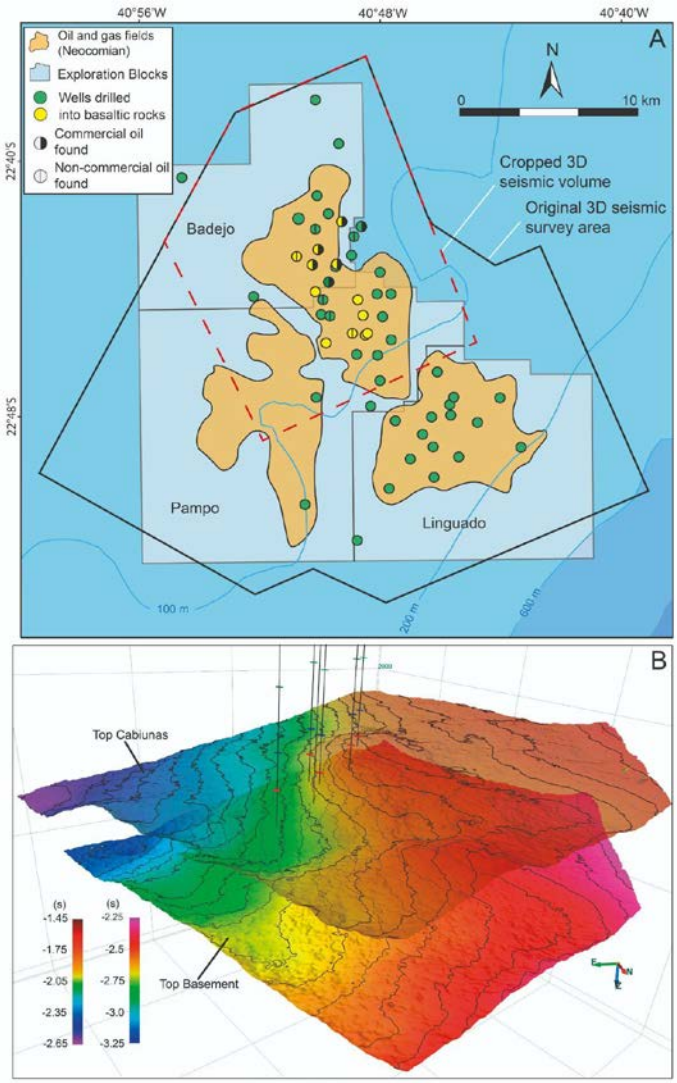

Figure 3 - A) Location of the original seismic survey used in the study, covering the Badejo, Pampo, and Linguado fields. The wells drilled into the basaltic Cabiúnas Formation used in the study are depicted. The dashed red rectangle indicates the cropped seismic volume used for this study. The yellow circles indicate the wells used to create the porosity cube. The location of the six wells that produced commercial oil, and six that found non-commercial oil are indicated. B) Surfaces interpreted in the cropped seismic volume delineating the top of the volcanic succession (Cabiúnas Fm.), and the top of the Precambrian basement. Markers: red - top of Cabiúnas Fm., blue - top of the Lagoa Feia Group, green - top of the Macaé Group.

After preliminary screening, twelve wells were selected to create the acoustic impedance data (Fig. 3A). These were chosen because of the data quality and the depth drilled into the volcanic succession (Table 1 - supplementary material). Coordinates, depth of the top of the Cabiúnas Formation, thickness drilled into the basaltic rocks, and the mean porosity of

the interval drilled are shown in Table 1. The acoustic impedance was used to create the porosity cube by applying a neural network plugin. Table 1 also shows the mean porosity value calculated from the density log of the selected wells.

The porosity logs were obtained through Equation 1, which used the RHOB (bulk density - g/cm³) log values to estimate the apparent porosity of the basaltic rocks (Fig. 4).

$$\textbf{Porosity} = \frac{Rhoma - Rhob}{Rhoma - Rhof} \quad \text{(Eq. 1)}$$

This approach is based on the relative constant density of basaltic rocks; thus, *Rhoma* represents the matrix density, *Rhob* refers to the apparent density, and *Rhof* represents the density of the fluid saturating the rock (brine). We have considered the massive fresh basalt (without porosity) as the reference matrix (*Rhoma*), with a value of 2,98 g/cm³, the density used for the fluid (*Rhof*) was 1 g/cm³ (Gupta et al., 2012).

An acoustic impedance log was also created, by using the data from the RHOB (density) and DT (formation sonic velocity - $\mu s/m$) logs (Fig. 4) (Gardner et al., 1974; Lindseth, 1979), by using Equation 2 (Fig. 4):

$$\textbf{AI} = \frac{Rhobv}{DTv} \quad \text{(Eq. 2)}$$

The $Rhob_v$ represents the value of the log in g/cm^3, and the DT_v represents the value of the acoustic signal in $\mu s/m$.

The log data used to create the impedance and porosity logs were analyzed to avoid spikes and artifacts. Data intervals with indications of problems (drilling reports, caliper log), were carefully screened and eventually discarded.

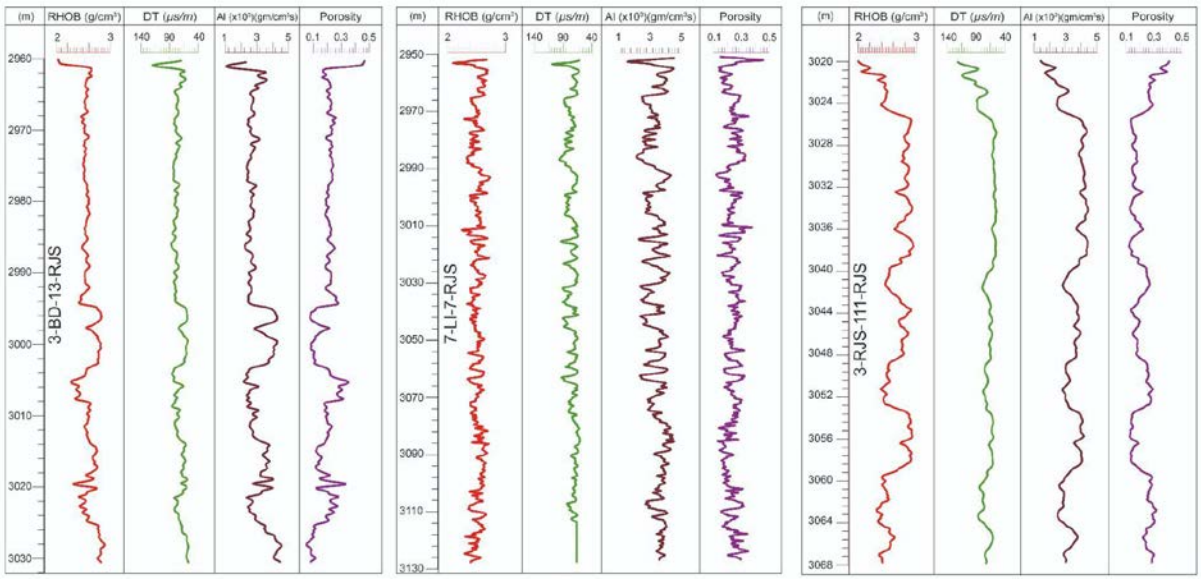

Figure 4 - Well log processing used in the study. Three examples of logs computed from the original borehole geophysical logs (density - RHOB, and sonic - DT). Acoustic impedance log (brown line) and porosity log (purple line).

Two procedures were adopted for the post-processing of the 3D seismic legacy data (Fig. 5): First, a dip steered cube was created to enhance the original data quality (Jibrin, 2014), second, three filters were applied on the steered cube: Dip Steered Median Filter, Ridge Enhancement Filter, and Fault Enhancement Filter, focusing on the detection of faults and fractures planes (Kumar & Mandal, 2018; Ismail et al., 2023) (Fig. 5). Second, a set of 6 seismic attributes were extracted from the steered seismic data. The attributes chosen are applied to detect and quantify discontinuities like faults and fractures (Kumar & Mandal, 2018; Ismail et al., 2023). The similarity attribute, which represents a coherence-type attribute, and the curvature attribute (most positive curvature), were used to highlight discontinuities created by faults and fractures in surfaces (Chopra & Marfurt, 2007a; Barnes, 2000; Taner et. al., 1994). The dip-azimuth attributes (dip angle and dip azimuth), were used to analyze the spatial behavior of fractures and faults (Marfurt et al., 1998; Chopra & Marfurt, 2007b; Barnes, 2000; Marfurt & Alves, 2015; Iacopini et al., 2016). The ridge enhancement filter highlights ridges in a similarity cube, and is useful to delineate fault zones (Bailey et. al., 2014). All the post-processing work was executed with the OpenDtect software (dGB Earth Sciences) (DGB Beheer, 2022).

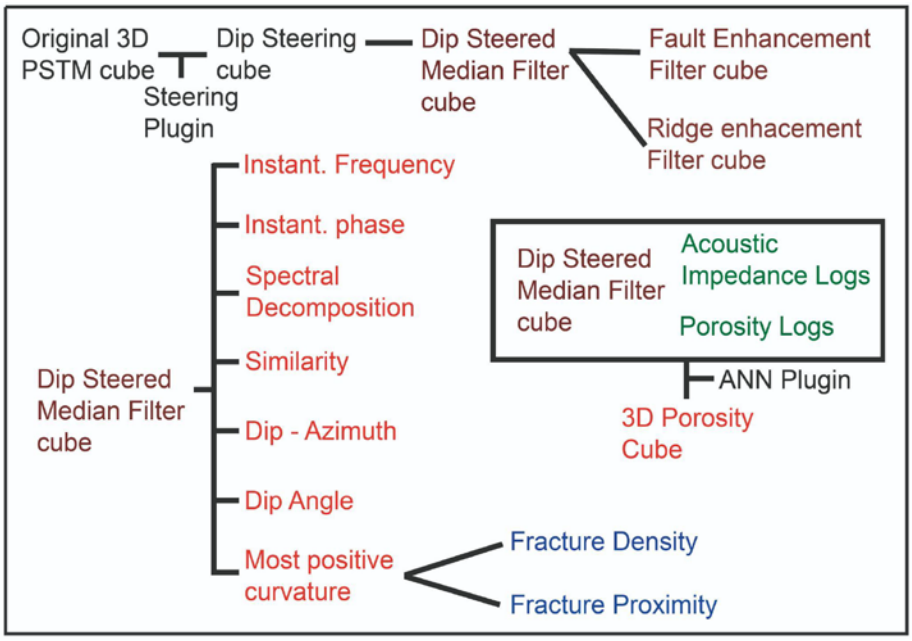

Figure 5 - Schematic chart showing the processing flow adopted for the cropped 3D seismic and well data. The well data was used to guide the seismic data interpretation and the creation of the porosity cube. Two meta-attributes (blue letters) were also extracted regarding fracture density and topology.

We also performed an analysis of the fracture traces interpreted on the surface of the top of the Cabiúnas Formation. This procedure aimed to capture the fracture network characteristics (Dershowitz & Einstein, 1988; Dershowitz & Herda, 1992; Rohrbaugh Jr et al., 2002). The discretization of the fracture networks can provide information about density and intensity parameters. Density represents the number of isolated fracture traces per unit length, area, or volume (Dershowitz & Einstein, 1988; Dershowitz & Herda, 1992; Rohrbaugh Jr et al., 2002). The fracture intensity (P21), considers density and size and represents the number of fractures per unit sample length, fracture length per unit surface area, or fracture area per unit rock volume, regarding 2D or 3D dimensions. We analyzed the Cabiúnas Formation subsurface, therefore the density related to fracture length per unit area. To perform this analysis, the fracture traces were manually discretized over the most positive curvature attribute (Figs. 3, 12, and 13). The topological analysis was performed with the NetworkGT plugin from the ArcGIS Pro software (Nyberg et al., 2018). Approximately 6.300 traces/planes were vectorized on the referred surface. The sampling grid for the intensity analysis used a cell size of 500 x 500 m. The fracture intensity map was created using the minimum curvature interpolation method.

2.1. Porosity Cube

The artificial neural network (ANN) represents a category of non-linear models in the artificial intelligence field that allow the solution of pattern-oriented problems and are useful in several applications regarding pattern recognition (categorization and trend analysis) in natural phenomena: lithofacies classification, fracture identification, modeling of petrophysical properties, seismic facies classification (Ashena & Thonhauser, 2024; Karpatne et al., 2018; Toms et. al., 2020). Supervised and unsupervised ANNs represent a powerful tool to address the task of detection, correlation, and classification of varied types of features (Basir et. al. 2013). The training aspect of the model represents a secondary metric used to ensure the most efficient decision, regarding the most robust justification (Toms et al., 2020). Thus, training the model represents a critical aspect of the application, and the results depend on the amount and quality of classified data. The ANN plugin used in this study is available in the OpenDtect software, and we executed the following steps for the porosity cube creation (Akinwale et al., 2022; Garia et al., 2023; Mojeddifar et. al., 2015). The first step was the creation of a *horizon cube*, between the top of the Cabiúnas Formation surface and a new surface 100 m below that (Fig. 6). We have selected 12 wells with a relatively similar penetration depth into the Cabiúnas Formation, of approximately 100 m (Table 1 - supplementary material), which were used for the calculation of the porosity cube. The horizon cube created a set of seismic horizons within the defined stratigraphic interval. This tool can be used in sequence stratigraphy modeling, geomorphological modeling, correlation of well markers, and the definition of low-frequency models for seismic inversion procedures like the porosity cube calculation (Garia et al., 2023). The horizon cube is based on the tracking of dip and azimuth values of the reflectors, which enables the delineation of the continuity of the stratigraphic framework (Brouwer et al., 2012, de Groot et al., 2010). It allows a data arrangement distributed in a chosen number of seismic horizons spaced regularly in the defined vertical interval. However, the spacing could change according to the lateral variation of the interval thickness. As observed in Figure 8, the throw of the rift faults, which cut the Cabiúnas Formation, present up to tens of meters, the horizon cube successfully recognized these changes to the lateral continuity of the beds (Fig. 6). The second step after creating the horizon cube was the creation of an acoustic impedance cube (AI). This step was achieved by creating AI logs based on the RHOB and DT logs through Equation 2, described above. A set of AI logs regarding the sampling interval from -12 to +12 ms was created. These logs were used to train the ANN by comparing the AI data against the porosity log from the wells. After the training, the ANN was used to calculate the porosity

distribution from the seismic data. Figure 6C shows a section with the porosity cube calculated for the upper 100 m of the top of the Cabiúnas Formations rocks.

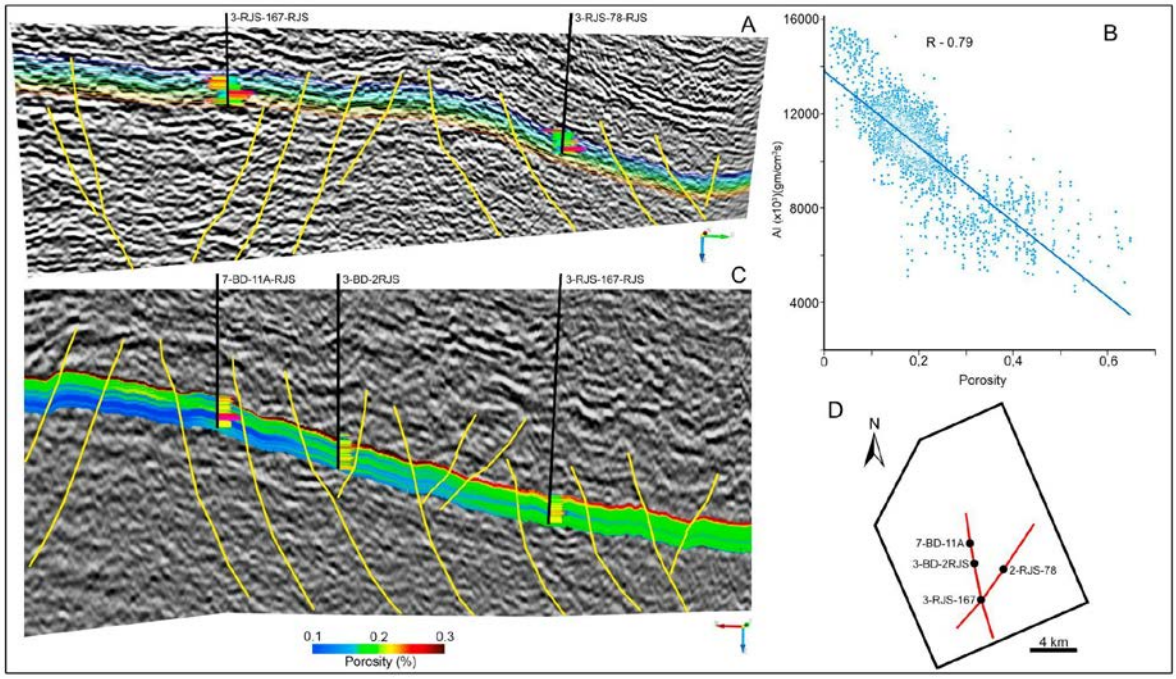

Figure 6 – Porosity model. A) 2D section showing the horizon cube encompassing the 100 m interval below the top of the basaltic succession. The wells show the porosity (left), and the AI (right) tracks. B) Crossplot graph showing correlation of a set of samples picked from the AI values computed from the seismic traces, and the porosity computed from the well logs. C) 2D section showing the porosity data calculated by the ANN in the upper 100m interval. The wells are showing the AI track. D) Map of the cropped seismic volume with the location of the two random 2D sections and the wells shown in A and C.

3. RESULTS

3.1 - Porosity map from the well logs

Figure 7 shows a map with the interpolation of the mean porosity value calculated for the porosity data of 45 wells that penetrated the basaltic succession. The data shows that the higher porosity values are located in a region over the Badejo Field horst trending NE-SW, with 5 to 8 km width. All the wells that found commercial or non-commercial oil are located in this zone.

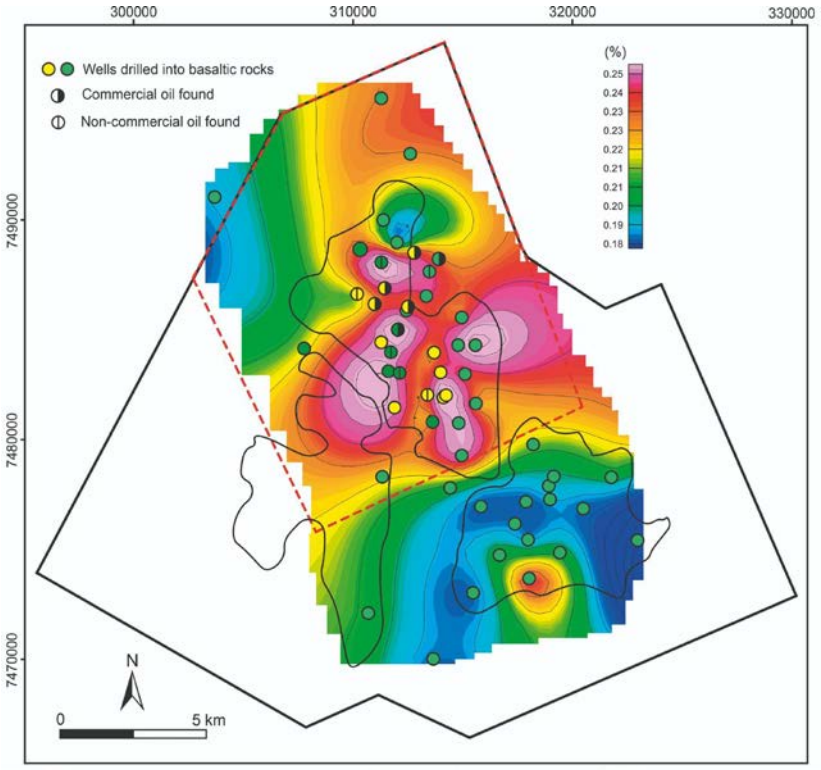

Figure 7 - Map with the interpolation of mean porosity values calculated for the 45 wells analyzed. Yellow circles indicate the wells used for the calculation of the porosity cube.

3.2 - Analysis of Seismic Attributes

Figures 8A and 8B show the seismic depth contour map for the top of the Cabiúnas Formation and the top of the Precambrian Basement, respectively. Figure 8B also shows the main fault traces interpreted in the seismic data, which were used herein to represent the tectonic framework. Attribute maps shown in Figures 9 to 12 were extracted from the top of the Cabiúnas Formation surface.

The oil accumulations in the basaltic rocks are related to a paleo-high bounded by normal faults in the northern part of the Badejo Field (Fig. 8), and they are aligned with major normal faults trending NNE-SSW that mark the continental platform border. These major faults represent normal and strike-slip synthetic and antithetic structures, trending NNE-SSW and NE-SW. The other main family of structures are normal and transfer faults trending NW-SE (de Castro & Picolini, 2015; Fetter, 2009; Strugale et al., 2021). The interception of the major fault zones (NNE-SSW) by transfer faults, created some segmentation of the main lineaments and relay ramps.

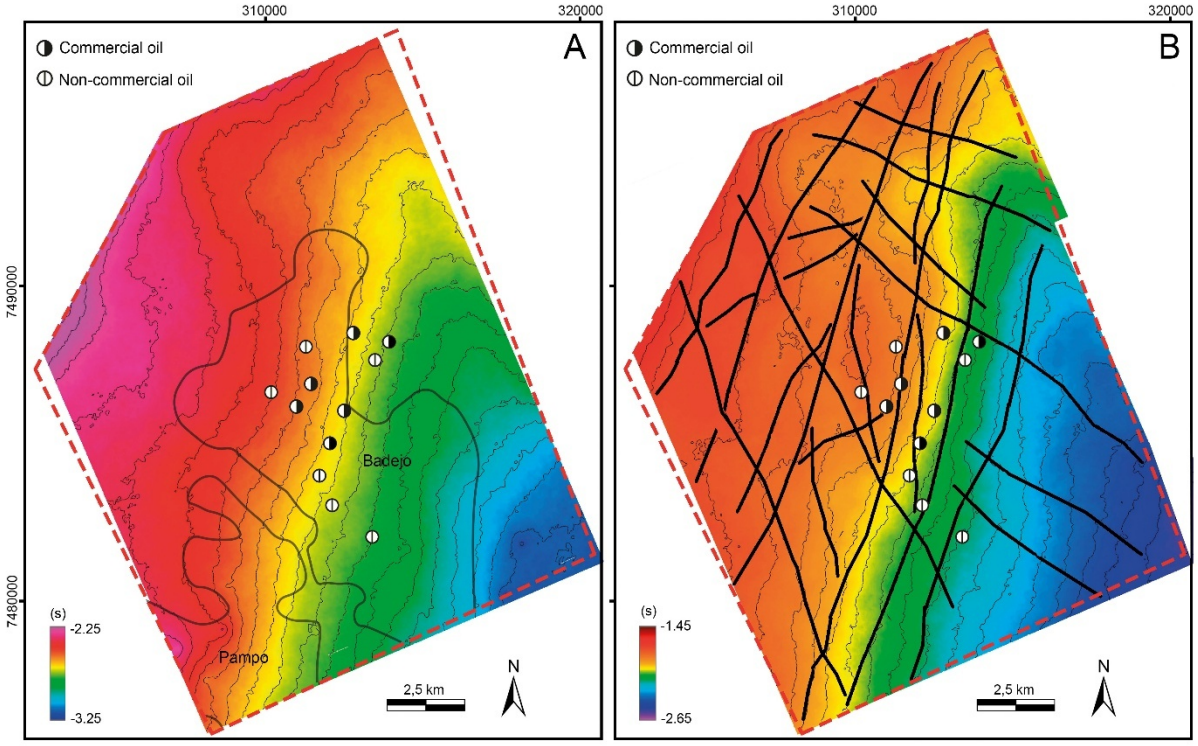

Figure 8 - A) Depth contour map of the Precambrian basement, B) Depth contour map of the top of Cabiúnas Formation. Major faults interpreted from the seismic data are represented by the black lines.

Figure 9 shows the Ridge Enhancement Filter and the Similarity attribute map. In these first maps, it is possible to observe larger traces related to the major fault zones (red arrows). However, no large continuous features are observed, possibly because of the segmentation of the faults. The relatively small throw of the faults (Fig. 2), can also explain the poor expression of the fault traces. Erosion due to the weathering could also reduce the topographic variation of the fault scarps, before the burial (Holland et al., 2006). In both maps a large number of small fractures are visible. These structures probably formed from the cooling of the basaltic lava flows, which generates an enormous number of centimeters to meter-scale discontinuities and also large fractures associated with lava inflation and deflation (Kattenhorn et al., 2008), and the formation of domed and collapsed zones (Bernardi et al 2019; Hamilton et al., 2020). Fractures delineated in the seismic attributes have tens to hundreds of meters, whose pattern varies from conjugate to apparent random. The distribution of the fractures also shows a circular to semi-circular arrangement in some areas. The fracture traces present linear to slightly concave geometries (Fig. 9). There is also an increase in fractures near the fault zones (Figs.

(9B and 9D), related to mechanic phenomena (Aydin & DeGraff, 1988; Holland et al., 2006; Walker et al., 2012, 2013).

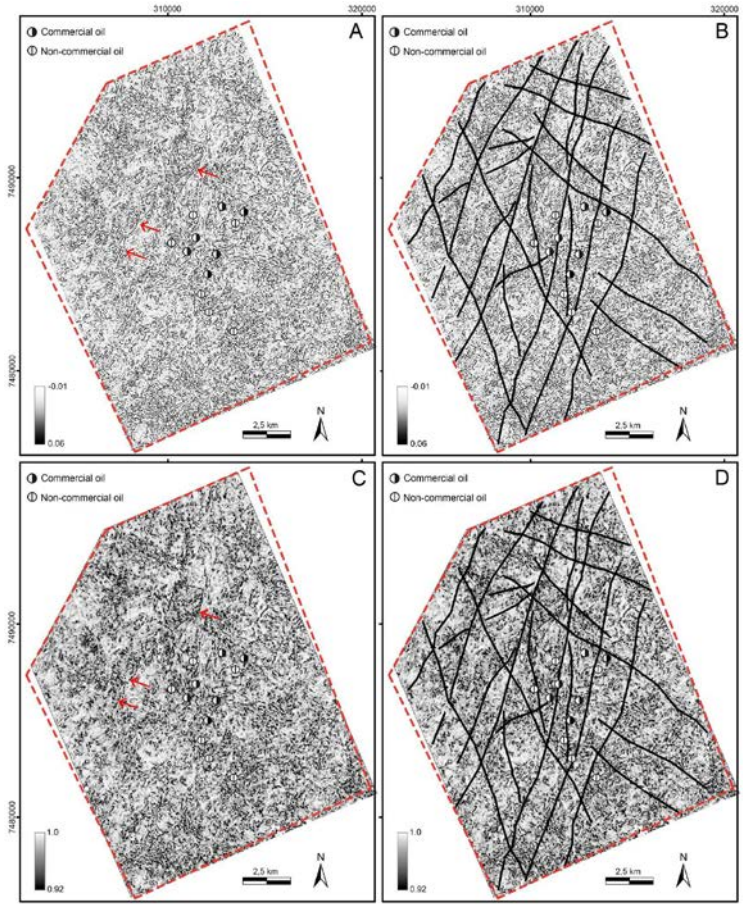

Figure 9 - A and B) Ridge Enhancement Filter map, C and D) Similarity attribute extracted on the full steered seismic data. Red arrows show the position of large discontinuity traces associated with major fault planes. The left image shows the map in the right picture with the major faults interpreted in the study area.

Figure 10 shows the Spectral Decomposition and the Maximum Curvature attribute maps. These attributes are specially integrated to delineate fractures and fault zones (Akinwale et al., 2022; Afife et al., 2024). The spectral decomposition attribute successfully showed the regions along the fault zones, which are increased in fractures (higher values) (Marfurt and Chopra, 2006; Akinwale et al., 2022), associated with cooling and syn-formational processes of the basaltic rocks (Fig. 10B) (Holland et al., 2006). The most positive curvature attribute map showed the intense formation of fractures and their relationship with the fault zones (Fig. 10D) (Aydin & DeGraff, 1988; Holland et al., 2006; Walker et al., 2012, 2013).

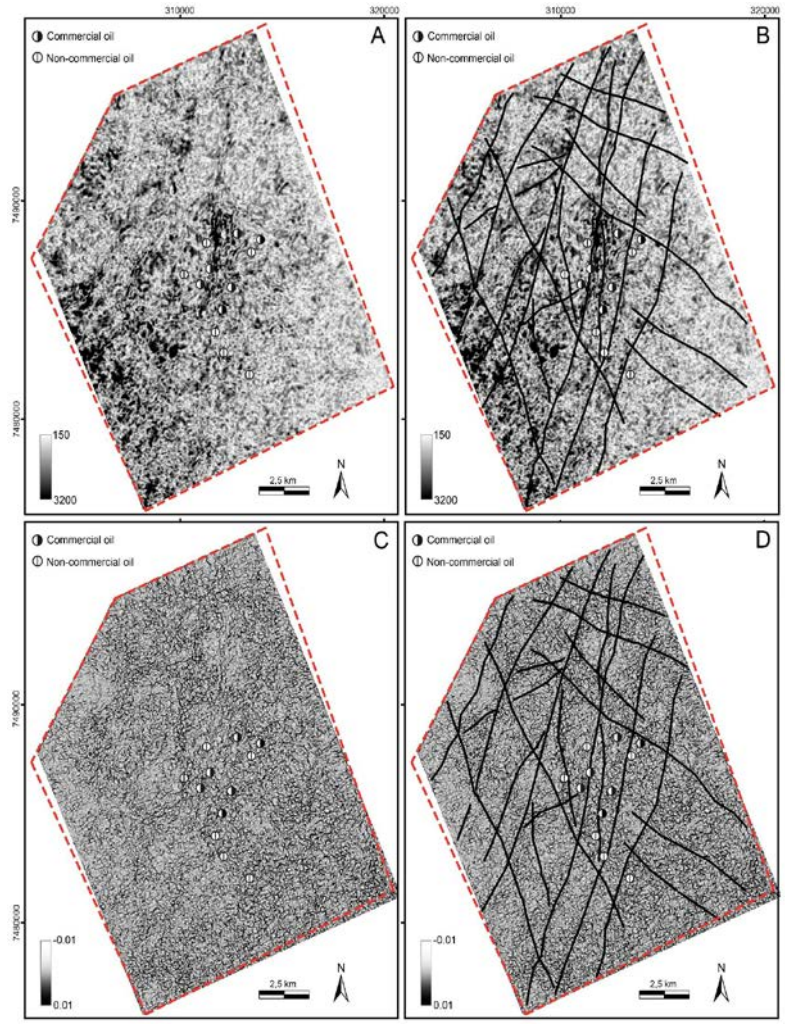

Figure 10 - A and B) Spectral Decomposition attribute map, C and D) Most Positive Curvature attribute map.

The most positive curvature attribute highlighted the reticulate aspect of the fracture traces distribution, and it also showed zones less affected by the fracturing. The topography does not show marked scarps of the rift faults, possibly due to the small fault throws and the weathering/erosion that affected part of these rocks (Mizusaki 1988; Mizusaki et al., 1992; Marins et al., 2022). Qualitative interpretation suggests that near the fault zones the small fractures tend to be parallel to the fault axis (Holland et al., 2006), and in the other regions it assumes a conjugate to a random general pattern (Fig. 10). It suggests that besides the fractures formed by syn-formational processes, a large number of fractures also was formed near the rift fault zones. Some fractures could be created by post-rift reactivation of some fault zones, and we did not address this aspect in our analysis.

Figures 11 show the dip angle and dip azimuth attribute maps. The dip angle map indicates the dip of reflectors related to fault planes (Figs. 11A and 11B), and the dip azimuth

attribute shows the dip direction of the fault planes (Figs 11B and 11C). The dip angle map shows a scattered distribution of dip values. Fractures formed near the fault zones exhibit higher dip angles (Fig. 11B). In the west part of the map there is a predominance of low dip values which coincides with the top of the Badejo Horst. In the east sector, east of the main faults trending NNE-SSW, there is a zone marked by steep dip angles. This zone was highlighted with a white dotted line polygon (Fig. 11B). The occurrence of commercial oil accumulations is related to this zone, marked by higher throw values of the rift faults, trending NNE-SSW. In this region, the interval of the basaltic succession also showed higher porosity (Fig. 7) (Ramos et al., 2023).

The dip azimuth map shows that the dip direction of the fracture planes in the top of the Badejo Horst (west sector) varies between NE and NW, with planes also dipping locally to SE, SSE, E-W, NW, NNE (Figures 11C and 11D), which demonstrates the effect of conjugated to random dip direction variation of fractures planes. In the west sector of the map, the main dip direction of fractures and fault planes varies from SE to SSE and ESE. These fracture planes are not associated with the tectonic control, and the dip directions vary significantly (Figs. 11C and 11D). The map shows no marked features related to the main fault zones trending NNE-SSW, corresponding to the extensional regime. The dip of the faults along these corridors also varies between NE and NW, due to possible oblique stress. In the northern upper part of the map, there is a corridor bounded by fault zones trending WNW-ESE, and the dip direction of the fracture planes is mainly NW. Some regions between major fault zones, associated with strike-slip features show marked SE and SSE dip direction, which indicates an inverted pattern created by relay ramp structures.

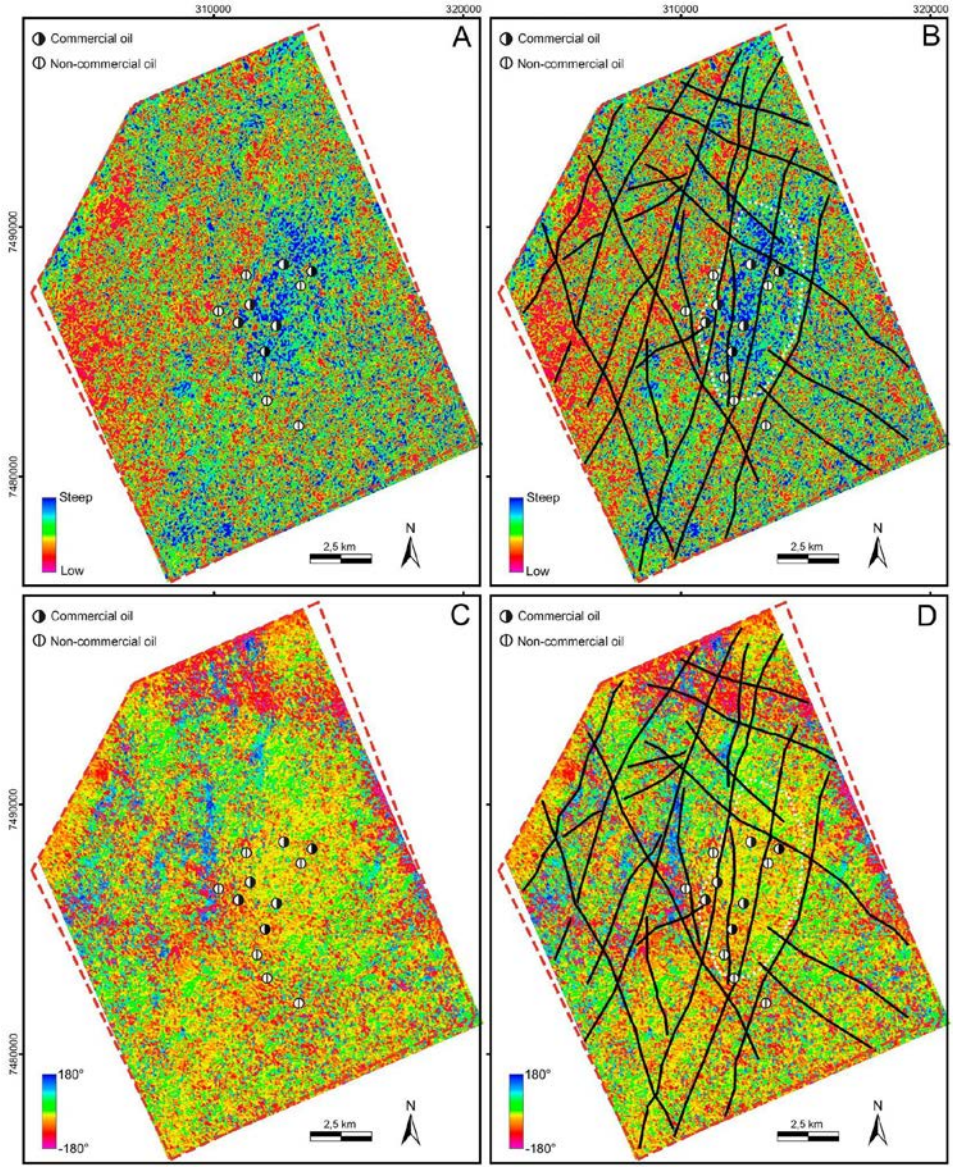

Figure 11 - A and B) Dip Angle attribute map, C and D) Dip Azimuth attribute map. The white dotted line polygon shows a zone with higher dip values on the eastern border of the Badejo paleo high.

Figures 12A and 12B show the meta-attribute calculated from the most positive curvature attribute map (Fig. 10D), used to analyze the fracture density. The discontinuities are identified as fault/fracture traces and the density was calculated regarding the cropped area. The map successfully showed the zones with a higher number of fracture traces, and this result is in agreement with the similarity and spectral decomposition maps (Figs. 9D and 10B). It also showed the increased density of fractures near the major fault zones.

Figures 12C and 12D show a map with the fracture intensity calculated from the manually assigned fracture traces over the Most Positive Curvature attribute map (Fig. 10D). This information is important because of its application in reservoir characterization regarding the prediction of fracture connectivity. This map emphasizes the influence of fault zones in forming areas with a high number of fractures, and also higher connectivity. As observed in Figure 12C there is a dominance in the orientation of the fault planes in two main directions, NE-SW and NW-SE (see rosette diagrams), and the major rift fault zones are trending NNE-SSW, with transfer faults mainly trending NNW-SSE to NW-SE (Fig. 12D). This aspect suggests that most of the fractures are not conditioned by the tectonic framework, and were generated by local syn-formational mechanical processes (cooling, inflation and deflation of the basaltic rocks) (Kattenhorn & Schaefer, 2008; Hamilton et al., 2020).

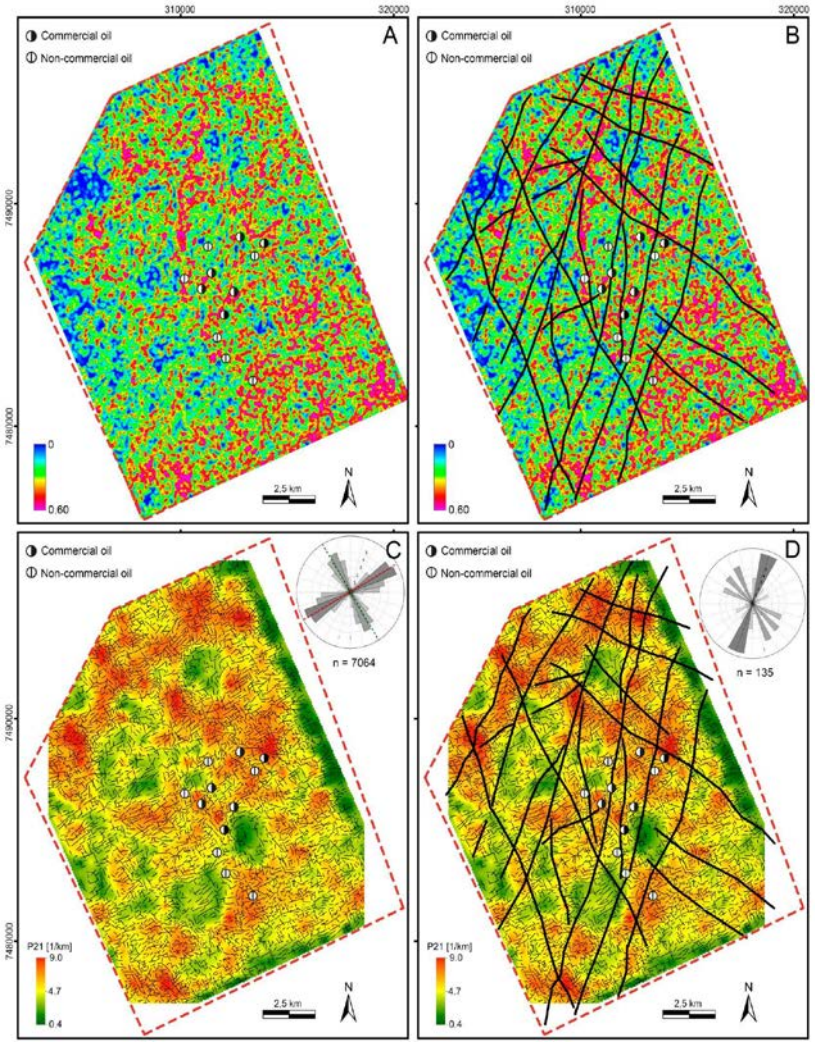

Figure 12 - A) Fracture Density attribute map obtained from the Most Positive Curvature attribute map. Higher values indicate a higher concentration of fracture traces. B) Fracture Intensity attribute map calculated from the manual identification of fracture traces over the

Most Positive Curvature map. Higher values indicate a higher number of fractures in a given area unit.

The model presented in Figure 13A shows the co-rendered instantaneous frequency and most positive curvature attributes extracted from the surface of the top of the Cabiúnas Formation. The scene also shows a 2D section co-rendered with the full steered seismic reflection and the spectral decomposition attribute (Fig. 13A). The green horizon in the 2D section shows the base of the evaporite deposits (Retiro Fm.), and the top of the basaltic succession is marked by the red horizon. This interval represents the Lagoa Feia Group (Figs. 1 and 2), which comprises the sin-rift sequence including the source rocks (Atafona Fm.), which directly overlie the basaltic rocks (Fig. 1). The surface of the basaltic succession showed a large number of fractures and ridges. Some ridges and escarpments delineate major fault zones that controlled the paleo relief. The regions near the fault zone corridors, marked with yellow dashed lines, exhibit higher fracturing intensity, and some areas relatively away from these faults show fewer fault traces. The black arrows indicate rift faults highlighted by the spectral decomposition attribute in the 2D section, which cut through the rift and sag sequences, below the evaporite (transitional) deposits. The lateral projection of these fault zones is highlighted on the surface of the basaltic formation by the yellow dashed lines. It demonstrates that the source rocks in the base of Lagoa Feia Group are in lateral contact with the basaltic rocks along these fault escarpments, and the white arrows indicate the interpreted hydrocarbon migration path. The six wells that were found to have commercial oil accumulation are shown in the scene. They found commercial accumulation over and near the escarpment that forms the eastern border of the Badejo Horst, which suggests that the migration of oil and gas to the fractured basaltic rocks occurred mainly in this zone with larger fault throws (Fig. 13A).

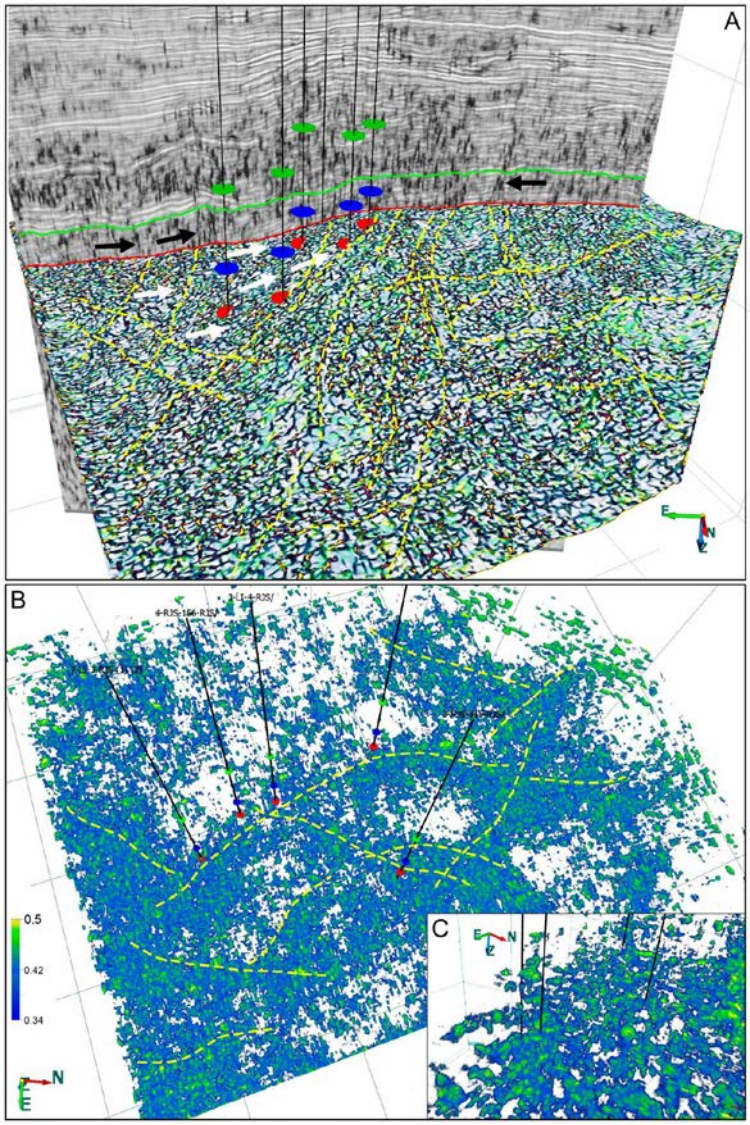

Figure 13 - Attributes modeling. A) 3D model showing the surface of the top of Cabiúnas Formation with co-rendered attributes of instantaneous phase and most positive curvature, and a random 2D section with co-rendered full steered seismic reflection and the spectral decomposition attribute. The sin-rift Lagoa Feia Group overlies the Cabiúnas Formation (green horizon), and is bounded by the base of the evaporite deposits (green horizon). Black arrows show the occurrence of rift faults cutting the Cabiúnas Fm and the overlying deposits of the Lagoa Feia Group (Fig. 2). The white arrows indicate the oil migration pattern controlled by the paleo topography and the normal faults, B) visualization of the Fracture Density Attribute, which shows the zones with higher concentration of fractures. Fault zones are marked by yellow dashed lines, C) inset showing the horizontal arrangement of regions with high fracture zones connected by vertical zones with higher fracture density.

The Most Positive Curvature attribute extracted from the top of the Cabiúnas surface showed the intense fracturing of the basaltic rocks (Fig. 13A), and the control of syn-rift faults in the paleo topography (Figs. 13A and 13B). The fracture intensity and connectivity can vary vertically and horizontally according to the rheology, lithofacies nature and formational processes of the lava flows (Reiter et al., 1987; Aydin & Degraf, 1988; DeGraff & Aydin, 1987, 1993; Helm-Clark et al., 2004; Kattenhorn & Schaefer, 2008; Navarro et al., 2020). We used the fracture density attribute to verify the distribution of the high fractured zones in the 3D volume of the Cabiúnas Formation (Fig. 13B). The data was adjusted to exhibit only the regions with higher values of fracture density (Figs. 13B and 13C). It demonstrates that: 1) fault zones present a high concentration of fractures and formed vertical connection planes through the fractured horizontal intervals (Fig. 13C, and, 2).

3.3 - Analysis of the Porosity Cube Created with the ANN

Figure 14 shows the porosity distribution (porosity cube), on a surface 5 ms below the top of the Cabiúnas Formation, into the upper portion of the basaltic formation.

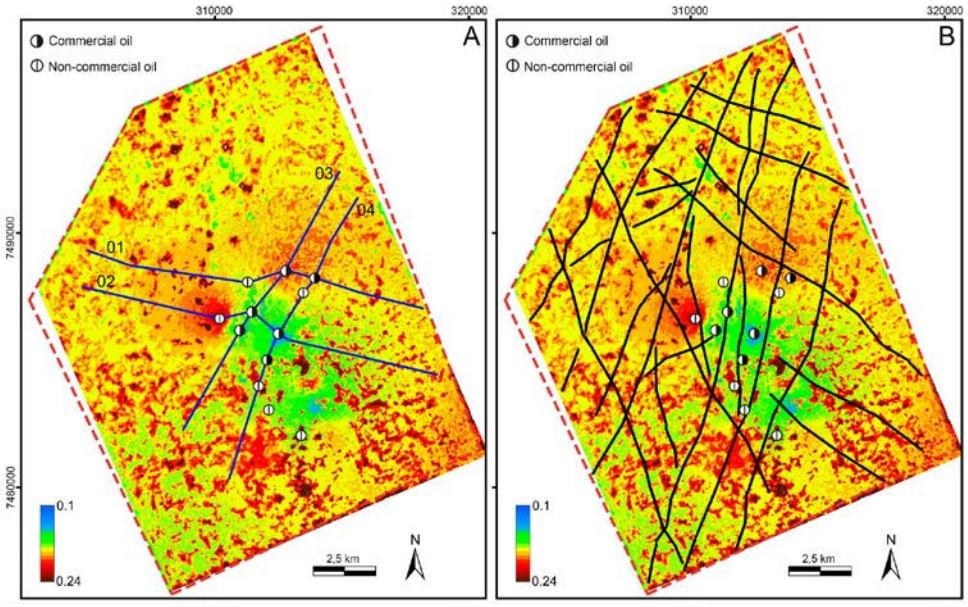

Figure 14 - Porosity values predicted with the neural network plugin at the top of the Cabiúnas Formation. A) Map with the location of random vertical sections. B) Map with the interpretation of major faults (black lines).

The distribution of estimated porosity values shows a complex pattern (Fig. 14). The mean porosity value varies from 15% to 18%. Most of the higher porosity values are related to the regions with higher fracture intensity and density. However, some contrasts are also observed. In the surface shown in Figure 14, some areas with high fracture density did not show higher porosity values. For example, the central part of the map, which shows higher density and intensity fracture values (Fig. 12), shows slightly smaller porosity values. This region coincides with the position of four wells that found commercial oil (Fig. 13). This aspect highlights the fact that porosity is not composed only of fractures, but also of primary structures like vesicles, as well as early (pre-burial) and later diagenetic structures like vugs (Lamur et al., 2017; Tang, 2022), which impacts the porosity, and permeability fields. Primary and secondary fractures can be filled during late diagenetic stages and the total porosity is reduced.

Figures 15 and 16 show random 2D sections with the calculated porosity values for the upper interval of the basaltic successions (see location in the map shown in Figure 14A). The figures also show the location of six wells drilled into the basaltic formation with the calculated acoustic impedance log (AI). The porosity values show a mean range between 10 and 20%, but some intervals present higher values, above 20%. The lateral porosity variation is strongly controlled by the stratigraphy, as expected due to the lithofacies variation of the magma flows, and diagenetic effects along different burial depths (Mizusaki et al., 1992; Marins et al., 2022).

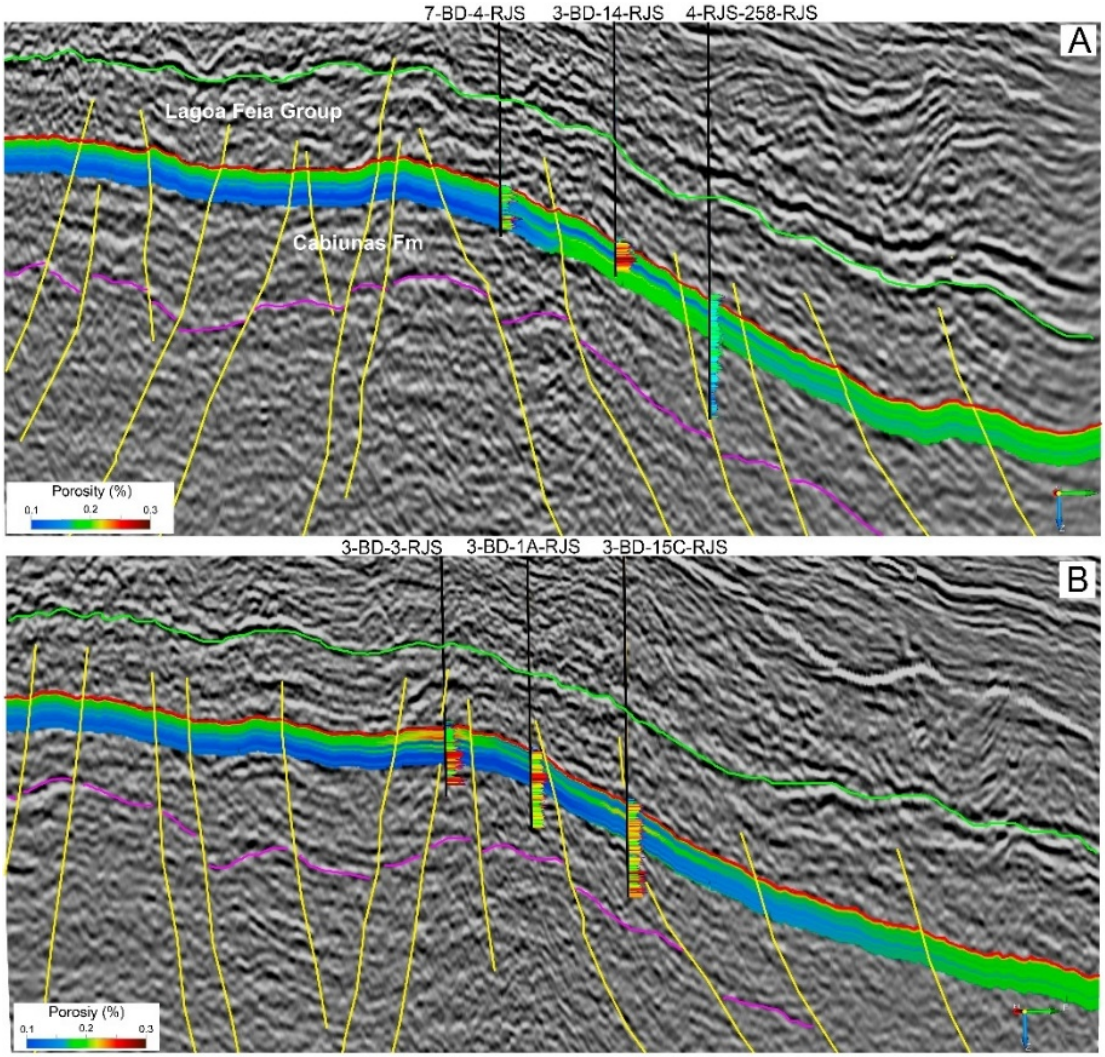

Figure 15 - A and B) 2D random sections showing the porosity values predicted for the upper 100 m interval of the Cabiúnas Formation (dip direction). The acoustic impedance logs are shown in the wells depicted in the sections (see location of sections 1 and 2 in the map shown in Figure 14A). Green horizon - base of the evaporites (Retiro Formation), red horizon - top of Cabiúnas Formation, and purple horizon - top of the seismic basement. Yellow lines - faults.

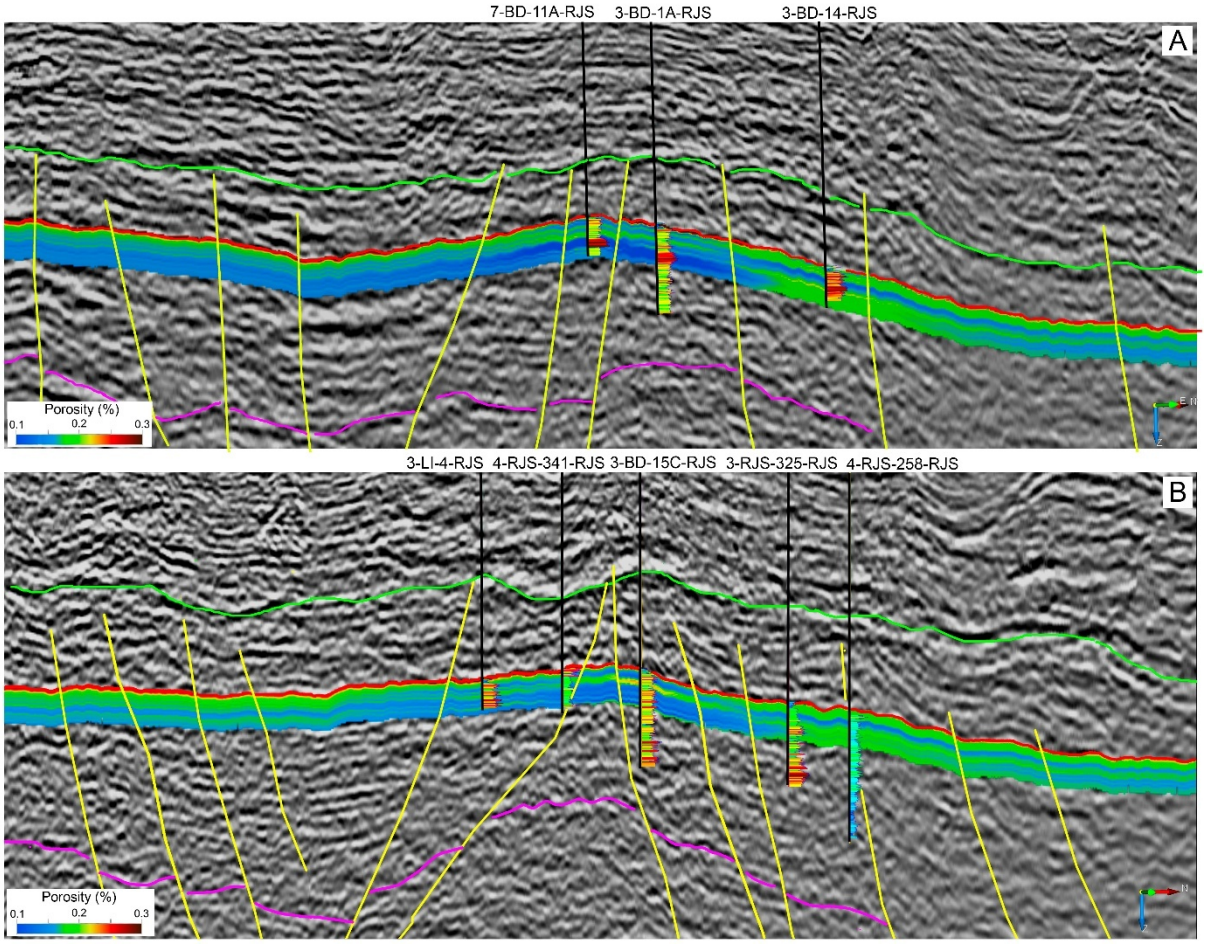

Figure 16 - A and B) 2D random sections showing the porosity values predicted for the upper 100 m interval of the Cabiúnas Formation (strike direction). The acoustic impedance logs are shown in the wells depicted in the sections (see location of sections 3 and 4 in the map shown in Figure 14A). Green horizon - base of the evaporites (Retiro Formation), red horizon - top of Cabiúnas Formation, and purple horizon - top of the seismic basement. Yellow lines - faults.

4. DISCUSSION

The study demonstrated that legacy data acquired by the oil industry during exploratory phases are valuable to developing GCS initiatives focusing on basaltic successions in offshore regions. We used the case of the Campos Basin because of the advantages related to the occurrence of flood basalt rocks that cover the shallow water domains, the available exploratory and production data acquired from the oil and gas production, and the proximity of the studied region of large CO_2 emitters (pre-salt fields production). We performed routine-based data interpretation and modeling to investigate critical aspects relate to the reservoir quality and investigation of the viability of CO_2 storage projects. Two key aspects were addressed, the tectonic influence in forming reservoir-like zones and the porosity distribution (Figs. 9 to 16). The map elaborated with the mean porosity value obtained from the studied wells showed a higher porosity zone at the top of the Badejo Horst. The general porosity seems to be very compartmentalized by faults in this region. Mizusaki (1986), and Mizusaki et al. (1988) argued that the oil accumulation and the better reservoir conditions in the Badejo basaltic reservoir were in part linked to the subaerial exposure and weathering of the rocks in the northern part of the field (Figs. 7 and 8).

Analysis of seismic attributes demonstrated the control of the rift faults trending mainly NNE-SSE, and transfer faults trending NW-SE to NNW-SSE (Figs. 8 to 12). However, many fractures formed due to cooling, inflation, and collapse (Kattenhorn & Schaefer, 2008; Hamilton et al., 2020), and this aspect was shown by seismic attributes extracted from the seismic data. The non-tectonic fractures were detected through the seismic attributes applied, and it can provide reliable information about the fracturing distribution of the stacked basalt flows. The ridge enhancement filter and the similarity and most positive curvature attributes showed the pattern created by the trace fractures (Figs. 9 and 10). The diffuse fracturing is not oriented according to the tectonic faults, and it exhibits two main orientations: NE-SW and NNW-SSE (Fig. 12). However, fault zones also formed fractures and the number of structures increases in these zones (Figs. 10A, 11A and 11B). The spectral decomposition attribute showed the increased fracturing near the fault zones (Fig. 10A). The analysis of the dip angle and dip azimuth attributes of faults and fractures showed that the rift and transfer faults created a relatively smooth relief in this part of the basin. Low angles are dominant in the west part of the top surface of the Cabiúnas Formation, over the Badejo Horst, and steeper angles to the east of the border of the Badejo Horst. The faults present relatively little throws, and they are not marked by continuous ridges and lineaments in attribute maps (Fig. 11). The dip angles of the

planes along the fault zones vary and also show some inversions because of the strike-slip component of some faults, and the interaction with the transfer faults. On the eastern border of the Badejo Horst, the planes are steeper and the fault throws are larger. In this zone, the source rocks of the Atafona Formation became in lateral contact with the fractured rocks of the Cabiúnas Formation. The large number of fractures created a varied pattern of angles, from low to steep values very locally (Fig. 11A and 11B). The dip azimuth attribute, similarly, showed a varied range of planes dip azimuth, ranging from NE to NW. Locally, planes are dipping to N, E, S, and W, related to the interaction between rift and transfer faults and the variation of the non-tectonic fracture planes (Fig. 11C and 11D).

Porosity, formed by fractures, vugs, and dissolution structures, is a critical factor controlling the variation in the physical properties of basalts (Navarro et al., 2020). Fracture patterns and paleo-topography are critical parameters in determining reservoir quality in basalt formations and confirm potential areas for fluid storage (Kattenhorn & Schaefer, 2008). To address this aspect, we used meta-attributes to extract information on the fracture density and intensity of the volcanic formation. Aspects like fracture density and intensity are critical to address reservoir characterization (Jaglan et al., 2015; Chopra et al., 2022; Feng et al., 2024). The two maps obtained with different tools showed similar results regarding the fracture distribution (Fig. 12). The density of fractures varies locally due to the lithofacies and mechanical properties of the rocks, as also observed for the fracture intensity. The higher values are observed along the fault zones, or in the intersection of the faults. The data provided here can be used to model reservoir response to CO_2 injection, as it is routinely executed for volcanic reservoirs (Jinghong et al 2011, Somasundaram et al., 2017).

The porosity cube created for the upper interval of the Cabiúnas Formation successfully demonstrated the complex patterns that involve the fractures and other features (Fig. 14). The variation of the porosity is related to the occurrence of non-tectonic fractures, but certainly by other factors not addressed in this study. Areas with higher density and intensity fractures do not necessarily imply bulk higher porosity values (Figs. 12 and 14). It is important because the porosity of these rocks is formed by primary structures like vesicles and cooling fractures, and by secondary structures like tectonic fractures and vugs. A high number of fractures does not necessarily mean higher porosity because the fractures could present local partial or total filling and consequently, porosity reduction. Or, the rock could show a smaller content of primary structures like vesicles. The porosity prediction was limited by the restricted thickness of well sampling into the Cabiúnas Formation and further studies could elucidate more details about

the influence of lithofacies and architecture of these lava flow successions in the reservoir characteristics (Asfahani, 2017; Navarro et al., 2020; Tang et al., 2022). The effect of subaerial weathering could be another aspect that can improve porosity, but also it can affect late diagenesis and reduce porosity due to the filling of fractures and pores (Sun et al., 2023; Xie et al., 2021; Marins et al, 2022). Analyzing the reservoir characteristics of basaltic rocks of the Deccan Traps, Chaudhary et al (2022), concluded that the identification of weathered and fractured zones in basalt alone is not an indication of good reservoir quality. The authors emphasized the use of flow analysis between the lithofacies to successfully determine the reservoir intervals.

The vertical distribution of porosity was shown in four 2D sections, regarding the behavior of porosity in strike and dip directions over the study area (Figs. 15 and 16). The porosity cube data shows a good correlation with values from the well logs used for validation. The main aspect observed is the lateral control of the porosity, due to the variation of lithofacies and the stacking pattern of the lava flows (Figs. 15 and 16). This variation is influenced by the rheology of the magma, the paleo topography, the extension and thickness of the flows, the content of gases, and cooling parameters (Rossetti et al., 2014; Rosenqvist et al., 2024).

The horizontal distribution of these zones, controlled by the stratigraphy of basalt flow layers, suggests that successive basaltic beds function as compartments that influence fracture connectivity (Helm-Clark et al., 2004). That variation could also be associated with weathering during the formation of the lava flows (Mizusaki, 1986). Nevertheless, the detailed characterization of porosity was also limited by the restricted sampling thickness, which may have affected the assessment of the fault zones influences.

As mentioned above, neither the weathering nor the fracturing isolated represent the main agent of porosity for basaltic systems. It is normally treated as a complex system involving primary features, sin-tectonic processes, pre-burial effects (weathering), and deep diagenetic effects (Sun et al., 2018; Fan et al., 2020; Tang et al., 2022). With the information provided by this research, and the information available in the literature, we built a schematic model to explain the mechanisms involved in the formation of oil and gas accumulation in the upper part of the Cabiúnas Formation in the Badejo Field (Fig. 17). The model shows that due to the rift fault evolution, source rocks from the Atafona Formation became in lateral contact with basaltic rocks of the Cabiúnas Formation. After the hydrocarbon generation and expulsion, the oil entered the fractured basaltic rocks. Through lateral migration the hydrocarbons accumulated in the horst structures forming the paleo topography of the economic basement. The upper part

of the basaltic sequence in this paleo-high presents evidence of weathering that was important in improving their reservoir quality (Mizusaki, 1986; Mizusaki et al., 1988). However, the compartmentalization formed by fault zones possibly prevented a more effective migration of the hydrocarbons. Figure 14 shows that despite the porosity distribution, there were wells with no commercial oil located very near the few wells that found commercial oil (Fig. 14), which suggests a strong influence of fault zones (vertical barriers) in the flow and hydrocarbon accumulation. In this case, understanding these kinds of phenomena will help the study and predict the effect of CO_2 injection in the eventual reservoir for storage purposes.

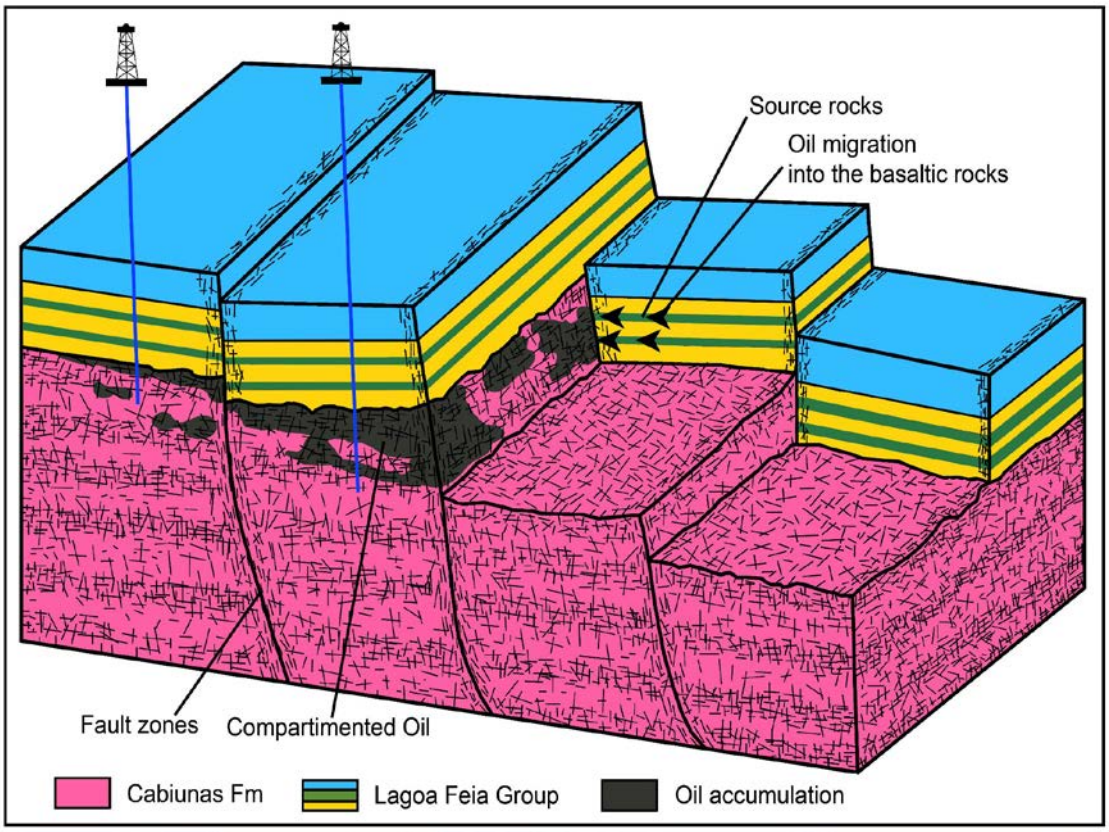

Figure 17 - Schematic model of the mechanism involved in the migration and accumulation of hydrocarbons in the fractured basalts of Cabiúnas Formation.

Thus, we demonstrated that the availability of well and seismic data allowed us to provide part of the framework of knowledge necessary to evaluate the eventual reservoir conditions for further decisions on GCS projects. This example showed that this approach could be applied in some potential offshore regions that possess volcanic formations for which there is good quality geophysical and well data acquired by the energy industry.

5. CONCLUSIONS

Our study aimed to present a case in which exploratory legacy data from the oil industry was used to study basaltic formations in shallow waters of a marginal basin (Campos Basin), a favorable region for the development of CO_2 geological storage. The study presented, took the advantage of treating the case of a mature volcanic reservoir (Badejo) for which there is an important set of geological and geophysical data. We demonstrated that understanding the mechanisms of oil migration and accumulation in the fractured basaltic rocks could help to predict how the injection of CO_2 will evolve. The results allowed us to reach the following conclusions:

The availability of data with reasonable quality allowed to access the main characteristics of the basaltic reservoir where oil accumulated in the Badejo Field;

The accumulation is related to the lateral migration of oil and gas from source rocks into the fractured economic basement formed by a volcaniclastic succession. It was a result of some factors, such as the evolution of basement paleo highs, the lateral contact of the rocks by rift faults, and the alteration of the basaltic rocks under subaerial conditions;

The migration and accumulation of the oil were primarily controlled by the fracturing of the rocks and major fault zones, corroborating previous observations of the literature. However, lithofacies distribution and late diagenetic effects also presented some degree of influence in the migration flow of hydrocarbons;

The prediction of the porosity values in the seismic cube by using an inversion method based on a neural network tool demonstrated the lateral control of the lithofacies succession on this parameter, but also the influence of the fault zones in the compartmentalization of the porosity field;

The occurrence of wells located very near each other with different contents in terms of oil accumulation demonstrated that porosity values are not the guarantee of permeability and fluid flow in the studied reservoirs;

The integrated information on the processes that favored the oil migration and accumulation can help the analysis and selection of other areas in the Campos Basin, where similar characteristics can result in good targets for CO_2 injection, concerning aspects like injectivity/flow assurance and storage capacity;

For the Cabiúnas Formation in this region, control factors like paleo topography, distribution of fault zones, fracturing, and paleoenvironmental conditions need to be considered for the reservoir quality;

The case presented here objectively demonstrated the feasibility of using the oil industry legacy data to develop GCS projects in offshore regions, saving costs and time.

Acknowledgments

We thank the National Agency for Petroleum, Natural Gas, and Biofuels (ANP) for providing the geological data used in this research. The National Council for Scientific and Technological Development (CNPq), provided the doctoral grant for GMSR. The dGB Earth Sciences for academic support with the licenses of the OpenDtect software. JAB acknowledges the financial support from CNPq, grant number 312294/2023-9.

References

Afife, M. M., Amawy, M. E., Mohammed, A. A., & Ahmed, M. A. 2024. Structural analysis, faulting system distribution, and geomechanical modeling of the Najmah Formation for improved drilling efficiency and well stability in Raudhatain and Sabriyah fields, North Kuwait. *Environmental Earth Sciences*, *83*(23), 658.

Ajayi, T., Gomes, J. S., & Bera, A. 2019. A review of CO_2 storage in geological formations emphasizing modeling, monitoring and capacity estimation approaches. *Petroleum Science*, *16*(5), 1028-1063.

Akinwale, R. P., Ayolabi, E., & Akinwale, S. A. 2022. 3D structural modelling and spectral decomposition analysis of Jay Field offshore Niger Delta, Nigeria. *Journal of Engineering and Applied Science*, *69*(1), 91.

Albertz, M., Stewart, S. A., & Goteti, R. 2023. Perspectives on geologic carbon storage. *Frontiers in Energy Research*, *10*, 1071735.

Alcalde, J., Flude, S., Wilkinson, M., Johnson, G., Edlmann, K., Bond, C. E., Scott, V., Gilfillan, S. M. V., Ogaya, Xènia & Haszeldine, R. S. 2018. Estimating geological CO_2 storage security to deliver on climate mitigation. *Nature communications*, *9*(1), 1-13.

Ali, M., Jha, N. K., Pal, N., Keshavarz, A., Hoteit, H., & Sarmadivaleh, M. 2022. Recent advances in carbon dioxide geological storage, experimental procedures, influencing parameters, and future outlook. *Earth-Science Reviews*, *225*, 103895.

Asfahani, J. 2017. Porosity and hydraulic conductivity estimation of the basaltic aquifer in Southern Syria by using nuclear and electrical well logging techniques. *Acta Geophysica*, *65*, 765-775.

Ashena, R., & Thonhauser, G. 2024. Application of artificial neural networks in geoscience and petroleum industry. In *Artificial intelligent approaches in petroleum geosciences* (pp. 115-154). Cham: Springer International Publishing.

Aydin, A., & DeGraff, J. M. 1988. Evolution of polygonal fracture patterns in lava flows. *Science*, *239*(4839), 471-476.

Aydin, G., Karakurt, I., & Aydiner, K. 2010. Evaluation of geologic storage options of CO_2: Applicability, cost, storage capacity and safety. *Energy Policy*, *38*(9), 5072-5080.

Bailey, A., King, R., Holford, S., Sage, J., Backe, G., & Hand, M. 2014. Remote sensing of subsurface fractures in the Otway Basin, South Australia. *Journal of Geophysical Research: Solid Earth*, *119*(8), 6591-6612.

Barnes, A. E. 2000. Attributes for automating seismic facies analysis. In *SEG International Exposition and Annual Meeting* (pp. SEG-2000). SEG.

Bernardi, M. I., Bertotto, G. W., Ponce, A. D., Orihashi, Y., & Sumino, H. 2019. Volcanology and inflation structures of an extensive basaltic lava flow in the Payenia Volcanic Province, extra-Andean back arc of Argentina. *Andean geology*, *46*(2), 279-299.

Braga, D. D., Valente, S. C., Marins, G. M., Parisek-Silva, Y. M., & Famelli, N. 2023. 3D Paleogeographic Reconstruction of the Cabiúnas formation lava flows in Campos basin, SE Brazil. *Journal of South American Earth Sciences*, *130*, 104537.

Brouwer, F., Huck, A., Hemstra, N. and Braga, I. 2012. Extracting full-resolution models from seismic data to minimize systematic errors in inversion: Method and examples. *The Leading Edge*, p. 546-554

Bruhn, C. H., Gomes, J. A. T., Del Lucchese Jr, C., & Johann, P. R. 2003. Campos basin: reservoir characterization and management-Historical overview and future challenges. In *Offshore Technology Conference*. Offshore Technology Conference.

Cao, X., Li, Q., Xu, L., & Tan, Y. 2024. A review of in situ carbon mineralization in basalt. Journal of Rock Mechanics and Geotechnical Engineering, 16(4), 1467-1485.

Chaudhary, M., Sharma, R., Kapoor, D., Sadiq, M., 2022. Formation evaluation of Deccan (basalt) trap basement of Kutch Offshore basin, Gulf of Kutch, India. Journal of Petroleum Science and Engineering, 217, 110854. https://doi.org/10.1016/j.petrol.2022.110854

Chen, L., He, A., Zhao, J., et al., 2022, Pore-scale modeling of complex transport phenomena in porous media. Progress in Energy and Combustion Science, 88: 100968.

Chopra, S., & Marfurt, K. J. 2007. *Seismic attributes for prospect identification and reservoir characterization*. Society of Exploration Geophysicists and European Association of Geoscientists and Engineers. https://doi.org/10.1190/1.9781560801900

Chopra, S., and Marfurt, K., 2007, Curvature attribute applications to 3D surface seismic data. The Leading Edge, 26(4), 404-414.

Chopra, S., Marfurt, K., Sharma, R., Pathak, R., & Srivastava, A. 2022. Seismic attribute characterization of fractured basement reservoirs. Geohorizons (Society of Petroleum Geophysicists India), 28(1), 35-50.

Clark, D. E., Oelkers, E. H., Gunnarsson, I., Sigfússon, B., Snæbjörnsdóttir, S. Ó., Aradottir, E. S., Gíslason, S. R., 2020. CarbFix2: CO_2 and H_2S mineralization during 3.5 years of continuous injection into basaltic rocks at more than 250°C. Geochimica et Cosmochimica Acta, 279, 45-66. https://doi.org/10.1016/j.gca.2020.03.039

d'Almeida, K.S., Vilela, P.C., Cardoso, R.A., Fernandes, R.F., Souza, M.F.F, 2018. Ocorrência de CO_2 em campos petrolíferos na margem leste brasileira. Empresa de Pesquisa Energética.

de Castro, R.D., Picolini, J.P. 2016. Main features of the Campos Basin regional geology. In: Kowsmann, R.O., editor. Geology and Geomorphology. Rio de Janeiro: Elsevier. Habitats, v. 1. p. 1-12.

de Groot, P., Huck, A., de Bruin, G., Hemstra, N., & Bedford, J. 2010. The horizon cube: A step change in seismic interpretation! The Leading Edge, 29(9), 1001–1184.

DeGraff, J. M., & Aydin, A. 1993. Effect of thermal regime on growth increment and spacing of contraction joints in basaltic lava. *Journal of Geophysical Research: Solid Earth*, *98*(B4), 6411-6430.

Dershowitz, W. S., & Einstein, H. H. 1988. Characterizing rock joint geometry with joint system models. *Rock mechanics and rock engineering*, *21*(1), 21-51.

Dershowitz, W. S., & Herda, H. H. 1992. Interpretation of fracture spacing and intensity. In *ARMA US rock mechanics/geomechanics symposium* (pp. ARMA-92). ARMA.

DGB Beheer B.V. 2022. OpendTect User Documentation - 6.6 dGB Earth Sciences. Netherlands.

Dziejarski, B., Krzyżyńska, R., & Andersson, K. 2023. Current status of carbon capture, utilization, and storage technologies in the global economy: A survey of technical assessment. *Fuel*, *342*, 127776.

Energy, I. G. 2021. CO_2 Status Report 2020. *IEA: Paris, France*.

Fan, M., McClure, J. E., Armstrong, R. T., Shabaninejad, M., Dalton, L. E., Crandall, D., & Chen, C. 2020. Influence of clay wettability alteration on relative permeability. *Geophysical Research Letters*, *47*(18), e2020GL088545.

Fan, C., Li, H., Qin, Q., Shang, L., Yuan, Y., & Li, Z. 2020. Formation mechanisms and distribution of weathered volcanic reservoirs: A case study of the carboniferous volcanic rocks in Northwest Junggar Basin, China. *Energy Science & Engineering*, *8*(8), 2841-2858.

Feng, R., Mosegaard, K., Mukerji, T., & Grana, D. 2024. Estimation of reservoir fracture properties from seismic data using Markov chain Monte Carlo methods. *Mathematical Geosciences*, 1-24.

Fernández-Ibáñez, F., Jones, G. D., Mimoun, J. G., Bowen, M. G., Simo, J. T., Marcon, V., & Esch, W. L. 2022. Excess permeability in the Brazil pre-Salt: Nonmatrix types, concepts, diagnostic indicators, and reservoir implications. *AAPG Bulletin*, *106*(4), 701-738.

Fernandez-Ibanez, F., Nolting, A., Breithaupt, C. I., Darby, B., Mimoun, J., & Henares, S. 2022. The properties of faults in the Brazil pre-salt: A reservoir characterization perspective. *Marine and Petroleum Geology*, *146*, 105955.

Fetter, M. 2009. The role of basement tectonic reactivation on the structural evolution of Campos Basin, offshore Brazil: Evidence from 3D seismic analysis and section restoration. *Marine and Petroleum Geology*, *26*(6), 873-886.

Fuss, S., Canadell, J. G., Ciais, P., Jackson, R. B., Jones, C. D., Lyngfelt, A., Peters, G. P. & Van Vuuren, D. P. 2020. Moving toward net-zero emissions requires new alliances for carbon dioxide removal. *One Earth*, *3*(2), 145-149.

Gardner, G. H. F., Gardner, L. W., & Gregory, A. 1974. Formation velocity and density—The diagnostic basics for stratigraphic traps. *Geophysics*, *39*(6), 770-780.

Garia, S., Pal, A. K., Katre, S., Nayak, S., Ravi, K., & Nair, A. M. 2023. Mapping petrophysical properties with seismic inversion constrained by laboratory-based rock physics model. *Earth Science Informatics*, *16*(4), 3191-3207.

Goldberg, D. S., Kent, D. V., & Olsen, P. E. 2010. Potential on-shore and off-shore reservoirs for CO_2 sequestration in Central Atlantic magmatic province basalts. *Proceedings of the National Academy of Sciences*, *107*(4), 1327-1332.

Goldberg, D., Aston, L., Bonneville, A., Demirkanli, I., Evans, C., Fisher, A., ... & White, S. 2018. Geological storage of CO_2 in sub-seafloor basalt: the CarbonSAFE pre-feasibility study offshore Washington State and British Columbia. *Energy Procedia*, *146*, 158-165.

Guardado, L. R., Gamboa, L. A. P., & Lucchesi, C. F. 1990. Petroleum geology of the Campos Basin, Brazil, a model for a producing Atlantic type basin ResearchGate Petroleum Geology of the Campos Basin, Brazil, a Model for a Producing Atlantic Type Basin.

Gupta, S. D., Chatterjee, R., & Farooqui, M. Y. 2012. Formation evaluation of fractured basement, Cambay Basin, India. *Journal of Geophysics and Engineering*, *9*(2), 162-175.

Hamilton, C. W., Scheidt, S. P., Sori, M. M., de Wet, A. P., Bleacher, J. E., Mouginis-Mark, P. J., ... & Crumpler, L. S. 2020. Lava-rise plateaus and inflation pits in the McCartys lava flow field, New Mexico: An analog for pāhoehoe-like lava flows on planetary surfaces. *Journal of Geophysical Research: Planets*, *125*(7), e2019JE005975.

Helm-Clark, C. M., Rodgers, D. W., & Smith, R. P. 2004. Borehole geophysical techniques to define stratigraphy, alteration and aquifers in basalt. *Journal of Applied Geophysics*, *55*(1-2), 3-38.

Holland, M., Urai, J. L., & Martel, S. 2006. The internal structure of fault zones in basaltic sequences. *Earth and Planetary Science Letters*, *248*(1-2), 301-315.

Iacopini, D., Butler, R. W. H., Purves, S., McArdle, N., & De Freslon, N. 2016. Exploring the seismic expression of fault zones in 3D seismic volumes. *Journal of Structural Geology*, *89*, 54-73.

IPCC, 2019. Summary for Policymakers. In: Global Warming of 1.5°C. An IPCC Special Report on the impacts of global warming of 1.5°C above pre-industrial levels and related global greenhouse gas emission pathways, in the context of strengthening the global response to the threat of climate change, sustainable development, and efforts to eradicate poverty.

Ismail, A., Radwan, A. A., Leila, M., Abdelmaksoud, A., & Ali, M. 2023. Unsupervised machine learning and multi-seismic attributes for fault and fracture network interpretation in the Kerry Field, Taranaki Basin, New Zealand. *Geomechanics and Geophysics for Geo-Energy and Geo-Resources*, *9*(1), 122.

Jaglan, H., Qayyum, F., & Hélène, H. 2015. Unconventional seismic attributes for fracture characterization. *First Break*, *33*(3).

Jibrin, B. 2014. Enhanced detection of faults using dip-steered multitrace similarity-computation techniques: Example using offshore niger delta 3D seismic data. *The Leading Edge*, *33*(4), 428-434.

Jinghong, W., Caineng, Z., Jiuqiang, J., & Rukai, Z. 2011. Characteristics and controlling factors of fractures in igneous rock reservoirs. *Petroleum Exploration and Development*, *38*(6), 708-715.

Karpatne, A., Ebert-Uphoff, I., Ravela, S., Babaie, H. A., & Kumar, V. 2018. Machine learning for the geosciences: Challenges and opportunities. *IEEE Transactions on Knowledge and Data Engineering*, *31*(8), 1544-1554.

Kattenhorn, S. A., & Schaefer, C. J. 2008. Thermal–mechanical modeling of cooling history and fracture development in inflationary basalt lava flows. *Journal of Volcanology and Geothermal Research*, *170*(3-4), 181-197.

Kelemen, P., Benson, S. M., Pilorgé, H., Psarras, P., & Wilcox, J. 2019. An overview of the status and challenges of CO_2 storage in minerals and geological formations. *Frontiers in Climate*, *1*, 9.

Khandoozi, S., Hazlett, R., & Fustic, M. 2023. A critical review of CO_2 mineral trapping in sedimentary reservoirs–from theory to application: Pertinent parameters, acceleration methods and evaluation workflow. *Earth-Science Reviews*, 104515.

Kumar, A., & Shrivastava, J. P. 2019. Carbon capture induced changes in Deccan basalt: a mass-balance approach. *Greenhouse Gases: Science and Technology*, *9*(6), 1158-1180.

Kumar, P. C., & Mandal, A. 2018. Enhancement of fault interpretation using multi-attribute analysis and artificial neural network (ANN) approach: A case study from Taranaki Basin, New Zealand. *Exploration Geophysics*, *49*(3), 409-424.

Lamur, A., Kendrick, J. E., Eggertsson, G. H., Wall, R. J., Ashworth, J. D., & Lavallée, Y. 2017. The permeability of fractured rocks in pressurised volcanic and geothermal systems. *Scientific reports*, *7*(1), 6173.

Lindseth, R. O. 1979. Synthetic sonic logs—A process for stratigraphic interpretation. *Geophysics*, *44*(1), 3-26.

Marfurt, K. J., Kirlin, R. L., Farmer, S. L., & Bahorich, M. S. 1998. 3-D seismic attributes using a semblance-based coherency algorithm. *Geophysics*, *63*(4), 1150-1165.

Marfurt, K. J., & Alves, T. M. 2015. Pitfalls and limitations in seismic attribute interpretation of tectonic features. *Interpretation*, *3*(1), SB5-SB15.

Marins, G. M., Parizek-Silva, Y., Millett, J. M., Jerram, D. A., Rossetti, L. M., e Souza, A. D. J., ... & Carmo, I. D. O. 2022. Characterization of volcanic reservoirs; insights from the Badejo and Linguado oil field, Campos Basin, Brazil. *Marine and Petroleum Geology*, 105950.

McGrail, B.P., Schaef, H.T, Ho, A.M., Chien, Y.J., Dooley, J.J., Davidson, C.L., 2006. Potential for carbon dioxide sequestration in flood basalts. Journal of Geophysical Research: Solid Earth, 111(B12). https://doi.org/10.1029/2005JB004169

McGrail, B.P., Spane, F.A., Amonette, J.E., Thompson, C.R., Brown, C.F., 2014. Injection and monitoring at the Wallula basalt pilot project. Energy Procedia, 63, 2939-2948. https://doi.org/10.1016/j.egypro.2014.11.316

McLaughlin, H., Littlefield, A. A., Menefee, M., Kinzer, A., Hull, T., Sovacool, B. K., ... & Griffiths, S. 2023. Carbon capture utilization and storage in review: Sociotechnical implications for a carbon reliant world. *Renewable and Sustainable Energy Reviews*, *177*, 113215.

Mendes, L. D. C., Correia, U. M., Cunha, O. R., Oliveira, F. M., & Vidal, A. C. 2022. Topological analysis of fault network in naturally fractured reservoirs: A case study from the pre-salt section of the Santos Basin, Brazil. *Journal of Structural Geology*, *159*, 104597.

Mizusaki, A. M. P. 1986. Rochas Ígneo-Básicas do Neocomiano da Bacia de Campos: Caracterização como reservatório de hidrocarbonetos. Tese. Programa de Pós Graduação em Geologia. Universidade Federal do Rio de Janeiro. xiii, 104 p.

Mizusaki, A. M. P, Thomaz Filho, Antônio, & Valença, J. 1988. Volcano Sedimentary Sequence of Neocomian Age In (Campos Basin (Brazil). *Revista Brasileira De Geociências*, *18*.

Mizusaki, A. M. P., Petrini, R., Bellieni, P., Comin-Chiaramonti, P., Dias, J., De Min, A., & Piccirillo, E. M. 1992. Basalt magmatism along the passive continental margin of SE Brazil (Campos Basin). *Contributions to Mineralogy and Petrology*, *111*, 143-160.

Mohriak, W.U., Mello, M.R., Dewey, J.F., & Maxwell, J.R., 1990. Petroleum geology of the Campos Basin, offshore Brazil. Geological Society, London, Special Publications, 50(1), 119-141. https://doi.org/10.1144/GSL.SP.1990.050.01.07

Mojeddifar, S., Kamali, G., & Ranjbar, H. 2015. Porosity prediction from seismic inversion of a similarity attribute based on a pseudo-forward equation (PFE): a case study from the North Sea Basin, Netherlands. *Petroleum Science*, *12*, 428-442.

Mwakipunda, G. C., Mgimba, M. M., Ngata, M. R., & Yu, L. 2024. Recent advances on carbon dioxide sequestration potentiality in salt caverns: A review. *International Journal of Greenhouse Gas Control*, *133*, 104109.

Navarro, J., Teramoto, E.H., Engelbrecht, B.Z., Kiang, C.H., 2020. Assessing hydrofacies and hydraulic properties of basaltic aquifers derived from geophysical logging. Brazilian Journal of Geology, 50 (04). https://doi.org/10.1590/2317-4889202020200013

Nisbet, H., Buscarnera, G., Carey, J. W., Chen, M. A., Detournay, E., Huang, H., ... & Viswanathan, H. S. 2024. Carbon mineralization in fractured mafic and ultramafic rocks: A review. *Reviews of Geophysics*, *62*(4), e2023RG000815.

Nyberg, B., Nixon, C. W., & Sanderson, D. J. 2018. NetworkGT: A GIS tool for geometric and topological analysis of two-dimensional fracture networks. *Geosphere*, *14*(4), 1618-1634.

Ramos, G. M. S., Barbosa, J. A., de Araújo, A. F. L., Correia Filho, O. J., Barreto, C. J. S., Oliveira, J. T. C., & de Medeiros, R. S. 2023. Potential for permanent CO_2 sequestration in depleted volcanic reservoirs in the offshore Campos basin, Brazil. International Journal of Greenhouse Gas Control, 128, 103942.

Rasool, M. H., & Ahmad, M. 2023. Reactivity of basaltic minerals for CO_2 sequestration via in situ mineralization: a review. *Minerals*, *13*(9), 1154.

Raza, A., Glatz, G., Gholami, R., Mahmoud, M., & Alafnan, S. 2022. Carbon mineralization and geological storage of CO_2 in basalt: Mechanisms and technical challenges. *Earth-Science Reviews*, *229*, 104036.

Reiter, M., Barroll, M. W., Minier, J., & Clarkson, G. 1987. Thermo-mechanical model for incremental fracturing in cooling lava flows. *Tectonophysics*, *142*(2-4), 241-260.

Ren, K., Zhao, J., Liu, Q., & Zhao, J. 2020. Hydrocarbons in igneous rock of Brazil: A review. *Petroleum Research*, *5*(3), 265-275.

Ringrose, P. S., & Meckel, T. A. 2019. Maturing global CO_2 storage resources on offshore continental margins to achieve 2DS emissions reductions. *Scientific reports*, *9*(1), 1-10.

Rohrbaugh Jr, M. B., Dunne, W. M., & Mauldon, M. 2002. Estimating fracture trace intensity, density, and mean length using circular scan lines and windows. *AAPG bulletin*, *86*(12), 2089-2104.

Rosenqvist, M. P., Millett, J. M., Planke, S., Johannesen, R. M., Passey, S. R., Sørensen, E. V., ... & Jamtveit, B. 2024. The architecture of basalt reservoirs in the North Atlantic Igneous Province with implications for basalt carbon sequestration. *Geological Society, London, Special Publications*, *547*(1), SP547-2023.

Rossetti, L. M., Lima, E. F., Waichel, B. L., Scherer, C. M., & Barreto, C. J. 2014. Stratigraphical framework of basaltic lavas in Torres Syncline main valley, southern Parana-Etendeka Volcanic Province. *Journal of South American Earth Sciences*, *56*, 409-421.

Rossetti, L. M., Healy, D., Hole, M. J., Millett, J. M., de Lima, E. F., Jerram, D. A., & Rossetti, M. M. 2019. Evaluating petrophysical properties of volcano-sedimentary sequences: A case study in the Paraná-Etendeka Large Igneous Province. *Marine and Petroleum Geology*, *102*, 638-656.

Ruz-Ginouves, J., Gerbault, M., Cembrano, J., Iturrieta, P., Leiva, F. S., Novoa, C., & Hassani, R. 2021. The interplay of a fault zone and a volcanic reservoir from 3D elasto-plastic models: Rheological conditions for mutual trigger based on a field case from the Andean Southern Volcanic Zone. *Journal of Volcanology and Geothermal Research*, *418*, 107317.

Sampaio, T. P. 2012. Complementary Development of Siri Reservoir. *Third Meeting of the Heavy Oil Working Group*. México DF. México.

Slagle, A.L., Goldberg, D.S., 2011. Evaluation of ocean crustal Sites 1256 and 504 for long-term CO_2 sequestration. Geophysical research letters, 38(16). https://doi.org/10.1029/2011GL048613

Snæbjörnsdóttir, S. Ó., Gislason, S. R., Galeczka, I. M., & Oelkers, E. H. 2018. Reaction path modelling of in-situ mineralisation of CO_2 at the CarbFix site at Hellisheidi, SW-Iceland. *Geochimica et Cosmochimica Acta*, *220*, 348-366.

Snæbjörnsdóttir, S. Ó., Sigfússon, B., Marieni, C., Goldberg, D., Gislason, S. R., & Oelkers, E. H. 2020. Carbon dioxide storage through mineral carbonation. *Nature Reviews Earth & Environment*, *1*(2), 90-102.

Somasundaram, S., Mund, B., Soni, R., & Sharda, R. 2017. Seismic attribute analysis for fracture detection and porosity prediction: A case study from tight volcanic reservoirs, Barmer Basin, India. *The Leading Edge*, *36*(11), 947b1-947b7.

Stanton, N., Kusznir, N., Gordon, A., & Schmitt, R. 2019. Architecture and Tectono-magmatic evolution of the Campos Rifted Margin: Control of OCT structure by basement inheritance. *Marine and Petroleum Geology*, *100*, 43-59.

Strugale, M., da Silva Schmitt, R., & Cartwright, J. 2021. Basement geology and its controls on the nucleation and growth of rift faults in the northern Campos Basin, offshore Brazil. *Basin Research*, *33*(3), 1906-1933.

Sun, X., Cao, S., Pan, X., Hou, X., Gao, H., & Li, J. 2018. Characteristics and prediction of weathered volcanic rock reservoirs: A case study of Carboniferous rocks in Zhongguai paleouplift of Junggar Basin, China. *Interpretation*, *6*(2), T431-T447.

Sun, L., Liu, Y., Cheng, Z., Jiang, L., Lv, P., & Song, Y. 2023. Review on multiscale CO_2 mineralization and geological storage: mechanisms, characterization, modeling, applications and perspectives. *Energy & Fuels*, *37*(19), 14512-14537.

Taner, M. T., Schuelke, J. S., O'Doherty, R., & Baysal, E. 1994. Seismic attributes revisited. In *SEG technical program expanded abstracts 1994* (pp. 1104-1106). Society of Exploration Geophysicists.

Tang, H., Tian, Z., Gao, Y., Dai, X., 2022. Review of volcanic reservoir geology in China. Earth-Science Reviews, 104158.

Toms, B. A., Barnes, E. A., & Ebert-Uphoff, I. 2020. Physically Interpretable Neural Networks for the Geosciences: Applications to Earth System Variability. Journal of Advances in Modeling Earth Systems, 12(9).https://doi.org/10.1029/2019MS002002

Tutolo, B. M., Awolayo, A., & Brown, C. 2021. Alkalinity Generation Constraints on Basalt Carbonation for Carbon Dioxide Removal at the Gigaton-per-Year Scale. Environmental Science & Technology, 55(17), 11906–11915. https://doi.org/10.1021/acs.est.1c02733

Vitillo, J. G., Eisaman, M. D., Aradottir, E. S., Passarini, F., Wang, T., & Sheehan, S. W. 2022. The role of carbon capture, utilization, and storage for economic pathways that limit global warming to below 1.5° C. *IScience*, *25*(5).

Walker, R. J., Holdsworth, R. E., Imber, J., & Ellis, D. 2012. Fault-zone evolution in layered basalt sequences: A case study from the Faroe Islands, NE Atlantic margin. *Bulletin*, *124*(7-8), 1382-1393.

Walker, R. J., Holdsworth, R. E., Imber, J., Faulkner, D. R., & Armitage, P. J. 2013. Fault zone architecture and fluid flow in interlayered basaltic volcaniclastic-crystalline sequences. *Journal of Structural Geology*, *51*, 92-104.

Wei, H., Tang, Z., Qiu, Z., Yan, D., & Bai, M. 2020. Formation of large carbonate concretions in black cherts in the Gufeng Formation (Guadalupian) at Enshi, South China. *Geobiology*, *18*(1), 14-30.

White, S.K., Spane, F.A., Schaef, H.T., Miller, Q.R., White, M.D., Horner, J.A., McGrail, B.P. 2020. Quantification of CO_2 mineralization at the Wallula basalt pilot project. Environmental Science & Technology, 54(22), 14609-14616. https://doi.org/10.1021/acs.est.0c05142

Winter, W. R., Jahnert, R. J., & França, A. B. 2007. Bacia de campos. *Boletim de Geociências da PETROBRAS*, *15*(2), 511-529.

Xie, H., Li, C., He, Z., Li, C., Lu, Y., Zhang, R., Gao, M. & Gao, F. 2021. Experimental study on rock mechanical behavior retaining the in situ geological conditions at different depths. *International Journal of Rock Mechanics and Mining Sciences*, *138*, 104548.

Zahasky, C., & Krevor, S. 2020. Global geologic carbon storage requirements of climate change mitigation scenarios. *Energy & Environmental Science*, *13*(6), 1561-1567.

Zakharova, N.V., Goldberg, D.S., Sullivan, E.C., Herron, M.M., Grau, J.A., 2012. Petrophysical and geochemical properties of Columbia River flood basalt: Implications for carbon sequestration. Geochemistry, Geophysics, Geosystems, 13(11). https://doi.org/10.1029/2012GC004305

Zhang, L., Chen, L., Hu, R., & Cai, J. 2022. Subsurface multiphase reactive flow in geologic CO_2 storage: Key impact factors and characterization approaches. *Advances in Geo-Energy Research*, *6*(3), 179-180.

Supplementary Material

Table 1 - Wells used in the study. The mean porosity (simple mean value from all the porosity values in the log) was calculated from the porosity log obtained through Equation 1 (Fig. 6). The acoustic impedance log was obtained from Equation 2. The code column indicates wells used for the porosity cube inversion (grey squares), wells with commercial oil production (blue squares), and wells with non-commercial oil found (green squares).

N°	Well name	X	Y	Depth to the Top Cabiunas (m)	Thickness (m)	Mean porosity (%)	Code		
1	1-RJS-13-RJS	7488968	312005	-3191	71	18,8%			
2	1-RJS-23-RJS	7495543	311298	-2938	39	23,0%			
3	3-BD-13-RJS	7488525	310280	-3096	48	23,6%			
4	3-BD-14-RJS	7488497	312780	-3095	109	23,8%			
5	3-BD-15C-RJS	7485985	312483	-2927	259	22,9%			
6	3-BD-1A-RJS	7486908	311427	-2964	230	24,2%			
7	3-BD-2-RJS	7484452	311300	-3115	104	25,3%			
8	3-BD-3-RJS	7486622	310185	-2961	196	21,3%			
9	3-LI-1-RJS	7483081	313991	-3050	100	24,4%			
10	3-LI-2-RJS	7484314	314815	-2960	76	23,7%			
11	3-LI-4-RJS	7483999	311729	-3021	76	25,3%			
12	3-LI-5-RJS	7481657	315600	-3125	125	22,2%			
13	7-BD-10D-RJS	7488070	311305	-3262	112	31,2%			
14	7-BD-11A-RJS	7486161	310983	-2957	101	22,7%			
15	7-BD-12D-RJS	7488070	311310	-3076	504	28,7%			
16	7-BD-16DA-RJS	7485927	312449	-3289,5	48,5	22,2%			
17	7-BD-4-RJS	7488069	311308	-3042	133	23,3%			
18	7-BD-5D-RJS	7488067	311309	-3047	888	27,1%			
19	7-BD-6D-RJS	7488068	311306	-3090	500	28,9%			
20	7-BD-7D-RJS	7488066	311307	-2970	434	27,7%			
21	7-BD-8-RJS	7489983	311389	-3133	37	22,4%			
22	7-BD-9D-RJS	7488067	311304	-2983	368	34,2%			
23	7-LI-3-RJS	7482048	313377	-2973	97	22,8%			
24	7-LI-7-RJS	7483125	311600	-2936	185	27,1%			
25	7-LI-9-RJS	7484305	315586	-3047	43	28,4%			
26	1-RJS-165-RJS	7491044	303689	-2587	183	19,1%			
27	1-RJS-262-RJS	7493023	312612	-3156	82	21,6%			
28	1-RJS-43A-RJS	7484189	307781	-3392	142	21,7%			
29	1-RJS-49-RJS	7479306	314949	-3135	65	29,6%			
30	1-RJS-74-RJS	7482998	315108	-3100	94	22,2%			
31	1-RJS-92-RJS	7478341	311316	-2940	195	22,2%			
32	3-RJS-140D-RJS	7479307	314964	-2982	369	21,7%			
33	3-RJS-157C-RJS	7480818	313632	-3159	91	22,4%			
34	3-RJS-167-RJS	7481446	311909	-3050	100	25,5%			
35	3-RJS-315-RJS	7487635	313467	-3025	216	24,3%			
36	3-RJS-73B-RJS	7480762	314826	-3110	80	26,7%			
37	3-RJS-78-RJS	7483983	313698	-3127	119	22,6%			
38	4-RJS-139A-RJS	7482003	314213	-3052	113	24,5%			
39	4-RJS-139-RJS	7481929	314143	-3040	137	34,2%			
40	4-RJS-156-RJS	7483030	312130	-2945	69	24,2%			
41	4-RJS-258-RJS	7488238	313925	-2972	343	23,1%			
42	4-RJS-264-RJS	7485579	314955	-3036	112	23,0%			
43	4-RJS-266-RJS	7486566	313325	-3054	121	24,2%			
44	4-RJS-341-RJS	7485021	312056	-3016	107	28,1%			

Table 2 - Editable Excel version of Table 1.

Well	X		hick	Top Cabiúnas (m)	Avg Porosity	ode
1-RJS-13-RJS	7488968	12005	1	-3191	18,8 %	
1-RJS-23-RJS	7495543	11298	9	-2938	23,0 %	
3-BD-13-RJS	7488525	10280	8	-3096	23,6 %	
3-BD-14-RJS	7488497	12780	09	-3095	23,8 %	
3-BD-15C-RJS	7485985	12483	59	-2927	22,9 %	
3-BD-1A-RJS	7486908	11427	30	-2964	24,2 %	
3-BD-2-RJS	7484452	11300	04	-3115	25,3 %	
3-BD-3-RJS	7486622	10185	96	-2961	21,3 %	
3-LI-1-RJS	7483081	13991	00	-3050	24,4 %	
3-LI-2-RJS	7484314	14815	6	-2960	23,7 %	
3-LI-4-RJS	7483999	11729	6	-3021	25,3 %	
3-LI-5-RJS	7481657	15600	25	-3125	22,2 %	
7-BD-10D-RJS	7488070	11305	12	-3262	31,2 %	

Well	X		hick	Top Cabiúnas (m)	Avg Porosity	ode
1-RJS-13-RJS	7488968	12005	1	-3191	18,8 %	
1-RJS-23-RJS	7495543	11298	9	-2938	23,0 %	
3-BD-13-RJS	7488525	10280	8	-3096	23,6 %	
3-BD-14-RJS	7488497	12780	09	-3095	23,8 %	
3-BD-15C-RJS	7485985	12483	59	-2927	22,9 %	
3-BD-1A-RJS	7486908	11427	30	-2964	24,2 %	
7-BD-11A-RJS	7486161	10983	01	-2957	22,7 %	
7-BD-12D-RJS	7488070	11310	04	-3076	28,7 %	
7-BD-16DA-RJS	7485927	12449	8,5	-3289,5	22,2 %	
7-BD-4-RJS	7488069	11308	33	-3042	23,3 %	
7-BD-5D-RJS	7488067	11309	88	-3047	27,1 %	
7-BD-6D-RJS	7488068	11306	00	-3090	28,9 %	
7-BD-7D-RJS	7488066	11307	34	-2970	27,7 %	
7-BD-8-RJS	7489983	11389	7	-3133	22,4 %	

Well	X		hick	Top Cabiúnas (m)	Avg Porosity	ode
1-RJS-13-RJS	7488968	12005	1	-3191	18,8 %	
1-RJS-23-RJS	7495543	11298	9	-2938	23,0 %	
3-BD-13-RJS	7488525	10280	8	-3096	23,6 %	
3-BD-14-RJS	7488497	12780	09	-3095	23,8 %	
3-BD-15C-RJS	7485985	12483	59	-2927	22,9 %	
3-BD-1A-RJS	7486908	11427	30	-2964	24,2 %	
7-BD-9D-RJS	7488067	11304	68	-2983	34,2 %	
7-LI-3-RJS	7482048	13377	7	-2973	22,8 %	
7-LI-7-RJS	7483125	11600	85	-2936	27,1 %	
7-LI-9-RJS	7484305	15586	3	-3047	28,4 %	
1-RJS-165-RJS	7491044	03689	83	-2587	19,1 %	
1-RJS-262-RJS	7493023	12612	2	-3156	21,6 %	
1-RJS-43A-RJS	7484189	07781	42	-3392	21,7 %	
1-RJS-49-RJS	7479306	14949	5	-3135	29,6 %	

Well	X		hick	Top Cabiúnas (m)	Avg Porosity	ode
1-RJS-13-RJS	7488968	12005	1	-3191	18,8 %	
1-RJS-23-RJS	7495543	11298	9	-2938	23,0 %	
3-BD-13-RJS	7488525	10280	8	-3096	23,6 %	
3-BD-14-RJS	7488497	12780	09	-3095	23,8 %	
3-BD-15C-RJS	7485985	12483	59	-2927	22,9 %	
3-BD-1A-RJS	7486908	11427	30	-2964	24,2 %	
1-RJS-74-RJS	7482998	15108	4	-3100	22,2 %	
1-RJS-92-RJS	7478341	11316	95	-2940	22,2 %	
3-RJS-140D-RJS	7479307	14964	69	-2982	21,7 %	
3-RJS-157C-RJS	7480818	13632	1	-3159	22,4 %	
3-RJS-167-RJS	7481446	11909	00	-3050	25,5 %	
3-RJS-315-RJS	7487635	13467	16	-3025	24,3 %	
3-RJS-73B-RJS	7480762	14826	0	-3110	26,7 %	
3-RJS-78-RJS	7483983	13698	19	-3127	22,6 %	

Well	X		hick	Top Cabiúnas (m)	Avg Porosity	ode
1-RJS-13-RJS	7488968	12005	1	-3191	18,8 %	
1-RJS-23-RJS	7495543	11298	9	-2938	23,0 %	
3-BD-13-RJS	7488525	10280	8	-3096	23,6 %	
3-BD-14-RJS	7488497	12780	09	-3095	23,8 %	
3-BD-15C-RJS	7485985	12483	59	-2927	22,9 %	
3-BD-1A-RJS	7486908	11427	30	-2964	24,2 %	
4-RJS-139A-RJS	7482003	14213	13	-3052	24,5 %	
4-RJS-139-RJS	7481929	14143	37	-3040	34,2 %	
4-RJS-156-RJS	7483030	12130	9	-2945	24,2 %	
4-RJS-258-RJS	7488238	13925	43	-2972	23,1 %	
4-RJS-264-RJS	7485579	14955	12	-3036	23,0 %	
4-RJS-266-RJS	7486566	13325	21	-3054	24,2 %	
4-RJS-341-RJS	7485021	12056	07	-3016	28,1%	

6 CONCLUSÕES PRELIMINARES

Com base na pesquisa realizada, e nos artigos elaborados, foi possível definir as seguintes conclusões parciais, considerando que um dos artigos ainda deve ser submetido para avaliação/revisão e publicação:

1 - O estudo do cubo sísmico e dos perfis e outros dados dos poços permitiu definir a espessura e aspectos tectono-estratigráficos da sucessão vulcânica posicionada na sequência rifte da região plataformal da Bacia de Campos;

2 - As características da formação basáltica - valores de temperatura, pH, e pressão, são compatíveis com os ranges adequados para o desenvolvimento do processo de dissolução/precipitação e armazenamento do carbono via método de mineralização;

3 - O fato das formações basálticas serem capeadas por estratos selantes, carbonatos, folhelhos e evaporitos, oferece uma vantagem em termos de segurança, se a opção de injeção for o CO2 em estado supercrítico;

4 - O estudo demonstrou que existe um controle das zonas de falhas sobre as propriedades dos reservatórios vulcânicos, o que criou blocos ou compartimentos com propriedades significativamente distintas;

5 - A modelagem de um reservatório hipotético com cerca de 21 km^2 e 300 m de espessura, permitiu estimar volumes de armazenamento entre 16 e 47 milhões de toneladas de CO2, diluído em água;

6 - A modelagem e interpretação dos dados legados permitiu entender a distribuição de propriedades intrínsecas dos reservatórios vulcânicos no Campo de Badejo, e isto demonstrou como estes dados serão importantes no futuro para o desenvolvimento de projetos de GCS no contexto avaliado;

7 - Apesar dos dados legados permitirem a modelagem de aspectos como a espessura, morfologia sísmica, e distribuição de propriedades como a densidade de fraturas nos estratos vulcânicos, existem fatores relacionados a diagênese e que afetam a porosidade que precisam ser considerados em termos de desenvolvimento de projetos de GCS neste tipo de meio geológico;

7 REFERÊNCIAS

AJAYI, T.; GOMES, J. S.; BERA, A. A review of CO2 storage in geological formations emphasizing modeling, monitoring and capacity estimation approaches. **Petroleum Science**, 8 jul. 2019. v. 16, n. 5, p. 1028–1063.

ALCALDE, J. *et al.* Estimating geological CO2 storage security to deliver on climate mitigation. **Nature Communications**, 12 jun. 2018. v. 9, n. 1.

ALZATE RUBIO, V. CO_2 mineralization process in basalt rocks: study case, Serra Geral Formation, Paraná sedimentary Basin, São Paulo state. 2024. - Universidade de São Paulo. Agência de Bibliotecas e Coleções Digitais, [s. l.], 2024.

AMINU, M. D. et al. A review of developments in carbon dioxide storage. Applied energy, [s. l.], v. 208, p. 1389–1419, 2017. Disponível em: http://dx.doi.org/10.1016/j.apenergy.2017.09.015.

ANDERSON, S. T. Risk, liability, and economic issues with long-term CO_2 storage—A review. Natural resources research, [s. l.], v. 26, n. 1, p. 89–112, 2017. Disponível em: http://dx.doi.org/10.1007/s11053-016-9303-6.

ANTHONSEN, K. L. *et al.* Characterisation and Selection of the Most Prospective CO2 Storage Sites in the Nordic Region. **Energy Procedia**, 2014. v. 63, p. 4884–4896. Acesso em: 17 dez. 2022.

AYDIN, G.; KARAKURT, I.; AYDINER, K. Evaluation of geologic storage options of CO_2: Applicability, cost, storage capacity and safety. Energy policy, [s. l.], v. 38, n. 9, p. 5072–5080, 2010. Disponível em: http://dx.doi.org/10.1016/j.enpol.2010.04.035.

BACHU, S. Sequestration of CO_2 in geological media: criteria and approach for site selection in response to climate change. Energy conversion and management, [s. l.], v. 41, n. 9, p. 953–970, 2000. Disponível em: http://dx.doi.org/10.1016/s0196-8904(99)00149-1.

BAILEY, A. *et al.* Remote sensing of subsurface fractures in the Otway Basin, South Australia. **Journal of Geophysical Research: Solid Earth**, 1 ago. 2014. v. 119, n. 8, p. 6591–6612. Acesso em: 2 dez. 2023.

BARNES, A. E. Attributes for automating seismic facies analysis. In **SEG International Exposition and Annual Meeting**. 2000. (pp. SEG-2000). SEG.

BENSON, S. M. et al. Underground geological storage, IPCC special report on carbon dioxide capture and storage, Intergovernmental Panel on Climate Change. Interlachen: [s. n.], 2005. v. 5

BÉREST, P. *et al.* Review and analysis of historical leakages from storage salt caverns wells. **Oil & Gas Science and Technology – Revue d'IFP Energies nouvelles**, 2019. v. 74, p. 27. Acesso em: 20 jul. 2019.

BRAGA, D. D. *et al.* 3D Paleogeographic Reconstruction of the Cabiúnas formation lava flows in Campos basin, SE Brazil. **Journal of South American Earth Sciences**, 1 out. 2023. v. 130, p. 104537–104537. Acesso em: 5 ago. 2024.

BRUHN, C. *et al.* Campos Basin: Reservoir Characterization and Management - Historical Overview and Future Challenges. **Offshore Technology Conference**, 1 jan. 2003. Acesso em: 1º maio 2023.

CAO, C. et al. A review of CO_2 storage in view of safety and cost-effectiveness. Energies, [s. l.], v. 13, n. 3, p. 600, 2020. Disponível em: http://dx.doi.org/10.3390/en13030600.

CAO, X. *et al.* A review of in-situ carbon mineralization in basalt. **Journal of Rock Mechanics and Geotechnical Engineering**, 1 dez. 2023. v. 16, n. 4. Acesso em: 10 abr. 2024.

CELIA, M. A. Geological storage of captured carbon dioxide as a large-scale carbon mitigation option. **Water Resources Research**, maio. 2017. v. 53, n. 5, p. 3527–3533.

CHOPRA, S.; MARFURT, K. J.; SOCIETY OF EXPLORATION GEOPHYSICISTS. **Seismic attributes for prospect identification and reservoir characterization**. Tulsa, Ok: Society Of Exploration Geophysicists, 2007.

CIOTTA, M. R. Estudo de possibilidades para armazenar CO_2 em reservatórios geológicos offshore na Bacia de Santos. 2020. - Universidade de Sao Paulo, Agencia USP de Gestao da Informacao Academica (AGUIA), [s. l.], 2020.

CIOTTA, M. R.; TASSINARI, C. C. G. Preliminary basin scale assessment of CO_2 geological storage potential in santos basin, southeastern Brazil: merluza field study case / avaliação preliminar do potencial para armazenamento geológico de CO_2 da bacia de santos, sudeste do Brasil: estudo de caso do campo de merluza. Brazilian Journal of Development, [s. l.], v. 6, n. 9, p. 65961–65977, 2020. Disponível em: http://dx.doi.org/10.34117/bjdv6n9-140.

CLARK, D. E. *et al.* The chemistry and potential reactivity of the CO2-H2S charged injected waters at the basaltic CarbFix2 site, Iceland. **Energy Procedia**, jul. 2018. v. 146, p. 121–128. Acesso em: 20 fev. 2020.

CLARK, D. E. et al. CarbFix2: CO2 and H2S mineralization during 3.5 years of continuous injection into basaltic rocks at more than 250 °C. Geochimica et Cosmochimica Acta, abr. 2020. v. 279, p. 45–66. Acesso em: jun. 2022.

DE FREITAS, L. C.; KANEKO, S. Decomposing the decoupling of CO_2 emissions and economic growth in Brazil. Ecological economics: the journal of the International Society for Ecological Economics, [s. l.], v. 70, n. 8, p. 1459–1469, 2011. Disponível em: http://dx.doi.org/10.1016/j.ecolecon.2011.02.011.

DGB Beheer B.V. OpendTect User Documentation - 6.6 dGB Earth Sciences. Netherlands. 2022

EPE [Empresa De Pesquisa Energética]. 2018. Ocorrência de CO_2 em campos petrolíferos na margem leste brasileira. Retrieved from <https://www.epe.gov.br/pt/publicacoes-dados-abertos/publicacoes/ocorrencia-de-co2-em-campos-petroliferos-na-margem-leste-brasileira>, Website accessed Jul. 15th, 2022.

EPE [Empresa De Pesquisa Energética]. 2021. Brazilian oil and gas report 2020/2021. Retrieved from <https://www.epe.gov.br/en/publications/publications/brazilian-oil-gas-report>, Website accessed Sep. 05th, 2022.

FEDORIK, J. *et al.* Structure and fracture characterization of the Jizan group: Implications for subsurface CO2 basalt mineralization. **Frontiers in earth science (Lausanne)**, 10 jan. 2023. v. 10.

FLEMING, F. P.; ASSIS, J. V. M. de. Monetização e descarbonização de gás natural do pré-sal via GTW (gas-to-wire), captura de CO_2 e EOR (enhanced oil recovery): uma análise de engenharia de sistemas. [S. l.]: Universidade Federal do Rio de Janeiro, 2020.

FRIEDMANN, S. J. et al. The low cost of geological assessment for underground CO_2 storage: Policy and economic implications. Energy conversion and management, [s. l.], v. 47, n. 13–14, p. 1894–1901, 2006. Disponível em: http://dx.doi.org/10.1016/j.enconman.2005.09.006.

GALECZKA, I. et al. An experimental study of basaltic glass-H2O-CO_2 interaction at 22 and 50°C: Implications for subsurface storage of CO_2. Geochim. Cosmochim. Acta, [s. l.], v. 126, p. 123–145, 2014.

GAMBOA, L. et al. Geotectonic controls on CO_2 formation and distribution processes in the Brazilian pre-salt basins. Geosciences, [s. l.], v. 9, n. 6, p. 252, 2019. Disponível em: http://dx.doi.org/10.3390/geosciences9060252.

GISLASON, S. R. et al. Mineral sequestration of carbon dioxide in basalt: A pre-injection overview of the CarbFix project. International journal of greenhouse gas control, [s. l.], v. 4, n. 3, p. 537–545, 2010. Disponível em: http://dx.doi.org/10.1016/j.ijggc.2009.11.013.

GISLASON, S. R. et al. Rapid solubility and mineral storage of CO_2 in basalt. Energy procedia, [s. l.], v. 63, p. 4561–4574, 2014. Disponível em: http://dx.doi.org/10.1016/j.egypro.2014.11.489.

GISLASON, S. R.; OELKERS, E. H. Carbon storage in basalt. Science (New York, N.Y.), [s. l.], v. 344, n. 6182, p. 373–374, 2014. Disponível em: http://dx.doi.org/10.1126/science.1250828.

GOLDBERG, D. *et al*. Geological storage of CO2 in sub-seafloor basalt: the CarbonSAFE pre-feasibility study offshore Washington State and British Columbia. **Energy Procedia**, 1 jul. 2018. v. 146, p. 158–165. Disponível em: <https://www.sciencedirect.com/science/article/pii/S1876610218301528>.

GOLDBERG, D. S.; KENT, D. V.; OLSEN, P. E. Potential on-shore and off-shore reservoirs for CO2 sequestration in Central Atlantic magmatic province basalts. **Proceedings of the National Academy of Sciences**, 4 jan. 2010. v. 107, n. 4, p. 1327–1332. Acesso em: 20 mar. 2020.

GOULART, M. B. R. *et al*. Technology readiness assessment of ultra-deep salt caverns for carbon capture and storage in Brazil. **International Journal of Greenhouse Gas Control**, 1 ago. 2020. v. 99, p. 103083. Disponível em: <https://www.sciencedirect.com/science/article/pii/S1750583619307170>. Acesso em: 11 out. 2021.

GUARDADO, R. Petroleum Geology of the Campos Basin, Brazil, a Model for a Producing Atlantic Type Basin: PART 1. **Datapages.com**, 2023. v. 132, p. 3–36. Disponível em: <https://archives.datapages.com/data/specpubs/basinar3/data/a132/a132/0001/0000/0003.htm>. Acesso em: 5 ago. 2024.

GUZMÁN, E. L. V. Petrofísica de rochas arenosas da bacia do Paraná para a estocagem e mineralização de CO_2. 2024. - Universidade de São Paulo. Agência de Bibliotecas e Coleções Digitais, [s. l.], 2024.

GUPTA, S. D.; CHATTERJEE, R.; FAROOQUI, M. Y. Formation evaluation of fractured basement, Cambay Basin, India. **Journal of Geophysics and Engineering**, 7 fev. 2012. v. 9, n. 2, p. 162–175. Acesso em: 1º mar. 2021.

GYSI, A. P.; STEFÁNSSON, A. CO_2-water–basalt interaction. Low temperature experiments and implications for CO_2 sequestration into basalts. Geochimica et cosmochimica acta, [s. l.], v. 81, p. 129–152, 2012. Disponível em: http://dx.doi.org/10.1016/j.gca.2011.12.012.

HE, H. *et al.* Characteristics and quantitative evaluation of volcanic effective reservoirs: A case study from Junggar Basin, China. **Journal of Petroleum Science and Engineering**, 1 dez. 2020. v. 195, p. 107723–107723. Acesso em: 1º jun. 2023.

HERMES, B. Análise de injeção alternada de água e CO_2 (wag-CO_2) em reservatórios semelhantes aos do pré-sal brasileiro. [S. l.]: Universidade Federal do Rio Grande do Norte, 2017.

HONG, S. et al. Effects of Mg ions on the structural transformation of calcium carbonate and their implication for the tailor-synthesized carbon mineralization process. Journal of CO_2 utilization, [s. l.], v. 60, n. 101999, p. 101999, 2022. Disponível em: http://dx.doi.org/10.1016/j.jcou.2022.101999.

IEA. Global Energy Review 2020. [S. l.], 2020. Disponível em: https://www.iea.org/reports/global-energy-review-2020. Acesso em: 15 abr. 2024.

IEA. World Energy Outlook. [S. l.], 2019. Disponível em: https://www.iea.org/reports/world-energy-outlook-2019,. Acesso em: 15 abr. 2024.

IPCC, 2005: Relatório Especial do IPCC sobre Captura e Armazenamento de Dióxido de Carbono. Preparado pelo Grupo de Trabalho III do Painel Intergovernamental sobre Mudanças Climáticas [Metz, B., O. Davidson, HC de Coninck, M. Loos e LA Meyer (eds.)]. Cambridge University Press, Cambridge, Reino Unido e Nova York, NY, EUA, 442 pp.

IPCC, 2018. Summary for Policymakers. In: Global Warming of 1.5°C. An IPCC Special Report on the impacts of global warming of 1.5°C above pre-industrial levels and related global greenhouse gas emission pathways, in the context of strengthening the global response to the threat of climate change, sustainable development, and efforts to eradicate poverty. Masson-Delmotte, V., P. Zhai,

ISMAIL, A. *et al.* Unsupervised machine learning and multi-seismic attributes for fault and fracture network interpretation in the Kerry Field, Taranaki Basin, New Zealand. **Geomechanics and Geophysics for Geo-Energy and Geo-Resources**, 26 set. 2023. v. 9, n. 1. Disponível em: <https://link.springer.com/article/10.1007/s40948-023-00646-9>. Acesso em: 5 ago. 2024.

KELEMEN, P. et al. An overview of the status and challenges of CO_2 storage in minerals and geological formations. Frontiers in climate, [s. l.], v. 1, 2019. Disponível em: http://dx.doi.org/10.3389/fclim.2019.00009.

KELEMEN, P. B. et al. Engineered carbon mineralization in ultramafic rocks for CO_2 removal from air: Review and new insights. Chemical geology, [s. l.], v. 550, n. 119628, p. 119628, 2020. Disponível em: http://dx.doi.org/10.1016/j.chemgeo.2020.119628.

KIM, K. *et al.* A review of carbon mineralization mechanism during geological CO2 storage. **Heliyon**, 1 dez. 2023. v. 9, n. 12, p. e23135–e23135. Disponível em: <https://www.cell.com/heliyon/fulltext/S2405-8440(23)10343-4>. Acesso em: 5 ago. 2024.

KOUKOUZAS, N. *et al.* Potential for Mineral Carbonation of CO2 in Pleistocene Basaltic Rocks in Volos Region (Central Greece). **Minerals**, 11 out. 2019. v. 9, n. 10, p. 627. Acesso em: 23 mar. 2021.

KUMAR, P. C.; MANDAL, A. Enhancement of fault interpretation using multi-attribute analysis and artificial neural network (ANN) approach: a case study from Taranaki Basin, New Zealand. **Exploration Geophysics**, jun. 2018. v. 49, n. 3, p. 409–424. Acesso em: 29 ago. 2021.

LARKIN, P. et al. Uncertainty in risk issues for carbon capture and geological storage: findings from a structured expert elicitation. International journal of risk assessment and management, [s. l.], v. 22, n. 3/4, p. 429, 2019. Disponível em: http://dx.doi.org/10.1504/ijram.2019.103335.

LEUNG, D. Y. C.; CARAMANNA, G.; MAROTO-VALER, M. M. 2014. An overview of current status of carbon dioxide capture and storage technologies. Renewable and Sustainable Energy Reviews, [s. l.], v. 39, p. 426–443, Disponível em: http://dx.doi.org/10.1016/j.rser.2014.07.093.

MAIA DA COSTA, A. et al. Potential of storing gas with high CO_2 content in salt caverns built in ultra-deep water in Brazil. Greenhouse Gases: Science and Technology, 7 dez. 2018. Acesso em: 1o jun. 2020.

MARCELLOS, C. F. C.; DA SILVA, C. H. de L.; KABOUK, N. B. Processamento de gás natural e Recuperação Avançada de Petróleo (EOR) de águas ultraprofundas com CO_2. [S. l.]: Universidade Federal do Rio de Janeiro, 2011.

MARINS, G. M. *et al.* Characterization of volcanic reservoirs; insights from the Badejo and Linguado oil field, Campos Basin, Brazil. **Marine and Petroleum Geology**, 1 dez. 2022. v. 146, p. 105950–105950. Acesso em: 5 ago. 2024.

MARTIN-ROBERTS, E. et al. Carbon capture and storage at the end of a lost decade. One earth (Cambridge, Mass.), [s. l.], v. 4, n. 11, p. 1645–1646, 2021. Disponível em: http://dx.doi.org/10.1016/j.oneear.2021.10.023.

MATTER, J. M. *et al.* Monitoring permanent CO2 storage by in situ mineral carbonation using a reactive tracer technique. **Energy Procedia**, 2014. v. 63, p. 4180–4185. Acesso em: 28 fev. 2020.

MCGRAIL, B. P. *et al.* Potential for carbon dioxide sequestration in flood basalts. **Journal of Geophysical Research: Solid Earth**, dez. 2006. v. 111, n. B12, p. n/a-n/a.

MCGRAIL, B. P. *et al.* Injection and Monitoring at the Wallula Basalt Pilot Project. **Energy Procedia**, 2014. v. 63, p. 2939–2948. Acesso em: 9 maio 2020.

MIZUSAKI, A. M. P. *et al.* Basalt magmatism along the passive continental margin of SE Brazil (Campos basin). **Contributions to Mineralogy and Petrology**, 1 jun. 1992. v. 111, n. 2, p. 143–160. Disponível em: <https://link.springer.com/article/10.1007/BF00348948>. Acesso em: 5 ago. 2024.

NAVARRO, J. *et al.* Assessing hydrofacies and hydraulic properties of basaltic aquifers derived from geophysical logging. **Brazilian Journal of Geology**, 2020. v. 50, n. 4. Acesso em: 2 out. 2022.

NOAA. Trends in Atmospheric Carbon Dioxide (CO_2). [S. l.], 2024. Disponível em: https://gml.noaa.gov/ccgg/trends/index.html.

OELKERS, E. H.; GISLASON, S. R.; MATTER, J. Mineral carbonation of CO_2. Elements (Quebec, Quebec), [s. l.], v. 4, n. 5, p. 333–337, 2008. Disponível em: http://dx.doi.org/10.2113/gselements.4.5.333.

OLIVEIRA, L. C. *et al.* Seismic interpretation of the Mero Field igneous rocks and its implications for pre- and post-salt CO2 generation – Santos Basin, offshore Brazil. **Marine and Petroleum Geology**, 1 maio. 2024. v. 163, p. 106775–106775. Acesso em: 5 ago. 2024.

ORITA, G. K. L.; CRUZ, V. G. P. da. Captura e armazenamento de CO_2: um revisão das tecnologias existentes, carbonatação in situ de basaltos e avaliação do potencial da Formação Serra Geral como reservatório de CO_2. Geociências, [s. l.], v. 41, n. 3, p. 779–795, 2023. Disponível em: http://dx.doi.org/10.5016/geociencias.v41i03.16760.

PELISSARI, M. R. Avaliação de reservatórios potenciais para armazenamento geológico de CO_2 emitido pelo Complexo Termelétrico Jorge Lacerda, Santa Catarina. 2021. - Universidade de Sao Paulo, Agencia USP de Gestao da Informacao Academica (AGUIA), [s. l.], 2021.

POGGE VON STRANDMANN, P. A. E. *et al.* Rapid CO2 mineralisation into calcite at the CarbFix storage site quantified using calcium isotopes. **Nature Communications**, 30 abr. 2019. v. 10, n. 1. Disponível em: <https://www.nature.com/articles/s41467-019-10003-8>.

RAMOS, G. M. S. *et al.* Potential for permanent CO2 sequestration in depleted volcanic reservoirs in the offshore Campos Basin, Brazil. **International journal of greenhouse gas control**, 1 set. 2023. v. 128, p. 103942–103942. Acesso em: 5 ago. 2024.

RAZA, A. et al. A screening criterion for selection of suitable CO_2 storage sites. Journal of natural gas science and engineering, [s. l.], v. 28, p. 317–327, 2016. Disponível em: http://dx.doi.org/10.1016/j.jngse.2015.11.053.

RAZA, A. et al. Carbon mineralization and geological storage of CO_2 in basalt: Mechanisms and technical challenges. Earth-science reviews, [s. l.], v. 229, n. 104036, p. 104036, 2022. Disponível em: http://dx.doi.org/10.1016/j.earscirev.2022.104036.

REN, K. *et al*. Hydrocarbons in igneous rock of Brazil: A review. **Petroleum Research**, 1 set. 2020. v. 5, n. 3, p. 265–275. Disponível em: <https://www.sciencedirect.com/science/article/pii/S2096249520300235>. Acesso em: 19 maio 2021.

ROCKETT, G. C. Associação de fontes emissoras e reservatórios potenciais para armazenamento geológico de CO_2 na Bacia de Campos, Brasil. 2010. - PUCRS, [s. l.], 2010.

ROSENBAUER, R. J. et al. Carbon sequestration via reaction with basaltic rocks: Geochemical modeling and experimental results. Geochimica et cosmochimica acta, [s. l.], v. 89, p. 116–133, 2012. Disponível em: http://dx.doi.org/10.1016/j.gca.2012.04.042.

RUBIN, E. S.; DAVISON, J. E.; HERZOG, H. J. The cost of CO_2 capture and storage. International journal of greenhouse gas control, [s. l.], v. 40, p. 378–400, 2015. Disponível em: http://dx.doi.org/10.1016/j.ijggc.2015.05.018.

SCHAEF, H. T.; MCGRAIL, B. P.; OWEN, A. T. Basalt reactivity variability with reservoir depth in supercritical CO_2 and aqueous phases. Energy procedia, [s. l.], v. 4, p. 4977–4984, 2011. Disponível em: http://dx.doi.org/10.1016/j.egypro.2011.02.468.

SCHMELZ, W. J.; HOCHMAN, G.; MILLER, K. G. Total cost of carbon capture and storage implemented at a regional scale: northeastern and midwestern United States. Interface focus, [s. l.], v. 10, n. 5, p. 20190065, 2020. Disponível em: http://dx.doi.org/10.1098/rsfs.2019.0065.

SILVA, G. C. R.; PARENTE, V.; DOS SANTOS, E. M. Road to net-zero carbon: a tecnologia CCUS e o mercado de créditos de carbono como instrumentos complementares à mitigação e

compensação das emissões de gases de efeito estufa no setor upstream. Revista Brasileira de Energia, [s. l.], v. 28, n. 4, 2023. Disponível em: http://dx.doi.org/10.47168/rbe.v28i4.754.

Singh, R. K., Nayak, N. P., Kumar, S., & Vishal, V. 2024. A Critical Meta-Analysis of CO2-Water-Rock Interaction in Basalt for CO2 Storage: A Review Based on Global and Indian Perspective. *Marine and Petroleum Geology*, 107002.

SNÆBJÖRNSDÓTTIR, S. Ó. et al. Author Correction: Carbon dioxide storage through mineral carbonation. Nature reviews. Earth & environment, [s. l.], v. 1, n. 12, p. 695–695, 2020. Disponível em: http://dx.doi.org/10.1038/s43017-020-00120-0.

SNÆBJÖRNSDÓTTIR, S. Ó.; GISLASON, S. R. CO_2 storage potential of basaltic rocks offshore Iceland. Energy procedia, [s. l.], v. 86, p. 371–380, 2016. Disponível em: http://dx.doi.org/10.1016/j.egypro.2016.01.038.

SPAN, R.; WAGNER, W. A New Equation of State for Carbon Dioxide Covering the Fluid Region from the Triple-Point Temperature to 1100 K at Pressures up to 800 MPa. **Journal of Physical and Chemical Reference Data**, nov. 1996. v. 25, n. 6, p. 1509–1596.

STENHOUSE, M. J.; GALE, J.; ZHOU, W. Current status of risk assessment and regulatory frameworks for geological CO_2 storage. Energy procedia, [s. l.], v. 1, n. 1, p. 2455–2462, 2009. Disponível em: http://dx.doi.org/10.1016/j.egypro.2009.02.007.

STICA, J. M.; ZALÁN, P. V.; FERRARI, A. The evolution of rifting on the volcanic margin of the Pelotas Basin and the contextualization of the Paraná–Etendeka LIP in the separation of Gondwana in the South Atlantic. **Marine and Petroleum Geology**, 1 fev. 2014. v. 50, p. 1–21.

TAKAGI, M. et al. Cost estimates for the CO_2 geological storage in deep saline aquifers offshore japan: A case study. Energy procedia, [s. l.], v. 37, p. 3374–3378, 2013. Disponível em: http://dx.doi.org/10.1016/j.egypro.2013.06.225.

TANER, M. T. *et al.* Seismic attributes revisited. **SEG Technical Program Expanded Abstracts 1994**, 1 jan. 1994. p. 1104–1106. Acesso em: 10 dez. 2023.

TANG, H. *et al.* Review of volcanic reservoir geology in China. **Earth-Science Reviews**, 1 set. 2022. v. 232, p. 104158–104158. Acesso em: 24 mar. 2024.

TIGRE, C. A. *et al.* Pampo, Linguado, and Badejo Fields: Their Discoveries,Appraisals, and Early Production Systems. *In*: OFFSHORE TECHNOLOGY CONFERENCE. Houston, Texas: 1983. Acesso em: 5 ago. 2024.

TUTOLO, B. M.; AWOLAYO, A.; BROWN, C. Alkalinity Generation Constraints on Basalt Carbonation for Carbon Dioxide Removal at the Gigaton-per-Year Scale. **Environmental Science & Technology**, 20 ago. 2021. v. 55, n. 17, p. 11906–11915. Acesso em: 8 jan. 2023.

VIEIRA, D. P. *et al.* Simulation Of The Conceptual Design Of Offshore Salt Caves For CO2 Storage. ECMS 2020 Proceedings: **ECMS 2020 Proceedings**, 1 jun. 2020. v. 34, n. 1. Acesso em: 5 ago. 2024.

VILARRASA, V.; CARRERA, J. Geologic carbon storage is unlikely to trigger large earthquakes and reactivate faults through which CO_2 could leak. Proceedings of the National Academy of Sciences of the United States of America, [s. l.], v. 112, n. 19, p. 5938–5943, 2015. Disponível em: http://dx.doi.org/10.1073/pnas.1413284112.

VULIN, D. et al. Development of CCUS clusters in Croatia. International journal of greenhouse gas control, [s. l.], v. 124, n. 103857, p. 103857, 2023. Disponível em: http://dx.doi.org/10.1016/j.ijggc.2023.103857.

WANG, Y. *et al.* Characteristics, controls and geological models of hydrocarbon accumulation in the Carboniferous volcanic reservoirs of the Chunfeng Oilfield, Junggar Basin, northwestern China. **Marine and Petroleum Geology**, 1 jun. 2018. v. 94, p. 65–79.

WANG, F.; DREISINGER, D. Status of CO_2 mineralization and its utilization prospects. **Minerals and Mineral Materials**, 25 abr. 2022. v. 1, n. 1, p. 4. Disponível em: <https://www.oaepublish.com/minerals/article/4806.html>.

WHITE, S. K. *et al.* Quantification of CO_2 Mineralization at the Wallula Basalt Pilot Project. **Environmental Science & Technology**, 11 set. 2020. v. 54, n. 22, p. 14609–14616.

WOLFF-BOENISCH, D.; GISLASON, S. R.; OELKERS, E. H. The effect of crystallinity on dissolution rates and CO_2 consumption capacity of silicates. Geochimica et cosmochimica acta, [s. l.], v. 70, n. 4, p. 858–870, 2006. Disponível em: http://dx.doi.org/10.1016/j.gca.2005.10.016.

WORLD METEOROLOGICAL ORGANIZATION (WMO). Greenhouse Gas concentrations hit record high. Again. [S. l.], 2023. Disponível em: https://wmo.int/news/media-centre/greenhouse-gas-concentrations-hit-record-high-again. Acesso em: 26 mar. 2024.

ZAHASKY, C. *et al.* Multimodal imaging and stochastic percolation simulation for improved quantification of effective porosity and surface area in vesicular basalt. **Advances in Water Resources**, nov. 2018. v. 121, p. 235–244. Acesso em: 3 dez. 2021.